The belowground functioning of tropical biomes

André Butler

Thesis submitted to the University of Edinburgh for the degree of:

DOCTOR OF PHILOSOPHY

School of Geosciences

2010

Declaration

I confirm that this work is my own, except where indicated otherwise. No part of this thesis has been submitted for any other degree or qualification.

Name: ..... Date: .....

Acknowledgements

A PhD is an intense baptism into the world of research; it is a long arduous process with a lot of ups and downs. I would like to express my thanks to all the people that have helped me on the road to the completion of this thesis.

I have been fortunate with my supervisors. Patrick Meir and John Grace both helped to guide me in the right direction, and complemented each other really well. Patrick wrote an interesting research proposal which provided me with a good foundation, but at the same time gave me the freedom to explore my own interests. John provided a wealth of experience, a peculiar brand of refreshing insight, and a wonderful sense of humour. Apart from my principal supervisors, it has been a privilege to work alongside both Jan Čermák and Nicolas Barbier. I have benefited immensely from their experience, and friendship.

The collection of good quality data is the foundation of any good research. I would like to express an immense amount of gratitude to Leandro Maracahipes and Divino Vicente Silverio for their invaluable help with the collection of data used in this thesis. It has been a pleasure to work with the research group; especially Beatriz, Ben Hur and Eddie, at the 'Universidade do Estado de Mato Grosso', Brasil. In particular I would like to show my appreciation for their logistical support and hospitality.

I am very privileged to have such a supportive family. I would like to express a great deal of gratitude to my parents for all their advice and assistance. To end with, during my time in Edinburgh I met my wonderful wife Camille. She has been a companion through the whole process; she has travelled with me halfway around the world several times to do field work, she has provided advice on data analysis, and

she has patiently proof-read all my papers. I have been very lucky to have met and shared such wonderful times with such a special person.

Abstract

Within the field of ecosystem science, substantial progress has been made towards our knowledge of the factors which shape the global distribution of vegetation. However, factors which control the biogeography of belowground vegetation structure and function remain less understood than their aboveground counterpart. Vegetation types can differ substantially in terms of belowground processes such as root growth, root turnover, and resulting vertical root distributions. Fine roots provide an exchange surface, allowing transport of water and nutrients to the leaves. On the other hand they also represent a significant sink for photosynthetically fixed carbon to the soil in terms of maintenance and growth. Overall, root processes have a major influence on fluxes of water, carbon and nutrients within ecosystems.

In this thesis, an electrical impedance method was used to determine the area of 'active' root in contact with the soil for the purpose of absorption. These measurements were compared to the leaf area of the trees, for the first time allowing the aboveground and the belowground resource exchange areas of plant to be contrasted. This approach was first developed to compare the exchange surface areas of leaves and roots within a Sitka spruce (*Picea sitchensis*) managed forest, making measurements in adjacent stands of differing tree density, but identical in age. Stem density was found to significantly influence the proportion of absorbing root area

relative to leaves. Following the successful test of the method, it was used to compare the resource exchange areas of eight stands of forest and savanna vegetation in central Brazil. Across a broad gradient of vegetation structure, the results showed progressively more investment in fine root area relative to leaf area across the transition from dense forest to open savanna. However, a contrasting result showed that the forests had a higher absorbing root area to leaf area ratio than savannas. Furthermore, these measured ratios were strongly correlated with tree height across the eight structurally contrasting stands. It appears that absorbing root area index provides a physiologically meaningful way of characterising belowground water uptake ability, it is possible that excessive investment in fine root area, relative to leaf area, may reflect differences in the requirement for nutrient uptake in poor soils.

Complementary to the analysis of root absorbing area, measurements of root activity and belowground carbon cycling were made by focussing on two of the eight tropical study sites. Here, the carbon costs of root growth and respiration were quantified to develop a belowground carbon budget for two structurally contrasting Brazilian savannas, using soil respiration measurements and a root presence/absence manipulation experiment. Annual estimates showed that at least 60% of the total CO_2 efflux from the soil was contributed by autotrophic processes, with this value rising to 80% during the dry season. Seasonal fluctuations of soil respiration were strongly correlated with soil moisture for both the autotrophic (R^2=0.79, p-value<0.05) and heterotrophic (R^2=0.90, p-value<0.05) components, with maximum

flux rates corresponding with 16.4 and 17.7% soil moisture content respectively. Furthermore, autotrophic respiration was found to varied with phonological patterns of fine root growth (R^2=0.80, p-value<0.05). It follows that, the way in which phenological processes respond to a changing climate is of potential importance within seasonally dry regions. Diurnal fluctuations of heterotrophic CO_2 efflux were correlated with soil temperature (R^2=0.74, p-value<0.05), demonstrating a Q_{10} value of 1.6 across both sites. In contrast, total soil CO_2 efflux was not correlated with temperature (p-value=0.31), suggesting that autotrophic respiration is predominantly limited by substrate supply.

Table of Content

List of Tables and Figures

Symbols and Abbreviations

Where appropriate, units are indicated in parentheses.

Symbol/Abbreviation	*Description*
$\mathfrak{R}$	Universal gas constant (J K^{-1} mol^{-1})
A_{bas}	Basal area (m^2 or m^2 ha^{-1})
A_{crown}	Crown area (m^2)
A_{social}	Social area (m^2)
C	Carbon
D	Stomatal density (mm^{-2})
DBH	Diameter at breast height (cm)
EI	Earth Impedance
E_{max}	Maximum transpiration rate (mmol s^{-1} m^{-2})
k_{root}	Absorbing root hydraulic conductance per unit surface area (m^3 MPa^{-1} m^{-2} s^{-1})
k_s	Hydraulic conductance per unit sapwood area (m^3 MPa^{-1} m^{-2} s^{-1})
L	Guard cell length (μm)
LAI	Leaf Area Index (m^{-2} m^{-2})
LAI_{fall}	Index of surface area of litterfall expressed per unit ground area (m^{-2} m^{-2})
LAI_{max}	Maximum Leaf Area Index (m^{-2} m^{-2})
$LAI_{transpiring}$	Transpiring Leaf Area Index (m^{-2} m^{-2})

P	Atmospheric pressure (MPa)
P	Precipitation (mm)
Q_{10}	Quotient of change in respiration caused by a change in temperature by 10 degrees Celsius
R	Electrical impedance (Ohms)
R_a	Autotrophic respiration (μmol m^{-2} s^{-1})
$R_{aboveground}$	Plant aboveground respiration (μmol m^{-2} s^{-1})
RAI	Root Area Index (m^{-2} m^{-2})
$RAI_{absorbing}$	Absorbing Root Area Index (m^{-2} m^{-2})
RAI_{fine}	Fine Root Area Index (m^{-2} m^{-2})
$R_{belowground}$	Plant belowground respiration (μmol m^{-2} s^{-1})
R_e	Ecosystem respiration (μmol m^{-2} s^{-1})
R_h	Heterotrophic respiration (μmol m^{-2} s^{-1})
R_{rg}	Root growth respiration (μmol m^{-2} s^{-1})
R_{rm}	Root maintenance respiration (μmol m^{-2} s^{-1})
R_{soil}	Soil respiration (μmol m^{-2} s^{-1})
S	Total Root Absorption Surface (m^2)
SPI	Stomatal Pore Index (m^{-2} m^{-2})
T	Temperature (Celsius or Kelvin)
V_{stem}	Stem volume (m^{-3})
ΔB_{fr}	Fine root production (MgC/unit time)
ΔB_{leaf}	Leaf production (MgC/unit time)
Θ	Volumetric water content (m^3 m^{-3})

μ	Viscosity of water at a given temperature ($m^2\ s^{-1}$)
P	Electrical resistivity of water conducting tissue (ohm.meters)
Ψ	Water potential (MPa)

Part I: Context

1.1 Introduction and Overview

The distribution of terrestrial ecosystems is principally determined by climate (Bond et al., 2005; Malhi et al., 2009), and the resulting vegetation cover plays an important role within the climate system by influencing energy, water, and gas exchange with the atmosphere (Sellers et al., 1997; Eastman et al., 2001; Law et al., 2002). As a result the dynamic equilibrium that exists between vegetation and regional climate may be altered if either component changes (Foley et al., 1998). One such delicate balance exists at the boundaries between tropical forests and savannas. The distinct structure of these vegetation types has profound effects on their function (Breshears, 2006) by influencing rates of transpiration and production (Leuning et al., 2005; Gotsch et al., 2010), nutrient cycling (Singh et al., 1989), and consequently regional biogeochemical cycles (Neilson, 1993). Given that the transition between tropical forests and savannas is anticipated to be highly sensitive to changes in climate, disturbance regimes, and land use (House et al., 2003; Mayle et al., 2007; Sankaran et al., 2008; Malhi et al., 2009), a better understanding of the mechanistic processes regulating the dynamics and feed-backs of this putative transition is urgently needed.

The structure and distribution of ecosystems forming the transition between tropical forests and savanna is thought to be influenced by four major environmental

factors: water availability, nutrient availability, fire, and herbivory (Lopes and Cox, 1977; Furley and Ratter, 1988; Sankaran et al., 2008; Hoffmann et al., 2009; Furley, 2010). Sankaran et al. (2008) found that a combination of all these drivers explained 70% of the variation of woody cover across African savannas. However, mean annual precipitation was the most important predictor of vegetation structure. Consequently, water availability is considered to be one of the critical drivers of the distribution of tropical ecosystems. It has been forecast that an increase in drought frequency and severity within these environments may be induced by several factors including : (1) A temperature increase associated with global warming may increase the rate of evaporation from the soil surface (Nepstad et al., 2004). (2) The replacement of natural vegetation with agriculture or pasture reduces water cycling leading to a reduction in rainfall (Nobre et al., 1991; Zhang et al., 1996; Hoffmann and Franco, 2003). (3) Increases in atmospheric CO_2 may induce a decline in evapo-transpiration, consequently curtailing a major source of moisture for regional precipitation (Cox et al., 2000). Additionally, drought is often associated with an increase in fire frequency, which can further inhibit rainfall by creating condensation nuclei, thus reducing warm rain processes in convective tropical clouds (Graf, 2004; Koren et al., 2004; Beerling and Osborne, 2006). Consequently, such changes could induce shifts in ecosystem structure and composition between forests and savanna.

An important adaptation observed in tropical savannas is the partitioning of a greater proportion of biomass belowground relative to forest ecosystems (Castellanos

et al., 1991; De Castro and Kauffman, 1998). Root processes and functioning are therefore of fundamental importance to the comparative advantage of savanna vegetation. Roots perform a variety of functions that are critical to plant survival, including; acquisition of water and nutrient from the soil, mechanical stability of plants, and the storage of carbon compounds. However, the principal function of plant roots is to provide an exchange surface for water and nutrients between the plant and the soil. Roots thereby provide a pathway for fluxes of water and other materials via the plant canopy to the atmosphere. The flux of water from the leaves to the atmosphere is regulated by the stomata. However, assuming no hydraulic capacitance, the rate of transpiration cannot exceed the supply of water from the soil. Consequently, the hydraulic properties of root systems have the potential to limit the flow of water through plants and thereby photosynthesis (Magnani et al., 1998; Sperry et al., 1998). Conversely, the maintenance and growth of an extensive root system comes at a significant carbon cost. As a result, there exists a trade-off between the form and function of plant root systems.

The carbon demands of root production, maintenance and turnover require transport of carbon and energy from the canopy to the soil, consequently influencing the biogeochemical cycle in terrestrial ecosystems (Norby and Jackson, 2000; Lauenroth and Gill, 2003; Trumbore and Gaudinski, 2003). Fine roots (<2 mm in diameter) are considered to be the dynamic part of the root system, and thereby responsible for most belowground carbon and nutrient cycling. It has been estimated

that fine roots account for at least 33% of global annual terrestrial net primary production (Jackson et al., 1997). Optimality theory predicts that plants will minimize the carbon costs associated with their root network while maximizing water and nutrient uptake (Sperry et al., 1998). As a result, plants must balance the carbon costs of new root growth with the benefits of young, more efficient fine roots which can colonise nutrient-rich microsites. This balance is influenced by a multitude of factors including: increased maintenance costs associated with higher temperatures, nutrient status of the soil, plant water availability, and mycorrhizal colonization (Eissenstat et al., 2000; Joslin et al., 2000; Norby and Jackson, 2000; Pregitzer et al., 2000). Finally, when roots die and decompose, some of their carbon is released to the atmosphere while some may remain as soil organic matter pool. Hence, root turnover is a major component of ecosystem carbon cycling and is an important sink for plant primary productivity.

1.2 Aims and Objectives

Tropical forests and savannas have been seen to show contrasting belowground vegetation structure and function. It has been well documented that tree species which are adapted to dry climatic regimes generally have a higher root:shoot ratio (R:S), and deeper rooting systems than species that are more suited to a mesic climate (Schenk and Jackson, 2002). Measurements of fine root turnover produced varying results, however those reported for savanna ecosystems are at the high end of

the range for tropical biomes. Such high rates of fine root turnover represent a significant sink for photosynthetically fixed carbon. This high carbon cost is thought to have functional benefits in terms of an efficient exchange surface for both water and nutrients. Consequently, the main aim of this thesis was to better understand the links between form and function for root systems, and the associated carbon costs of root systems, in seasonally dry climates making comparisons between tropical deciduous forests and savanna ecosystems.

A newly developed earth impedance (EI) method for measuring the active absorbing root surface area of individual trees (Aubrecht et al., 2006; Čermák et al., 2006) was used to develop a novel approach allowing us to quantify and compare the belowground and aboveground resource absorbing areas at the ecosystem level. This approach was explored by comparing measurements of absorbing root area (using the EI method), fine root area, and leaf area across three Sitka spruce stands of contrasting tree density. Using this new and promising method, relationships between absorbing root surface areas and leaf areas across a natural gradient in vegetation structure in the zone of transition between the Amazon forest and Brazilian savanna were investigated. These results will allow us to better understand the physiological functioning of root systems in relation to structure within contrasting vegetation types.

Another aim of this thesis was to understand how vegetation structure (with respect to carbon allocation patterns), and climatic variables (ie. soil temperature and

moisture) independently influence the respiration costs of growth and maintenance of the root system in seasonally dry climates. The influence of vegetation structure can be assessed by making comparisons between the autotrophic component of soil respiration within two structurally contrasting woody savannas existing in the same climate and relating these measurements to seasonal fluctuations in fine root productivity. A root presence/absence manipulation experiment was used to determine how the soil respiration components independently respond to these abiotic and biotic variables.

This thesis has been divided into two main sections (Part II & Part III); the first of these sections focuses on quantifying and analysing resource exchange surface areas of plants, while the second section explores the belowground carbon dynamics of tropical savannas. Part II begins with a general introduction on plant hydrology and a discussion of different methods for measuring root systems. This is followed by two complementary research papers. The first research paper entitled '***Estimates and relationships between aboveground and belowground resource exchange surface areas in a Sitka spruce managed forest***' (Published in *Tree Physiology*) explores a new approach to measuring the belowground exchange surface area within a controlled experimental setting. The second reseach paper entitled '***Absorbing root areas and transpiring leaf areas at the tropical forest and savanna boundry in Brazil***' evaluates ecophysiological allocation patterns of leaves and absorbing roots across a natural gradient in vegetation structure. The second

main section (Part III) follows on from the analysis of absorbing root area to evaluate the influence of root activity on belowground carbon cycling. This section begins with some background information on the influence of root activity on soil respiration processes. This is followed by the final reseach paper entitled '***Soil respiration and belowground carbon dynamics in two structurally contrasting woody savannas in central Brazil***', which focuses on the influence of phenological cycles of fine root turnover and leaf litter fall on soil CO_2 efflux. Finally, the thesis concludes (Part IV) by considering the implications of this research within a general discussion.

Part II: Root Form and Function

2.1 Plant Hydrology

Terrestrial plants rely on the supply of water from the soil to replace the evaporation that occurs while atmospheric CO_2 is diffusing into photosynthetic tissue. Water used for transpiration moves from the soil through the plant to the atmosphere, along a continuum of increasingly negative water potential (ψ) which flows 'downhill' thermodynamically but 'uphill' physically from the roots to the leaves. Plant water loss is controlled by stomatal conductance and atmospheric demand. However, for the plant to avoid desiccation, water loss cannot exceed the maximum supply from the roots. Consequently, carbon assimilation may be significantly constrained by the hydraulic pathway from the soil to the leaf.

The movement of water from the soil through the plant is in many ways analogous to Ohm's law of electrical conductivity (Figure 2.1-1). The supply of water to the canopy ($E_{\max}$) is directly proportional to the water potential gradient from the soil to leaf ($\Delta\psi$) and inversely proportional to the resistance of the hydraulic pathway. The total resistance consists of a root (R_{root}) and shoot (R_{shoot}) component arranged in series:

$$E_{\max} = \frac{\Delta\psi_{soil}^{leaf}}{R_{root} + R_{shoot}} \quad (1)$$

Hydraulic limitations arise because the resistances experienced by the water flow are not constant. As the water potential deficit increases between the leaf and the soil the resistance to water flow also increases. This increased resistance occurs at two weak points in the soil-plant-atmosphere hydraulic continuum: (1) at the root-soil interface where steep water potential gradients can create dry non-conductive zones, and (2) in the xylem where cavitations can eliminate water transport. Additionally, the leaf water potential diminishes with increasing tree height due to a gravitational component, potentially resulting in cavitation processes.

The hydraulic resistance of the root system is predominantly determined by the radial resistance across the soil-root interface and is therefore inversely related to surface area of the absorbing roots:

$$R_{root} = \frac{1}{k_{root} S_{root}} \tag{2}$$

where k_{root} is the absorbing root hydraulic conductance per unit surface area, and S_{root} is the absorbing root surface area. However, due to the difficulties in measuring root hydraulic resistances they have been largely neglected in hydraulic models.

A model proposed by Whitehead et al. (1984) predicts that the leaf area (A_l) to sapwood area (A_s) ratio will decline with increases in tree height. Thereby preventing the development of damaging water potential gradients, while minimizing reductions in canopy conductance:

$$\frac{A_l}{A_s} = \frac{k_s \cdot \Delta\psi}{H \cdot \mu \cdot g_s \cdot D} \tag{3}$$

where k_s is the hydraulic conductance per unit sapwood area, $\Delta\psi$ is the soil to leaf water potential deficit, H is tree height, μ is the viscosity of water at a given temperature, g_s is canopy conductance to water vapour, and D is atmospheric vapour pressure deficit. However, this model is based on the assumption that all the hydraulic resistance is located in the shoot, and the effects of varying the root surface area have been largely ignored.

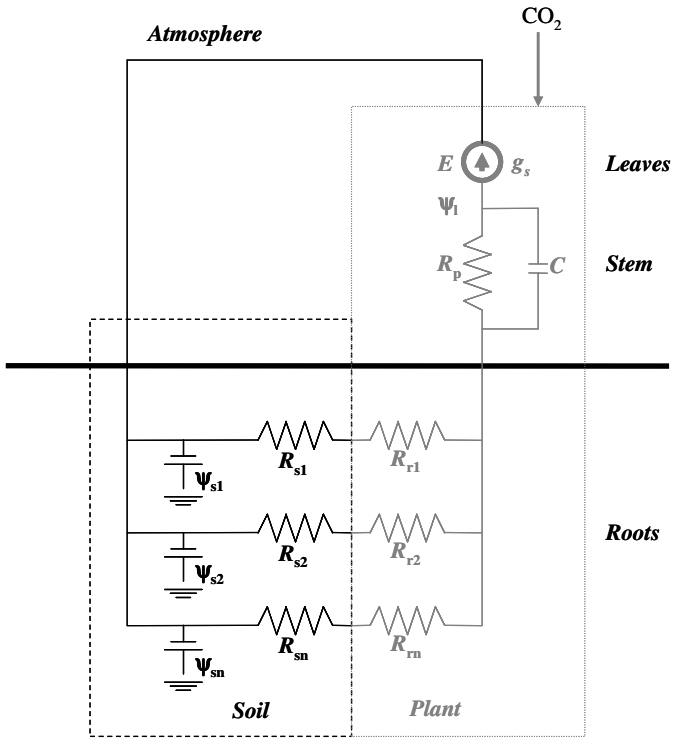

Figure 2.1-1: The resistance network for sap flow through the soil-plant-atmosphere system. Resistances to the supply of water to the absorbing roots through the soil are shown as R_s. Multiple (n) absorbing root resistances are shown in parallel, each with a specific resistance, R_r. The plant stem has a single resistance R_p and a capacitance (C) component. Current is generated by transpiration (Williams et al., 2001).

2.2 Methods for Measuring Root Systems

Increasing our knowledge of belowground processes has not simply been a matter of allocating more effort to the topic. We have fundamentally been limited by the methods that are available to assess belowground processes from the individual plant level right up to the ecosystem level. Conventional methods for measuring root systems have included both destructive excavation such as soil coring, monoliths and in-growth cores, and non-destructive monitoring such as minirhizotron imaging (Vogt et al., 1998). Digital photography along with specialist software has been adopted in conjunction with these methods to measure fine root surface areas (Himmelbauer et al., 2004). However, our limited ability to distinguish between absorbing and non-absorbing root surfaces represents a major shortcoming of traditional methods. Whereas it is easy to visually discriminate between foliage and branches as functional organs, absorbing and non-absorbing roots cannot be easily distinguished.

The electrical properties of roots can be exploited to measure the absorbing soil-root interface non-destructively. This approach was first explored through measurements of capacitance, which was thought to be related to the extent and active surface area of the root system (Chloupek, 1977; Preston et al., 2004; McBride et al., 2008). However, moisture in the soil-root system had a significant influence on the capacitance measurements (Dalton, 1995). More recently electrical impedance spectroscopy has been adopted for the study of root systems (Repo et al., 2005). This

technique has been developed to assess the absorbing root surface area of individual trees in field conditions (Aubrecht et al., 2006).

The earth impedance method is based on the physical principle of electrical current continuity. If a simple electrical circuit is established between a tree and the soil, the current will only enter (or exit) the tree through the same porous surface area used in water and nutrient uptake. From the difference in conductivity of tree tissue and the soil, the soil–root exchange surface area is estimated (Aubrecht et al., 2006). A large field trial has shown absorbing root surface area to be proportional to the cross-sectional area of aboveground conducting tissue (Čermák et al., 2006). Additionally, lab-based studies have found electrical resistance to be correlated with geometric root surface areas (Cao et al., 2010). It appears therefore, that the development of the earth impedance method for measuring soil-root interface has the potential to address questions related to root functioning.

2.3 Estimates and relationships between aboveground and belowground resource exchange surface areas in a Sitka spruce (*Picea Sitchensis*) managed forest

Butler, A., Barbier, N., Cermak, J., Koller, J., Thornily, C., McEvoy, C., Nicoll, B., Perks, M., Grace, J. & Meir, P. (2010) *Tree Physiology*, doi:10.1093/treephys/tpq022.

Abstract

Our knowledge of the nature of belowground competition for moisture and nutrients is limited. In this study we used an earth impedance method to determine the root absorbing area of Sitka spruce (*Picea sitchensis* (Bong.) Carr.) trees, making measurements in stands of differing density (2, 4, and 6 meter inter-tree spacing). We compared absorbing root area index ($RAI_{absorbing}$; based on the impedance measure) with fine root area index (RAI_{fine}; based on estimates of total surface area of fine roots) and related these results to investment in conductive roots. Root absorbing area was a near-linear function of tree stem diameter at 1.3 m height. At the stand level $RAI_{absorbing}$ which is analogous to and scaled with transpiring leaf area index (maximum stomatal pore area per unit ground area; $LAI_{transpiring}$) increased proportionally with basal area across the three stands. In contrast RAI_{fine} was inversely proportional to basal area. The ratio of $RAI_{absorbing}$ to $LAI_{transpiring}$ ranged from 7.7 to 17.1, giving an estimate of the relative above versus belowground resource exchange areas. $RAI_{absorbing}$ provides a way of characterising ecosystem functioning as a physiologically meaningful index of belowgound absorbing area.

Introduction

Plants acquire carbon and nutrients from the environment, which are then allocated to new tissue growth or maintenance of existing tissue (or storage). This partitioning of resources influences the efficiency of future acquisition rates of carbon and soil resources. For example, increased allocation to photosynthetically active leaf area must be supported by an increase in water supply from the soil through the absorbing root surface (Shipley and Meziane, 2002). Therefore, the ratio of absorbing root area to transpiring leaf area is of fundamental importance to plant survival (Sperry et al., 1998).

The pipe model theory predicts that a given unit of leaf area is supported by a continuation of conducting tissue of constant cross-sectional area, analogous to a pipe system (Shinozaki et al., 1964). More recent research suggests that plants adapt to hydrological pressures by differentially adjusting the cross-sectional area of xylem conducting tissue relative to their leaves (Magnani et al., 2000). However, this theory has never been extended to the belowground absorbing surface area of the roots. It has been estimated that the radial conductivity through the absorbing roots is eight orders of magnitude lower than that of the saturated conductivity of the xylem and soil (Steudle and Peterson, 1998). This may suggest that the supply of water to the leaves is predominantly controlled by the hydraulic properties of the absorbing roots (Sperry et al., 2002). Consequently, the absorbing root to leaf area ratio may provide useful insights into the way plants adapt to their environment.

Plant root systems perform a range of functions including structural support, storage, transport and absorption (Schulze et al., 1983; Körner, 1994). Conventionally, the functional components of the root system have often been differentiated according to soil depth and diameter. Coarse roots (>2 mm in diameter) are generally woody and provide mechanical support and conductive capacity to the tree (Jackson et al., 1996; Nicoll and Ray, 1996; Čermák et al., 2008). In contrast, fine roots (often defined as ≤2 mm in diameter) have been distinguished as the primary exchange surface for water and nutrients between the soil and plant, analogous to the role played by leaves for carbon and energy uptake (Hendrick and Pregitzer, 1992; Pregitzer et al., 1993, 2002; Jackson et al., 1997; Gill and Jackson, 2000). However, unlike leaves and branches, it is difficult to distinguish between absorbing and conducting (non-absorbing) roots. A recently established earth impedance (EI) method allows us to isolate the absorbing root surface area of individual trees (Aubrecht et al., 2006; Čermák et al., 2006), which has the potential to improve our understanding of water and nutrient uptake at the soil-root interface.

The EI method is based on the physical principle of electrical current continuity (Aubrecht et al., 2006). A large field trial has shown absorbing root surface area to be proportional to the cross-sectional area of aboveground conducting tissue (Čermák et al., 2006). Additionally, lab-based studies have found electrical resistance to be correlated with geometric root surface areas (Cao et al., 2010). However, it is important to establish how this method relates to the more

conventional measure of fine root area at the stand level. Therefore, the main objective of this study is to further evaluate the EI method within a Sitka spruce managed forest, making comparisons between stands of different tree densities. We will do this by establishing allometric relationships with aboveground biometric parameters and making comparisons with the geometric surface area of fine roots across different stand densities. An additional core objective is to use the EI method to evaluate the role of plantation density on ecophysiological allocation patterns of leaves and roots.

Materials and Methods

Study Site

The study was carried out during July-August 2007 at Cloich, which is part of the Forestry Commission's Glentress Forest, ~32 km outside of Edinburgh, UK, at 55°42'N, 03°16'W. The site was originally planted in 1970 with Sitka spruce *(Picea sitchensis* (Bong.) Carr.) at an average tree density of ~3000 stems per hectare (equivalent to approximately a 2 m inter-tree spacing). In early 1986, three plots of differing tree density were established by selectively thinning the existing forest to 625 and 278 stems per hectare, which corresponds to inter-tree spacings of ~ 4- and 6-m, respectively (Greens et al., 1995). This management intervention has resulted in trees with widely varying trunk diameters. These distinctive aboveground

characteristics may be supported by correspondingly distinctive belowground root distributions.

At the time of planting, the soil was prepared by ploughing the topsoil to excavate drainage trenches. The trees were planted on parallel-mounded ridges (also known as ribbons) separated by the drainage trenches. The soil on the ridges was ~15 cm deeper than the furrows. The trees in all three stands are sustained by a shallow peat (~30 cm deep in the furrows) overlaying Silurian Ordovician greywacke (Sheppard et al., 1995). There was no significant understorey in any of the plots.

Root Absorbing Area

Root absorbing area was evaluated using the EI method (Aubrecht et al., 2006). If a simple electrical circuit is established between a tree and the soil, the current will only enter (or exit) the tree through the same porous surface area used in water and nutrient uptake. From the difference in conductivity of tree tissue and the soil, we estimated the soil-root exchange surface area based on the equation:

$$S = \rho l \frac{I}{U} \tag{1}$$

where S is the total root absorption surface (m^2), ρ is the resistivity of the water conducting tissue (ohm.meters), l is the distance from the stem (m), I is the current flowing through the wood stem, root system and soil to auxiliary metal electrodes

from an external power supply (amperes), and U is the potential difference between the stem boundary and a potential electrode in the soil (volts).

We inserted six electrodes into the stem of the tree and eight soil electrodes in a 60° arch around the stem and connected them to an alternating current generator. The soil electrodes were 10 mm in diameter and inserted 20 cm into the soil to ensure a sufficient conducting surface. An auxiliary potential electrode was inserted at the base of the trunk and another in the soil at a defined distance, l, from the stem. The distance from the stem to both the current and potential soil electrodes was determined by the course of potential (voltage) characteristics. The amount of current flowing from the tree stem to the surrounding soil, via the root segment, decreases with increasing distance from the tree. This drop in voltage was mapped by progressively moving the soil potential electrode away from the stem in a radial direction. The point at which the drop in voltage plateaus is considered to be l, which corresponds to the mean distance of all the absorbing root segments of the tree.

Resistivity of the water conducting tissue (ρ_{wood}) of the roots was calculated using the four point Wenner method, where $\rho_{wood}=2\pi aR$ (Aubrecht et al. 2006). The four electrodes were inserted into the sapwood at an equal distance, a, apart. The electrical impedance, R, was measured with the electrodes 2-, 4-, and 6- cm apart and the mean was taken. Current was generated and the impedance measurements were made using a four pole Avo Megger DET 5/4D Earth/Ground Tester.

In each stand (2-, 4-, 6-m spaced trees) 6 trees were measured using the electrical impedance method. The target trees in each stand were chosen based on the quantiles of total method (Čermák et al., 2004), such that the whole range of tree sizes were covered and each tree represented approximately the same fraction of stand basal area. The measurement was repeated for four 60^{o} segments, each of which was multiplied by 1.5, and summed to estimate the whole tree root surface (360^{o}). Two segments were measured in opposite directions along rows where trees were planted, and two others were measured along perpendicular segments (across trenches), as there is reason to believe that roots preferentially grow within the ridges (Savill, 1976).

Fine Root Area

We sampled for fine root area by taking intact soil cores in each of the plots. Sampled soil cores had a diameter of 8 cm and a depth of 30 cm. Random stratified core samples were taken on the planting ridges (n=15) and in the furrows (n=15) in the 2 m spaced plot. In the 4 m spaced plot an additional 15 core samples were taken on ridges devoid of trees. Finally, in the 6 m spaced plot, a further 15 additional cores were taken in trenches surrounded by ridges with no trees. This sampling regime was applied to explore possible differences in fine root area both between treatments and within plots, which will allow us to accurately scale to the stand level. Samples were taken at 0-15 cm and 15-30 cm below the soil surface by splitting each

core into two. We carefully washed all the roots out of the soil and separated the live and dead roots based on a visual distinction in colour and resilience. Live roots ≤2 mm in diameter were then scanned dried and weighed. As there was no significant understorey we are confident that the vast majority of fine roots were produced by the large Sitka spruce trees. The roots were scanned at 600 dpi on an Epson GT 10000 A3 flat bed scanner and the images were analysed using Winrhizo^{TM} software to calculate surface area of fine roots (cm^2). We scaled root area to the plot level by multiplying the mean fine root area per unit ground area by the total area occupied by each of the sampling locations.

Coarse Root Volume

Roots of the target trees were also excavated using an air spade (Soil Pick; MBW, Slinger, Wisconsin, USA). Roots were exposed along two 30° horizontal angular sectors down to a depth of 30 cm. The centre of each sector corresponded to those measured by the EI method. The coarse root architecture of each of the target trees was mapped by measuring the root diameters (D_{tsxi}*:* Diameter of individual root *i* from tree *t*, sector *s* and distance *x*) at defined distances from the stem (50, 75, 125, 175, 250, 325 cm) using a calliper and a measuring tape anchored near the trunk.

The cross-sectional area (A_{tsxi}; m^2 of individual root *i* from tree *t*, sector *s* and distance *x*) of all the individual roots was calculated and summed at each distance for each angular sector:

$$A_{tsx} = \sum_i A_{tsxi} \quad (2)$$

For each sector a 2 or 3 degree polynomial function *f(x)* was used to link A_{ts} (m^2) with distance *x* (m). Root volume (V_{ts}, m^3) was calculated for each tree and sector, via the bounded integral of function *f(x)*:

$$V_{ts} = \int_a^b f(x)dx \quad (3)$$

a was defined as 50 cm from the stem, due to the presence of small buttresses, and *b* was the maximum radial distance of root growth from the stem. The total root volume for each tree was calculated by multiplying the two measured sectors of 30^o by 6 to account for the full 360^o of root extension.

Tree Social Area

We used a measure of social area (A_{social}, m^2) to estimate the apparent competitive environment surrounding a tree (Figure 2.3-5). Social area is a share of the stand area associated with a particular sample tree according to its size and the available surrounding space. A_{social} was calculated from Equation (4), where d_i (m) is a series of distances to nearest neighbouring trees which are weighted by the corresponding basal area of the sample tree (A_{bas_s}, m^2) and that of each neighbouring tree (A_{bas_i}, m^2) as a circular area (Čermák et al., 2006):

$$A_{social} = \pi\left(\sum_{i=1}^{n} d_i\left[\frac{A_{bas\_s}}{A_{bas\_s} + A_{bas\_i}}\right]\right)^2 \quad (4)$$

In addition projected tree crown area was calculated from field measurements and analysed using an irregular octagon approach.

Leaf Area Index (LAI)

Leaf area index (*LAI*) was estimated from a published allometric relationship between *DBH* and foliar biomass based on data from a Sitka spruce stand growing in similar conditions (Tobin et al., 2006). We applied this equation to all the trees in each of the treatment plots and summed the values to estimate the total foliar biomass in each stand. We calculated the foliar biomass per unit ground area and used a half-surface specific leaf area value of 4.48 m^2kg^{-1} to convert from foliar biomass to *LAI* (Tobin et al., 2006).

LAI accounts for the entire surface area of the leaf organ and is thus much larger than the water conducting surface area, which is determined by stomatal diameter and density (stomatal pore area). In order to make a direct comparison with our measure of root absorbing area we calculated stomatal pore area index (*SPI*), a dimensionless index of stomatal pore area per unit lamina area (Sack et al., 2003). Jeffree et al. (1971) measured the maximum possible surface area of an individual stomatal pore in Sitka spruce to be 127×10^{-8} cm^2 with 6000 pores per cm^2 across the needle lamina. Based on these measurements we calculate the *SPI* to be 7.62×10^{-3}

cm^2cm^{-2}, which we multiplied by our estimate of *LAI* to obtain the transpiring leaf area index ($LAI_{transpiring}$).

Data Analysis

Relationships between root absorbing surface area and *DBH*; stem resistivity and *DBH*; and stem/root volume and social area were determined using ordinary least squares regression analysis. Differences in the estimated parameters of the power functions for root absorbing area (EI method) fitted between soil segments that run parallel or perpendicular to the drainage trenches were determined using an analysis of covariance on linearized data (log-log transformation). Plot differences between fine root surface area were determined using a hierarchical nested analysis of variance with location (i.e. ridge or furrow with or without trees) nested within plot, to test for the effect of tree density on RAI_{fine}. Statistical tests were done in R (R Development Core Team, 2009).

Plot level coarse root volume was calculated by generating eight random neighbours for each of the sample trees from a population of 50 trees. The distances between neighbours were based on the assumption of systematically distributed grid tree spacing within each of the three plots. Equation (4) was applied to each of the 50 trees and the coarse root volume was calculated from the log-linear relationship between social area and coarse root volume (the intercept was set at the origin to avoid negative root volumes; Figure 2.3-6a).

Results

The management intervention of selective thinning resulted in distinctive tree metrics within the three treatment plots. Generally, the biometric parameters, such as tree diameter and crown projected area, were smallest in the 2 m plot and reached a maximum in the 6 m plot. In contrast, the basal area was highest in the 2 m plot and lowest in the 6 m plot. The thinning treatment has resulted in progressively fewer but larger trees (Table 2.3-1).

Using the EI method we found that trees with diameters in the range of 15-50 cm had absorbing root surface areas in the range of 4-10 m^2 (Figure 2.3-1). Within the range of trees that we measured, the relationship between *DBH* and absorbing root surface area was linear. However, a fitted non-linear power function (Figure 2.3-1) allowed the predicted values of the model to approach the origin. Given the high variance in absorbing root surface area, the effect of the curvature is small. In contrast, a linear model has a *y*-intercept of 2.6 m^2, thus overestimating the root absorbing area for small trees. Consequently, we applied the power function to our tree inventory data in order to extrapolate the total root absorbing area to the stand level. We used this measure of root area to estimate the absorbing root area index ($RAI_{absorbing}$). $RAI_{absorbing}$ ranged from 0.28 $m^2\ m^{-2}$ in the 6 m spaced plot to ~1.11 $m^2\ m^{-2}$ in the 2 m spaced plot (Table 2.3-1). These values are substantially lower in magnitude than the range in *LAI* (4.8-8.5 $m^2\ m^{-2}$). However, $RAI_{absorbing}$ is more closely analogous to and scales with $LAI_{transpiring}$, which represents 0.8% of the total

estimated *LAI* (Table 2.3-1). $LAI_{transpiring}$ ranged from 6.5×10^{-2} in the 2 m spaced plot to ~3.7×10^{-2} in the 6 m spaced plot. The resulting $RAI_{absorbing}$: $LAI_{transpiring}$ ratios fall in the range of 7.7-17.2, which is a functionally descriptive estimate of the relative aboveground versus belowground resource-capturing ability. The values are an order of magnitude greater than those for the RAI_{fine}:*LAI* ratio (0.7-1.6).

There was significantly more root absorbing surface area in segments that ran along ridges created by the drainage furrows ($p<0.01$). This distinction is the expression of a significantly different estimate of the power or allometric parameter, b in the power law function, $y=ax^b$ ($p<0.01$). That is, the proportional change in absorbing root surface area associated with *DBH* is distinct between segments that were oriented parallel to the drainage channels and those perpendicular to the drainage trenches (Figure 2.3-2). The observed difference is more pronounced for larger trees, indicating that there is continual preferential growth along ridges or ribbons as the trees mature. Additionally, we found the resistivity of the water-conducting tissue (ρ in Equation (1)) to be a negative power function of *DBH* (Figure 2.3-3) within the range of data ($p<0.01$, $r^2= 0.64$).

Table 2.3-1: A comparison of above and belowground resource capturing areas of three Sitka spruce (*Picea sitchensis*) stand of differing tree densities. Measurements of stand structure (including coarse root volume) show distinct biomass allocation patterns. Belowground resource capturing area is expressed as root area index, *RAI* (root area per unit ground area). RAI_{fine} is estimated from fine root excavation and geometric calculation, $RAI_{absorbing}$ is estimated from earth impedance method. Where applicable we report the standard errors. **a** and **b** indicate statistical distinction at the 5% level (where applicable).

	2 meter plot	4 meter plot	6 meter plot
Tree density [Stems ha^{-1}]	3000	625	278
Basal Area [A_{bas}, m^2ha^{-1}]	71.43	55.56	50.69
Mean diameter at breast height [cm]	19.9 (±0.69)	29.0 (±0.99)	42.3 (±1.06)
Mean crown projected area [m^2]	6.2 (±0.47)	15.9 (±1.16)	39.0 (±2.28)
Fine root area index [RAI_{fine}, m^2m^{-2}]	5.56 **a** (±0.44)	7.13 **b** (±0.57)	7.55 **b** (±0.54)
Absorbing root area index [$RAI_{absorbing}$, m^2m^{-2}]	1.11	0.50	0.28
Leaf area index [*LAI*, m^2m^{-2}]	8.5	5.8	4.8
Transpiring leaf area index [$LAI_{transpiring}$]	6.5×10^{-2}	4.4×10^{-2}	3.7×10^{-2}
RAI_{fine}*:LAI* ratio	0.7	1.2	1.6
$RAI_{absorbing}$:$LAI_{transpiring}$ ratio	17.1	11.3	7.7
Social area [A_{social}, m^2]	4.84 (±0.21)	19.51 (±0.43)	43.99 (±0.55)
Coarse root Volume [m^3ha^{-1}]	33.67	38.44	22.11
Absorbing root area per unit coarse root volume [m^2m^{-3}]	331.22	129.65	124.48

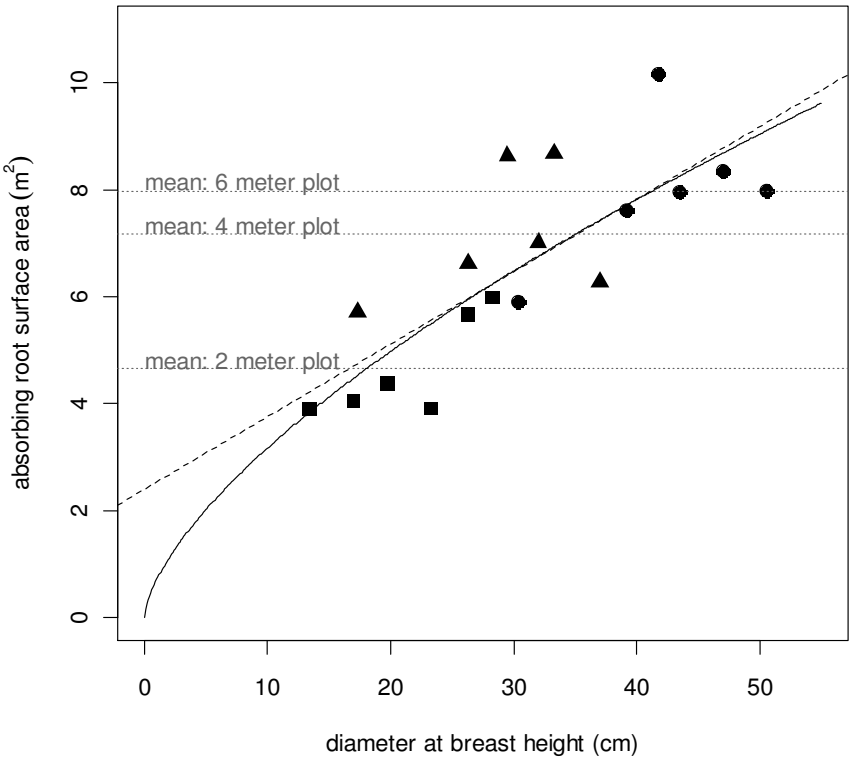

Figure 2.3-1: Absorbing root surface area of Sitka spruce (*Picea sitchensis*). Relationship between diameter at breast height and absorbing root surface area derived from the impedance method in 3 treatment plots (2 (■), 4 (▲) & 6 (●) meter spacing between trees). Both a linear ($y=2.4+0.14x$, R^2=0.60, p-value<0.01), and a power function ($y=0.7x^{0.65}$, R^2=0.67, p-value<0.01) was applied to the data.

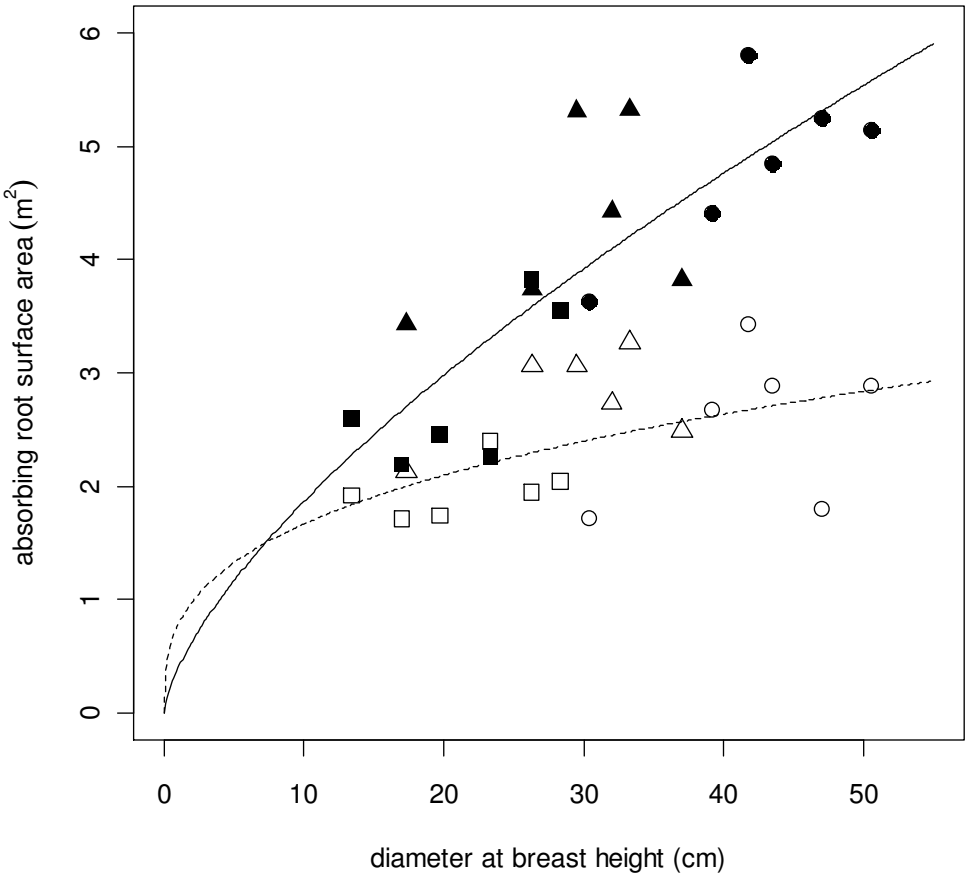

Figure 2.3-2: Comparison of absorbing root surface area of Sitka spruce (*Picea sitchensis*) based on earth impedance method. Measurements were taken parallel (solid symbols) and perpendicular (clear symbols) to drainage channels in 3 treatment plots (2 (■,□), 4 (▲,Δ) & 6 (●,○) meter spacing between trees). The stem segments (120 deg) parallel to the drainage channels are fitted by $y=0.39x^{0.68}$ (R^2=0.65, p-value<0.01). The stem segments (120 deg) perpendicular to the drainage channels are fitted by $y=0.78x^{0.3345}$ (R^2=0.22, p-value<0.05) (R development core team, 2008).

Calculations of mean RAI_{fine} from core samples, ranged from 5.56 m^2m^{-2} in the 2 m spaced plot to 7.55 m^2m^{-2} in the 6 m spaced plot (Table 2.3-1). There was a significant difference between the 2 m plot and both the 4- and 6-m plot. Though

there appears to be a slight negative trend with basal area, there was no significant difference between the 4- and the 6-m spaced plots (Table 2.3-1). Including the location where each core sample was taken (i.e. ridge or furrow with or without trees present), nested within each individual plot, significantly increased the explanatory power of the model (p<0.01, r^2=0.13; Figure 2.3-4).

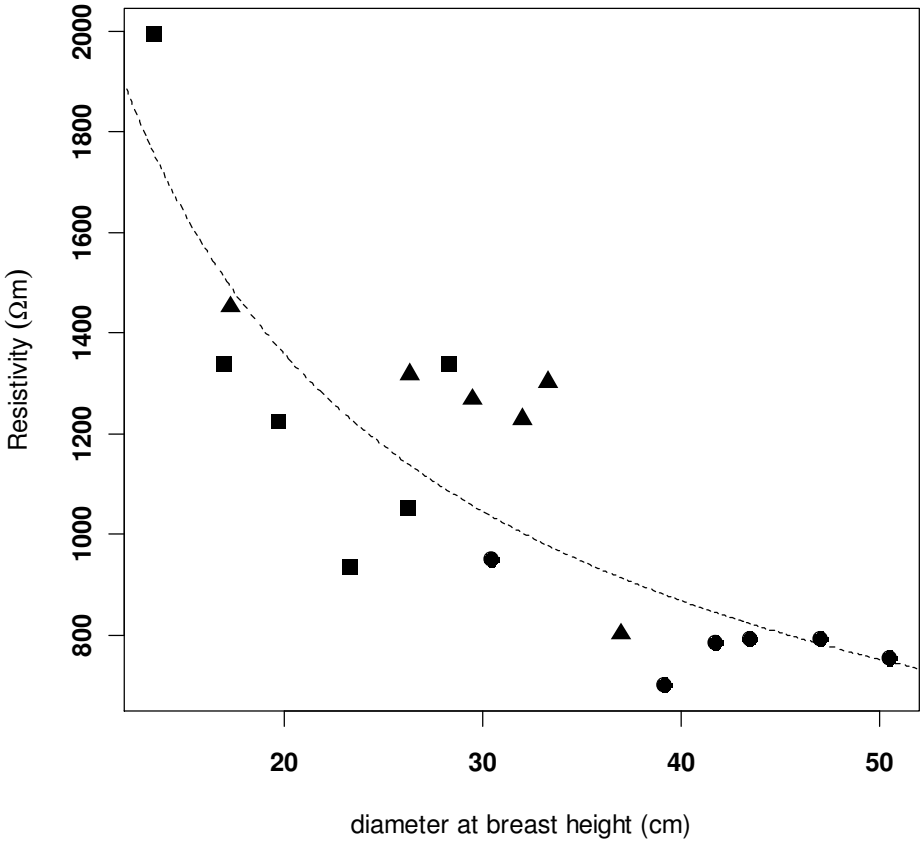

Figure 2.3-3: Resistivity of water conducting tissue as a function of diameter at breast height of Sitka spruce (*Picea sitchensis*) across 3 treatment plots (2 (■), 4 (▲) & 6 (●) meter spacing between trees). The fitted curve is a power function: $y=2204.6x^{-0.63}$ (R^2=0.64, p-value<0.01).

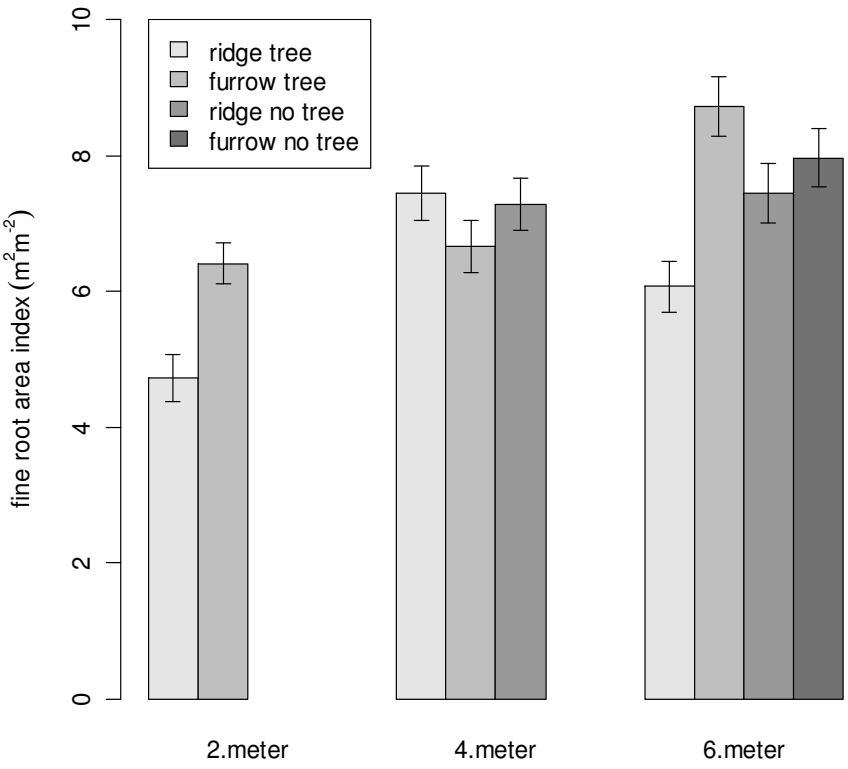

Figure 2.3-4: Fine root area index, based on surface area of root less than 2 mm in diameter, across all plots (2-, 4- and 6-m spacing between trees) and locations (error bars represent standard errors).The 2-m plot is significantly distinct from the 4- and 6-m plot (p-value<0.05)

We used social area as a measure of the competitive environment of individual trees, which can be compared with projected crown area (Figure 2.3-5). Our mean estimates for social area for a sample of 50 trees within each plot were: 4.8, 19.5, and 45 m^2 for the 2-, 4-, and 6-m plots respectively (Table 2.3-1). This shows that the trees in the 6 meter plot experience less competitive pressure despite the presence of larger neighbours.

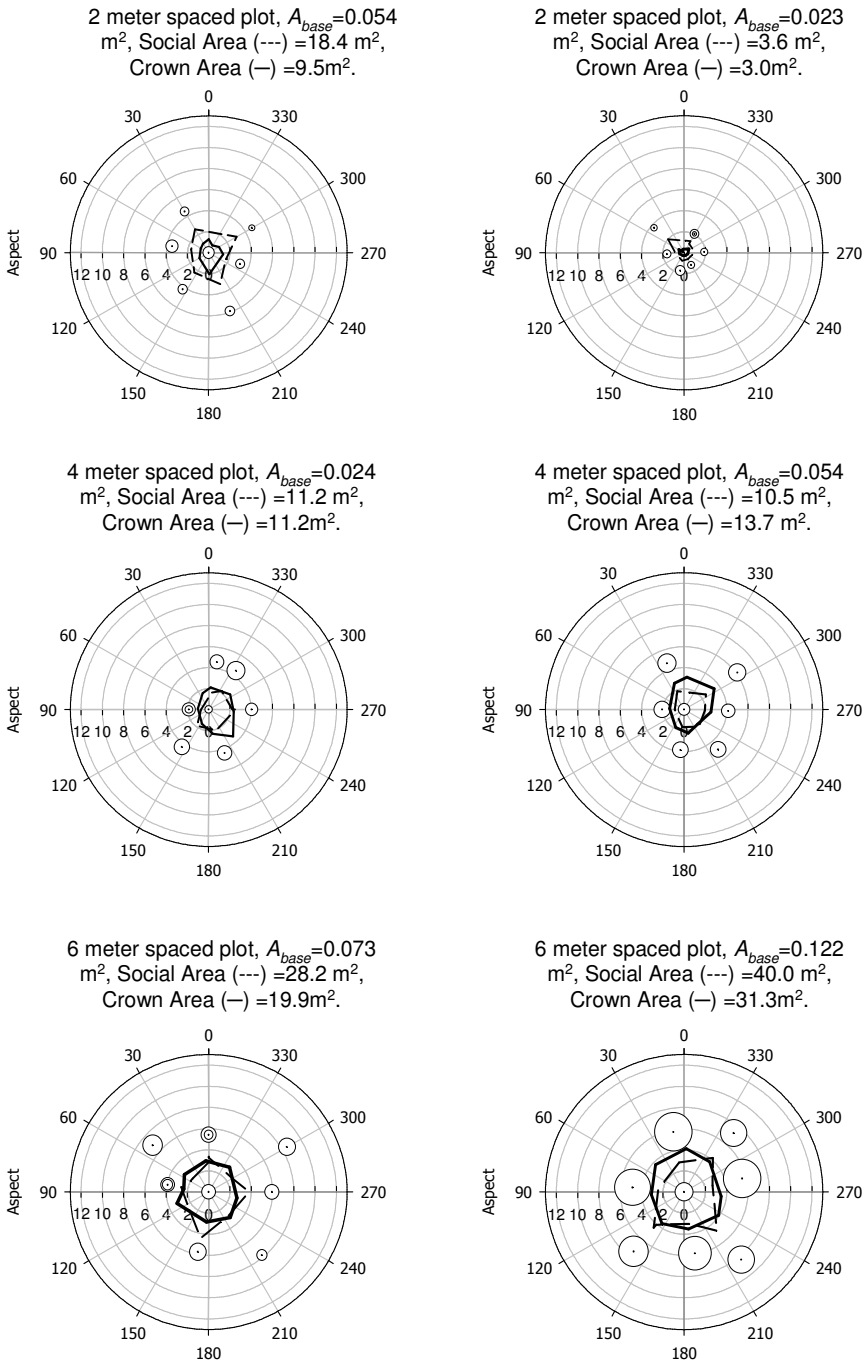

Figure 2.3-5: Spatial representation of six individual sample trees and their nearest neighbours from three differentially spaced Sitka spruce plots (2 meter, 4 meter and 6 meter). Tree location and basal area is represented by - ⊙. Social area of target trees are calculated according to Equation (4) (Čermák et al. 2006) and are represented by broken lines. Crown area is represented by the solid line.

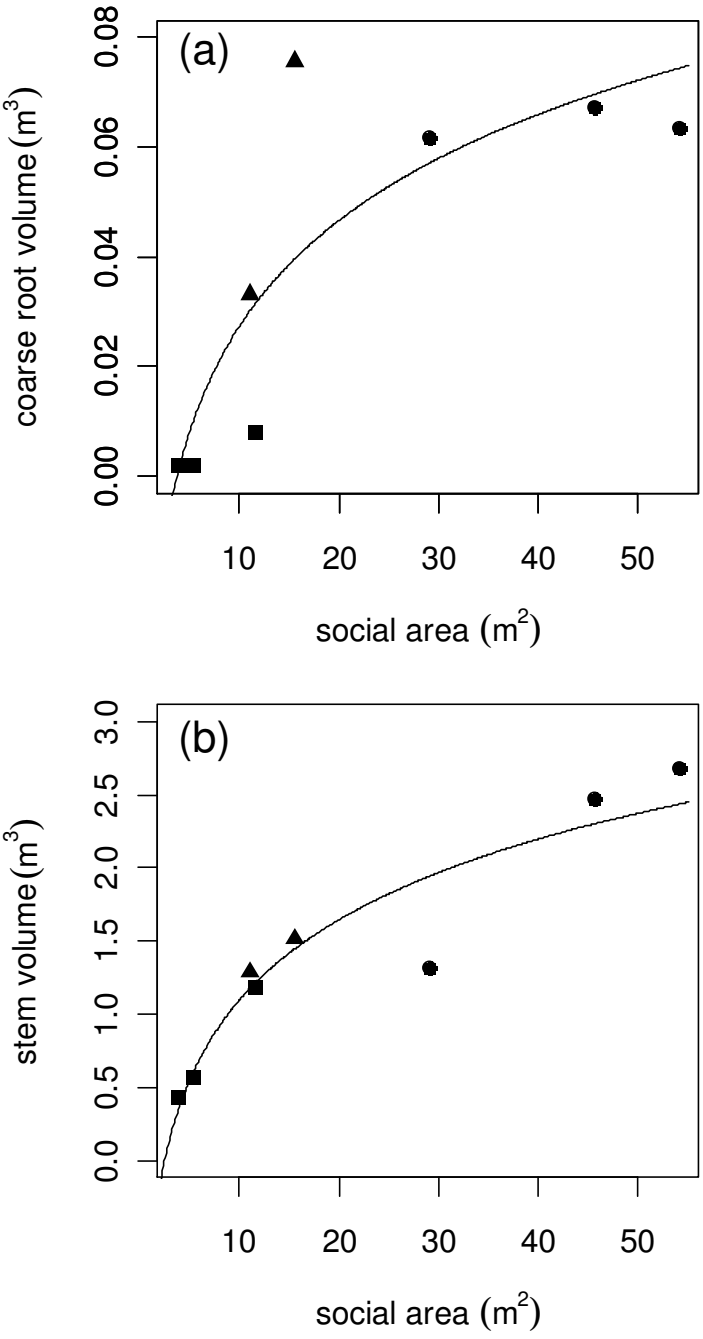

Figure 2.3-6: (a) Relationship between root volume and social area of individual Sitka spruce (*Picea sitchensis*) trees. The trend line is a logarithmic relationship V_{coarse_root} = 0.028Log$_e$(A_{social}) - 0.037 (R^2=0.71, *p*-value<0.01). **(b)** Relationship between shoot volume and social area of individual Sitka spruce (Picea sitchensis) trees. The trend line is a logarithmic relationship V_{coarse_root} = 0.7961Log$_e$(A_{social}) - 0.7391 (R^2=0.87, *p*-value<0.01). Symbols represent the 2 (■), 4 (▲) & 6 (●) meter spacing between trees.

The coarse root network was evaluated as each individual plant's investment in the total volume of coarse roots (for practical purposes, defined as roots ≥5 mm in diameter). The coefficients of determination for the polynomial fits *f(x)* used to link radial root area ($A_{ts,}$ m^2) with distance (*x,* m) within Equation (3), were fairly high (mean r^2=0.85). Social area accounts for ~71% of the variation in root volume investment (Figure 2.3-6a). This relationship appears to plateau as social area increases above ~30 m^2**.** The aboveground stem volume shows a similar relationship (Figure 2.3-6b) indicating a proportional investment in aboveground and belowground tissue. At the stand level, the proportion of absorbing root area per unit coarse root volume declines with reduced tree density (Table 2.3-1).

Discussion

For the most part, field studies of root systems have failed to address their resource capturing ability. Here, we use an EI method to measure the absorbing root surface area. The results from our study show a strong correlation between absorbing root surface area and *DBH* (Figure 2.3-1), and also show good agreement with measurements made on Norway spruce (*Picea abies*) (Čermák et al., 2006). The observed trend is in accordance with conventional hydraulic theory where a given unit of sapwood area would be expected to be supported by a proportional amount of absorbing root surface area (Sperry et al., 1998).

We observed a distinct asymmetry in the development of the root system around individual trees. The method of spaced-furrow ploughing is known to restrict root development, with roots preferentially proliferating along the lines of the ploughed ridges (Savill, 1976). This differential development of the root system is expressed in the amount of root absorbing surface area that was measured in segments along ridges and those across ridges. This disparity was more pronounced in the larger trees with a maximum discrepancy of ~3 m^2 of absorbing root surface area in the largest trees (Figure 2.3-2).

Conventionally it has been assumed that fine roots are the functional equivalent of leaves in their ability to capture resources. This idea is complicated by the ambiguous definitions used for fine roots, having been classified by various authors anywhere in the range of <1mm to as much as <5mm in diameter (Persson et al., 1995; Pregitzer et al., 1998; Vanninen and Makela, 1999). Here we quantified a measure of root area index (m^2 root area per unit ground area) based on fine root excavation (RAI_{fine}) and our estimates across the three plots (Table 2.3-1) correspond well to global estimates in temperate coniferous forests and boreal forests of 11 and 4.6 m^2m^{-2} respectively (Jackson et al., 1997). These estimates are comparable in magnitude to *LAI*, with the ratio of RAI_{fine}:*LAI* ranging from 0.7 to 1.6 (Table 2.3-1). RAI_{fine} was significantly lower in the 2 m plot relative to the other two study plots, despite having the largest basal area, which conflicts with the requirement for a correlation between the hydraulic conducting surface areas of the roots and stem. The

traditional approach of inferring root physiological function based on arbitrary size classification has been questioned before (Pregitzer, 2002). The widely held assumption that all roots of a given size class (fine roots) function in the same way in terms of water and nutrient uptake may not be true, and consequently, measurements of RAI_{fine} may be misleading in this context. Furthermore, there is evidence to suggest that the absorbing surface area of roots is only represented by a short zone (≈ 100–200 mm) behind the root tip (Steudle, 1994). Consequently, any inconsistency in the ratio of fine root biomass to number of root tips will introduce error into the measurements and interpretation of fine root surface area.

In contrast $RAI_{absorbing}$ (based on the EI method) was proportional to basal area across the three stands, ranging from 0.28 $m^2 m^{-2}$ in the 6 m spaced plot to ~1.11 $m^2 m^{-2}$ in the 2 m spaced plot (Table 2.3-1). Interestingly, $RAI_{absorbing}$ was not directly proportional to RAI_{fine}, with the absorbing component accounting for between 3.7 and 19.6% of the total fine root area (Table 2.3-1). This outcome probably reveals differences in the proportion of total fine root surface area that is used for nutrient and water uptake, although independent measures of the absorbing zone of the fine roots of each tree would be needed to explore this further.

Our measure of $RAI_{absorbing}$ is analogous to $LAI_{transpiring}$, which is the proportion of the total *LAI* accounted for by the *SPI*. Functionally, *SPI* has been shown to correlate well with the hydraulic conductance of the leaf lamina (Sack et al., 2003). The ratios of $RAI_{absorbing}$:$LAI_{transpiring}$ observed here may indicate a

comparatively higher root absorbing surface area with respect to stomatal pore area, possibly to compensate for dry non-conductive zones that may develop in the rhizosphere (Newman, 1969; Bristow et al., 1984; Sperry et al., 1998).

Electrical resistance (R, Ω) of an object (such as a tree stem) is dependent on tree height (h), stem cross-sectional area (A_{bas}), and the nature of the water-conducting tissue or resistivity, (ρ, Ωm) in Equation (5):

$$R = \frac{\rho h}{A_{bas}} \qquad (5)$$

Resistivity is a material specific constant, at a given temperature. Therefore, we would expect the observed differences in resistivity to be attributed to differences in the xylem structure, assuming constant temperature. The smaller trees have the highest electrical resistivity of the water conducting tissue (Figure 2.3-3). This is likely to be associated with differences in stem density. It is well understood that the space available for the growth of a tree will affect the characteristics of its woody tissue, with high stand densities yielding more dense wood (Brazier, 1970; Petty et al., 1990). Furthermore, the basic density of Sitka spruce wood depends primarily on tracheid diameter relative to wall thickness (Mitchell and Denne, 1997). This suggests that the trees in the 2 m plot will generally have thinner tracheids which are associated with lower cavitation risk, and consequently, low hydraulic conductivity. Accordingly, the higher $RAI_{absorbing}$:$LAI_{transpiring}$ ratio observed in the 2-m plot may correspond to lower plant hydraulic conductivity. This relationship is supported by

modelled predictions of root:leaf area ratios, with higher ratios corresponding to low soil and xylem conductivity (Sperry et al., 1998).

The conducting root system functions to mobilize soil resources across the soil profile, because unlike the atmosphere, the soil experiences little mixing (Carvalheiro and Nepstad, 1996). The network of coarse conducting roots of individual trees, measured as root volume, varies in accordance with the competitive environment (social area) (Figure 2.3-6a). It is well established that both competition and resource availability influence biomass allocation during tree growth (Gersani and Sachs, 1992; Reynolds and Pacala, 1993; Belcher et al., 1995; Maliakal et al., 1999). As tree density decreases, each individual tree will have more resources (both light and soil resources) available. Therefore, as social area increases, individual plants are more productive both aboveground and belowground. However, at large separation (large social areas) both these relationships plateau (Figure 2.3-6).

Hydraulic constraints associated with increasing tree height may account for a reduced investment in stem tissue (Schafer et al., 2000; Koch et al., 2004; Niklas, 2004). In contrast, root proliferation may be constrained by diminishing marginal returns (Bloom et al., 1985), assuming that a benefit is accured by maximising leaf area and stomatal conductance while minimising root biomass (Sperry et al., 1998; Shipley and Meziane, 2002). Mechanical constraints (e.g. increased wind loading) on trees with reduced density and increased crown dimensions may also contribute to additional investment in structural root architecture (Greens et al., 1995; Nicoll and

Ray, 1996). Furthermore, root efficiency can be determined by the differences between an individual's nutrient and water uptake, and the cost of growth and maintenance of servicing roots (Gersani et al., 2001). Consistent with these ideas, the efficiency of belowground investment can be illustrated in our data by the amount of absorbing root area per unit coarse root volume (Table 2.3-1). Our results demonstrate that, as the tree density decreases across the plots, every additional unit of absorbing root area is supported by a proportionally greater investment in coarse conducting roots (Table 2.3-1), rendering further investment progressively less efficient.

Conclusions

Conventionally, fine roots (commonly defined as being ≤2 mm in diameter) have been thought to function as the pathway for water and nutrient uptake by plants, analogous to the role that leaves play for carbon and energy uptake (Jackson et al., 1997; Pregitzer et al., 2002). Consequently, an accurate and physiologically meaningful measure of root area index is of fundamental importance in establishing a functional understanding of energy exchange and nutrient cycling. Despite the fundamental role that roots play in global biogeochemical cycles, they are poorly represented in global models relative to their foliar counterparts (Woodward and Osborne, 2000). Leaf area facilitates accurate simulation of carbon and energy gain

in terrestrial models. In a similar way, root area, measured using the EI method, may provide physiologically meaningful data for simulating soil resource acquisition.

The inherent difficulties in conducting studies with an integrated approach to the plant-soil continuum have dramatically hindered our understanding of this functional association (Högberg and Read, 2006). Here, we express a physiologically relevant estimate of *RAI* ($RAI_{absorbing}$), which is fundamental to our understanding of roots as functional plant organs. This variable has considerable potential to improve our efforts of modelling water and nutrient uptake. Additionally, comparison between leaf and root areas as resource capturing organs will improve our understanding of the functionally important exchange surfaces between plants and their environment.

2.4 Absorbing root areas and transpiring leaf areas at the tropical forest and savanna boundary in Brazil

Submitted to *Trees: Structure and Function*

Abstract

Plants capture essential resources for growth via absorbing surfaces on both roots and leaves. As a result, the allocation of assimilates to these resource exchange surface areas are of fundamental importance to plant growth and survival. Previous work on tropical forests and savanna vegetation has mainly focused on broad root:shoot biomass ratios. Yet, uptake of CO_2 (leaves), water and nutrients (roots) is a surface area phenomenon. In this study we compared the root:leaf ratio of the active absorbing area at the ecosystem scale, within eight structurally diverse stands, that were chosen to characterise the transition between the Amazonian forest (closed canopy) and Brazilian Cerrado (savanna). We use an earth impedance method to quantify the absorbing root area index ($RAI_{absorbing}$) at each site, and compare these measurements to the more widely used fine root area index (RAI_{fine}). Surprisingly, we found that $RAI_{absorbing}$ and RAI_{fine} were not correlated, leading us to conclude that the two measurements are not direct substitutes. Additionally, we compared both measures of *RAI* with the leaf area index (*LAI*) in these contrasting ecosystems. The resulting RAI_{fine}:*LAI* ratio (R^2=0.85) was inversely proportional to basal area, with the highest values in the savanna vegetation. On the other hand, the $RAI_{absorbing}$:*LAI*

ratio showed an opposite trend with basal area (R^2=0.83), with highest values in the forest. We suggest this paradox may reflect different growth patterns by plants to access adequate water and nutrient resources.

Introduction

Plants are capable of adjusting the relative size and distribution of organ systems, such as stems, leaves and roots, in response to changes in resource availability and disturbance regimes (De Castro and Kauffman, 1998; Magnani et al., 1998). As resources are generally partitioned either aboveground (with respect to carbon dioxide and light) or belowground (with respect to the availability of water and nutrients), it is thought that plants adjust their biomass partitioning to counterbalance the relative abundance of aboveground and belowground resources (Robinson, 1986; Johnson and Thornley, 1987; Gedroc et al., 1996). These adjustments are a functional response, which determine the efficiency of future resource acquisition. This theory of optimal partitioning has been used to explain distinct root:shoot ratios between forests and woody savannas (Reynolds and Pacala, 1993; Belcher et al., 1995). For example root:shoot ratios in Brazilian woody savannas (Cerrado) range from 2.9-7.7 (De Castro and Kauffman, 1998), while tropical dry forests have significantly lower ratios in the range 0.42-0.84 (Murphy and Lugo, 1986; Castellanos et al., 1991). These distinct biomass allocations in turn result in

contrasting vegetation structures which are thought to be associated with physiological adaptations to their contrasting environments.

Root:shoot ratios have often been interpreted as a differential investment of photosynthetically fixed carbon between above and belowground organs to maximise acquisition of limiting resources (Titlyanova et al., 1999). However, roots are known to perform a range of functions including structural support, storage, transport and absorption (Schulze et al., 1983). Acquisition of resources only occurs only through the absorbing surface area, which may not be strongly related to biomass (Butler et al., 2010). Therefore, the root:shoot biomass ratio may only be a coarse indicator of physiological processes. In contrast, the partitioning between actively absorbing roots and transpiring leaves is functionally more informative, especially with respect to maintaining an efficient water balance (Shackleton et al., 1988; Litton et al., 2003; Butler et al., 2010)

Quantifying the belowground resource capturing ability of terrestrial vegetation remains a major challenge in ecosystem science. Conventionally, it is thought that fine roots represent the absorbing surfaces for both water and nutrient uptake (Hendrick and Pregitzer, 1992; Pregitzer et al., 1993; Gill and Jackson, 2000). Accordingly, the belowground resource exchange surface area has previously been measured as the live fine root area index (RAI; surface area of fine roots per unit ground area). Resulting global estimates of RAI range from 4.6 in boreal forests to 42.5 in tropical grasslands and savannas (Jackson et al., 1997). However, in recent

methodological advancements electrical impedance spectroscopy has been used to provide a direct estimate of the area of root surface which is in physiological contact with the soil (Aubrecht et al., 2006; Čermák et al., 2006). This method has the potential to provide an independent measure of RAI, allowing us to explore the links between biomass allocation and the physiological function of root systems (Butler et al., 2010).

The main objectives of this study was to compare the absorbing root area and leaf area of different vegetation types characterising the transition zone between the Amazonian forest and the Brazilian Cerrado. We quantified and compared RAI estimates using both the earth impedance method, and live fine root surface area. We then contrasted these estimates with the analogous aboveground measure of leaf area index (LAI) across eight structurally contrasting stands. We evaluated the role of vegetation structure and density on ecophysiological allocation patterns of leaves and roots.

Materials and Methods

Study Site

The study area was located in the northeast region of the state of Mato Grosso, Brazil, within the municipalities of Nova Xavantina and Ribeirão Cascaliera (Table 2.4-1). The region is classified as an area of 'ecological tension' in the transition

zone between savanna (*cerrado*) and dry forest (*floresta estacional*) on the *Mapa de Vegetação do Brasil* (IBGE, 1993). The climate is characterised by a seasonal rainfall pattern, with close to no precipitation for three consecutive months of the year (Figure 2.4-1). We chose eight locations representing two main vegetation types, savanna and dry forest, growing on a variety of soil types (Table 2.4-2). The study sites spanned a broad vegetation gradient with a basal area between 3.22 and 28.47 m^2ha^{-1} and a mean tree height between 5.6 and 18.4 meters (Table 2.4-3). The three most dominant species for each of the study sites are listed in Table 2.4-1. All the plots had dominant woody vegetation of both trees and shrubs with very limited grass cover.

Seven one hectare (100 × 100 m) and one previously established 0.6 hectare plots were surveyed (Table 2.4-2). Four of the plots were located within the municipality of Nova Xavantina and four within the municipality of Ribeirão Cascaliera. A detailed inventory of the vegetation was carried out on all the trees larger than 10 cm diameter at breast height (*DBH*; 1.3 m). The species, *DBH* and crown diameter (two perpendicular measurements) were recorded for each tree in the plot. All measurements were taken in April 2007, at the end of the wet season when root biomass is expected to be at its maximum.

Table 2.4-1: Names of the three most dominant species from each study site.

Plot	Vegetation Type (Classification)	Dominant species
1	Cerrado *sensu stricto* (savanna)	*1. Qualea parviflora* *2. Davila eliptica* *3. Ropala Montana*
2	Cerradão (savanna)	*1. Hertella glandulosa* *2. Sclerolobium paniculatum* *3. Xylopia aromatic*
3	Evergreen mono-dominant (*Brosimum*) forest	*1. Brosimum rubescens* *2. Amaioua guianensis* *3. Cheiloclinium cognatum*
4	Dry deciduous forest	*1. Cheiloclinium cognatum* *2. Amaioua guianensis* *3. Tetragastris altissima*
5	Cerrado *sensu stricto* (savanna)	*1. Emmotum nitens* *2. Pouteria ramiflora* *3. Mouriri elliptica*
6	Cerradão (savanna)	*1. Xylopia sericea* *2. Mezilaurus crassiramea* *3. Pterodon pubescens*
7	Cerrado aberto (savanna)	*1. Mezilaurus crassiramea* *2. Eugenia dysenterica* *3. Bowdichia virgiliodes*
8	Dry deciduous forest	*1. Amaioua guianensis* *2. Soloanea simemariensis* *3. Cheiloclinium cognatum*

Absorbing Root Surface Area

Root absorbing area was quantified using an electrical impedance (EI) method (Aubrecht et al., 2006; Čermák et al., 2006; Butler et al., 2010). When a simple electrical circuit is established between a tree and the soil, current passes across the tree-soil interface through the same channels used for water and nutrient uptake

(Figure 2.4-2). From the difference in conductivity of the water-conducting tissue of the tree and the soil, we can estimate the soil-root exchange surface area (Equation 1).

$$S = \rho l \frac{I}{U} \quad (1)$$

where S is the total root absorbing surface area (m^2), ρ is the resistivity of the water conducting tissue (Ωm), l is the distance from the stem (m), I is the current (Amps) flowing between the tree and soil to auxiliary metal electrodes from an external power supply, and U is the potential difference between the stem boundary and a potential electrode in the soil (Volts).

Following established methods (Aubrecht et al., 2006; Čermák et al., 2006; Butler et al., 2010), we inserted between four and six (depending on the size of the tree) electrodes into the stem of the tree and ten soil electrodes in a 60° arc around the stem and connected them to an alternating current generator. The soil electrodes were 10 mm in diameter and inserted 20 cm into the soil to ensure a sufficient conducting surface. An auxiliary potential electrode was inserted at the base of the trunk and another in the soil at a defined distance, l, from the stem. The distance from the stem to both the current and potential soil electrodes was determined by the course of potential (voltage) characteristics. The amount of current flowing from the tree stem to the surrounding soil via the root segment decreases with increasing distance from the stem. This drop in voltage was mapped by progressively moving

the soil potential electrode away from the stem in a radial direction. The point at which the drop in voltage reached a plateau is considered to be *l*, which corresponds to the mean distance of all the absorbing root segments of the tree.

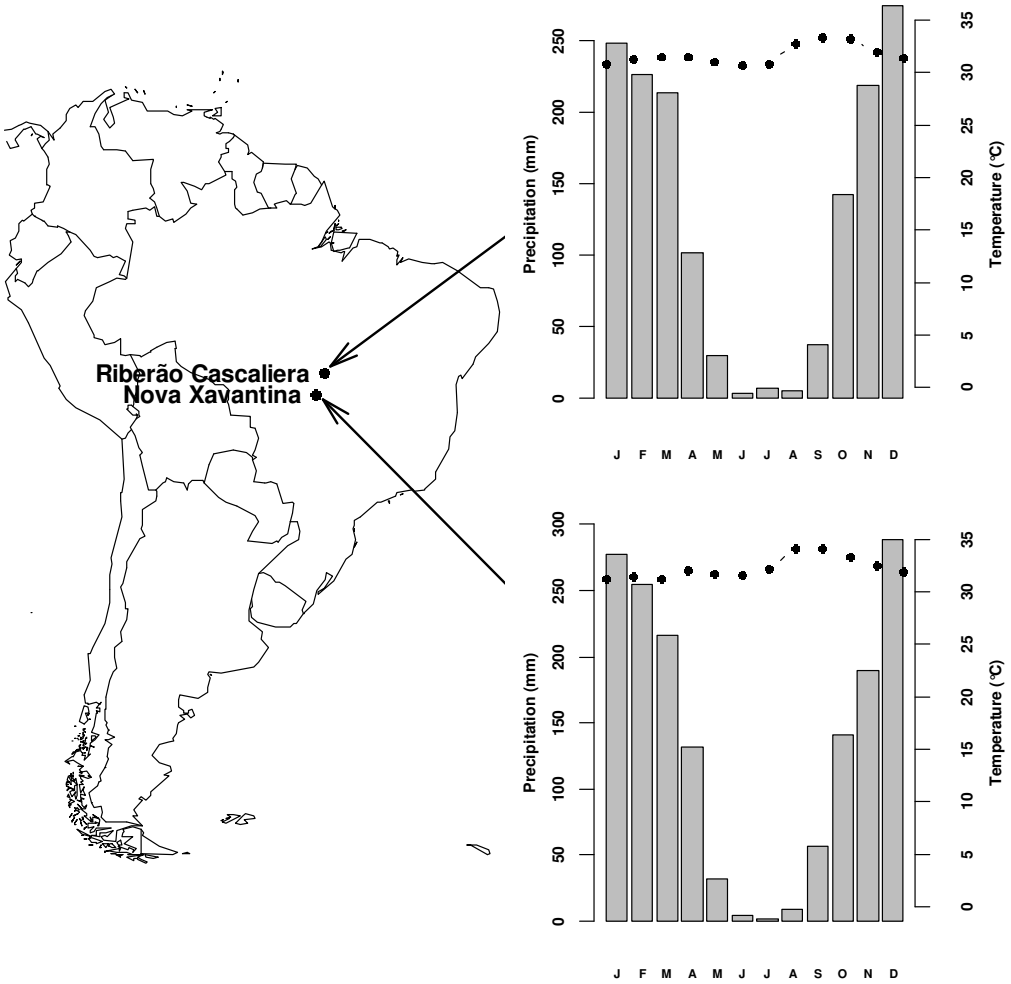

Figure 2.4-1 Geographical location of the study areas and mean monthly maximum temperature (circles) and precipitation (bars) (data obtained from WorldClim).

Table 2.4-1: Plot location and meteorological information

Plot	Vegetation Type (Classification)	Location (nearest town)	Latitude	Longitude	Mean Annual Precipitation (mm)	Mean Precipitation of the Wettest Quarter (mm)	Mean Precipitation of the Driest Quarter (mm)
1	Cerrado *sensu stricto* (savanna)	Reserva Biológica, Municipal Mário Viana (Nova Xavantina)	14°71'S	52°35'W	1508	747	16
2	Cerradão (savanna)	Reserva Biológica, Municipal Mário Viana (Nova Xavantina)	14°70'S	52°35'W	1508	747	16
3	Evergreen mono-dominant (*Brosimum*) forest	Fazenda Vera Cruz (Nova Xavantina)	14°83'S	52°16'W	1516	754	16
4	Dry deciduous forest	Fazenda Vera Cruz (Nova Xavantina)	14°83'S	52°17'W	1512	754	16
5	Cerrado *sensu stricto* (savanna)	Fazenda Santa Marta (Ribeirão Cascaliera)	12°82'S	51°77'W	1603	820	16
6	Cerradão (savanna)	Fazenda Santa Marta (Ribeirão Cascaliera)	12°82'S	51°77'W	1603	820	16
7	Cerrado aberto (savanna)	Fazenda Santa Marta (Ribeirão Cascaliera)	12°83'S	51°77'W	1599	818	16
8	Dry deciduous forest	Fazenda Floresta (Ribeirão Cascaliera)	12°81'S	51°85'W	1613	826	16

The resistivity of the water conducting tissue (ρ_{wood}) of the roots was calculated using the four point Wenner method, where $\rho_{wood}=2\pi aR$ (Aubrecht et al. 2006). The four (or six) stem electrodes were inserted into the sapwood at an equal distance, a, apart. The electrical impedance, R, was measured with the electrodes 2, 4, and 6 cm apart and the mean was taken. Current was generated and impedance measurements were made using a Earth/Ground Tester (Model 1623, Fluke, Utah, USA).

A minimum of 12 trees were measured within each plot using the electrical impedance method. The target trees were chosen from a stratified random sampling method based on diameter sizes classes. Due to methodological complications trees only single stem trees were measured. Measurements were repeated for two 60^{o} segments (Figure 2.4-2) which were multiplied by three to estimate the whole tree root surface (360^{o}). Two segments were measured in the opposite directions of North and South. For each of our target trees we recorded: species, *DBH*, height of the first branch, tree height and crown cover (based on longest and shortest crown diameters).

Fine Root Area

We measured fine root area by taking 15 intact soil cores in each of the 8 plots. Each core had a diameter of 8 cm and a depth of 30 cm. We carefully washed all the roots out of the soil and separated the live and dead roots based on visual distinction in colour and resilience. For each plot, a subsample of live fine roots (≤2 mm in

diameter) were scanned, dried and weighed. The images from the scans where then analysed using the WinRhizo software to calculate the surface area of fine roots (cm^2). The resulting relationship with the sample weights were used to estimate the total surface area of the remaining samples. We calculated the fine root area index (RAI_{fine}) as the surface area of fine roots per unit ground area.

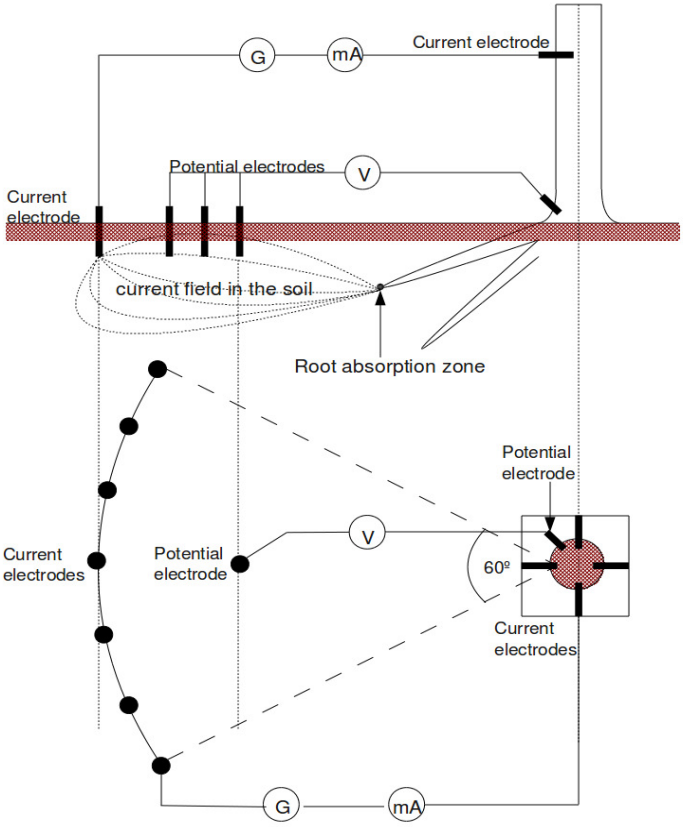

Figure 2.4-2: Diagramatic representation of the earth impedance method. *G* is an alternating current generator, *mA* is a milliammeter, *V* is a voltmeter.

Leaf Area Index

Images of the canopy were taken from the ground, at a height of 1m, with an upward-viewing digital camera and hemispherical lens (Nikon Coolpix 900, Nikon Corporation, Japan) at 25 locations within each plot (Breda, 2003). Images were always taken in the late afternoon with the bottom of the camera facing north, in the absence of direct sunlight. The images were then analyzed with image analysis software (Gap Light Analyser, ring 5, GLA). For the forest plots we calculated *LAI* (m^2m^{-2}) directly using the GLA software. However, the assumptions of this method are not consistent with the fragmented canopy structure found in savanna environments. Therefore, we used published values of leaf area per unit crown area within similar cerrado vegetation (Hoffmann et al., 2005). Canopy cover for the savanna plots was measured using the GLA software. Subsequently, to obtain an estimate of overall *LAI*, the leaf area per unit crown area was multiplied by the total canopy cover.

Stomatal Area

We measured the stomatal dimensions of the five most dominant species based on their importance value (IV), within all the plots located in the Nova Xavantina municipality. Species which presented difficulties in visualising the stomata were

excluded from the study and the next most important was taken. Each species was represented by a sample of two sun leaves from five individuals. Stomatal density, *D*, and guard cell lengths, *L*, were determined using an optical microscope (Carl Zeiss Microlmaging GmbH 37081 Gottingen, GERMANY). Measurements were taken on the abaxial surface located centrally, midway between the midrib and margin. The lengths of five guard cells were averaged within each sample leaf, and a species average was compiled from the five sampled individuals. We estimated the area of each individual stomate as *L* multiplied by the guard cell width, which we approximated as half *L*. We then calculated stomatal pore area index (*SPI*) which is a dimensionless index of the stomatal pore area per unit area of the leaf laminar (Sack et al., 2005; England and Attiwill, 2006).

Data Analysis

To explore general differences in absorbing root area between forest and savanna species we used an analysis of covariance to investigate vegetation specific correlations with various above ground biometric parameters. However, there was reason to believe that there may be variation associated with plot specific factors, such as vegetation structure, or soil type. Therefore the fixed effects assumptions of the analysis of covariance were untenable, leading to systematic error when scaling to the stand level. Consequently, we estimated plot specific coefficients in a mixed-

effects model taking into account the differences between plots in terms of there contribution to the variance (Model 1):

$$S = \alpha A^{\beta} + Zu + \varepsilon \qquad \textit{Model 1}$$

where S is root absorbing area (m^2), A is basal area, α and β are coefficient vectors, Z is the plot where the each tree was situated, u is a coefficient for the random plot level effects, and ε is the error term. Restricted Maximum likelihood estimates were used to derive the regression coefficients. We applied this model to the tree inventory data of each individual plot to estimate the total root absorbing area for each stand.

We investigated possible differences between the root absorbing area of evergreen and deciduous species within the savanna vegetation type using an analysis of covariance, as we felt any systematic differences would affect our results when scaling to the stand level. We pooled brevi-deciduous species as evergreen, as there is evidence to suggest they are physiologically similar (Jackson et al. 1999). Additionally, we evaluated differences between the stomatal size and density of forest and savanna species using the unpaired Wilcoxon rank sum test.

From our estimates of the total absorbing root area for each stand we estimated the absorbing root area index ($RAI_{absorbing}$), which is a dimensionless index of the total absorbing root area per unit ground area. The correlations between RAI to LAI ratios (both $RAI_{absorbing}$:LAI and RAI_{fine}:LAI) and other biometric parameters (including basal area, mean canopy height) were determined using ordinary least

squares regression analysis. We used a weighted average of *SPI,* based on the importance value of the measured species, which was multiplied by *LAI* to estimate to the transpiring leaf area index ($LAI_{transpiring}$). All statistical analyses were done using R (R Development Core Team, 2009).

Results

Vegetation Structure

The study plots spanned a wide gradient of basal area and tree density. At the low end of the range was the open savanna or '*Cerrado aberto*' (STM-03) with a basal area of 3.2 m^2ha^{-1} and tree density of 170 stems per hectare, while the high end was represented by the *Brosmium* mono-dominant forest (VCR-01) with a basal area of 28.5 m^2ha^{-1} and a tree density of 468 stems per hectare (Table 2.4-3). This structural gradient in the vegetation was also characterised by an increase in the mean tree height. Additionally, *LAI* increased rapidly with basal area among the savanna plots, saturating at basal areas represented by the forest stands (Table 2.4-3 & Figure 2.4-4). In summary, the climates of all the study plots were very similar, yet they spanned a large structural gradient.

Absorbing Root Surface Area

We found the absorbing root area of individual trees, defined from the impedance method, to vary between 0.25 and 5 m^2 across all tree sizes and vegetation types. We explored allometric relationships between absorbing root area (S) and basal area (A_{bas}), tree height (h), crown area (A_{crown}), and stem volume (V_{stem}), for both forest and savanna species. Each of the aboveground biometric parameters showed a reasonably good correlation with absorbing root surface area (S) with 39-69 % of the variation explained by each parameter ($p \leq 0.05$; Figure 2.4-3 & Table 2.4-4). There was considerably more unexplained variation within the savanna vegetation with R^2 values ranging from 0.39-0.55, with crown projected area performing the best in terms of explained variation in S. Generally, savanna trees had significantly ($p \leq 0.05$) less absorbing root area than their forest counterparts, with the difference increasing at larger tree sizes (Figure 2.4-3). Absorbing root area showed a power function relationship with A_{bas}, crown projected area and stem volume, saturating at high values (Figure 2.4-3:A, C, & D). In contrast, height showed a clearly linear correlation with absorbing root area (Figure 2.4-3B). Additionally, we found no significant difference between evergreen and deciduous species ($p > 0.05$).

Stomatal Area

We found that stomatal density ranged from 205-848 mm^{-2} across all species, while guard-cell length ranged from 9.3-36.2 μm. We did not find any significant

difference between the stomatal density of forest and savanna species (p=0.381), however, forest species had significantly (p=0.01) smaller stomata. Consequently, the stomatal cells of forest species occupied significantly (p=0.01) less leaf surface area. The stomata of the forest species in this study were on average about 30% smaller, and the mean proportion of the leaf laminar occupied by stomatal cells was 10% for forest species and 17% for savanna species (Table 2.4-5).

Table 2.4-3: Stand level biometric data, including root area index (*RAI*) estimates based on both fine root and earth impedance measurements (standard errors are reported where appropriate).

Plot	Vegetation	Tree Density (stems ha^{-1})	Basal Area ($m^2 ha^{-1}$)	Mean Tree Height (m)	Leaf Area Index (m^2m^{-2})	Fine Root Area Index (m^2m^{-2})	Absorbing Root Area Index (m^2m^{-2})
STM-03	Cerrado aberto (savanna)	170	3.22	5.61	0.48	4.5 (±0.3)	0.01
NXV-01	Cerrado *sensu stricto* (savanna)	341	5.27	6.56	1.55	7.4 (±0.3)	0.03
STM-01	Cerrado *sensu stricto* (savanna)	364	6.37	7.15	1.44	7.4 (±0.7)	0.04
STM-02	Cerradão (savanna)	411	7.11	7.88	1.22	6.9 (±0.5)	0.04
NXV-02	Cerradão (savanna)	564	10.27	9.95	2.36	7.3 (±0.4)	0.07
VCR-02	Dry deciduous forest	459	16.45	13.57	2.69	5.5 (±0.6)	0.11
FLO-01	Dry deciduous forest	604	18.44	15.49	2.62	6.8 (±0.4)	0.11
VCR-01	Evergreen mono-dominant (*Brosimum*) forest	468	28.47	18.44	2.65	6.4 (±0.5)	0.13

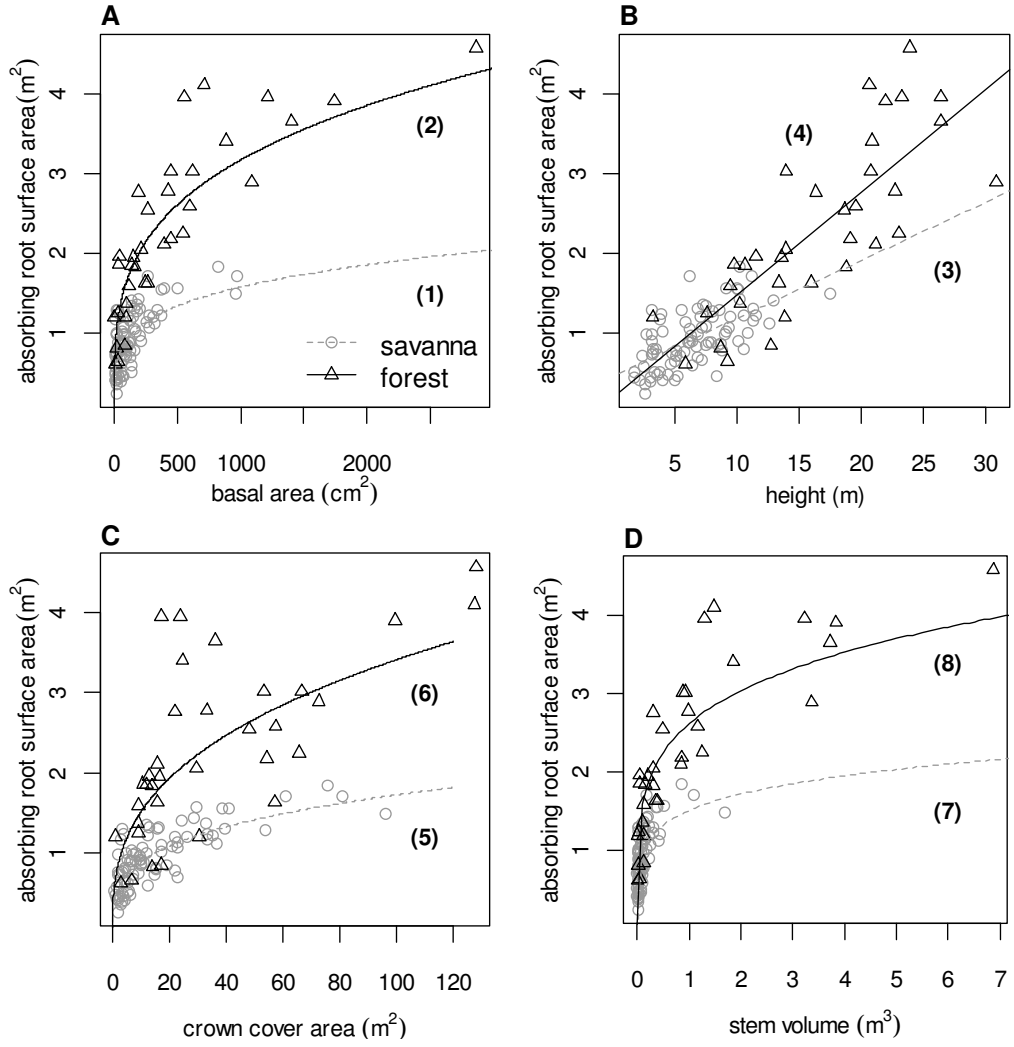

Figure 2.4-3: Absorbing root area derived from the EI method of forest and savanna trees. Correlation with, (**A**) basal area, (**B**) height, (**C**) crown area, and (**D**) stem volume. Equations for numbered regression lines are reported in Table 2.4-4 (all *p-values* are ≤0.05).

Table 2.4-4: Estimated parameters and statistics for relationships between absorbing root surface area and aboveground biometric parameters (corresponding to regression function in Figure 2.4-3).

Regression Line	Equations	Vegetation	Estimated parameters		R^2
			α	β	
1	$S = \alpha \cdot A_{bas}{}^{\beta}$	Forest	0.45	0.28	0.69
2		Savanna	0.31	0.23	0.41
3	$S = \alpha \cdot h + \beta$	Forest	0.13	0.18	0.62
4		Savanna	0.07	0.46	0.39
5	$S = \alpha \cdot A_{crown}{}^{\beta}$	Forest	0.67	0.35	0.47
6		Savanna	0.46	0.29	0.55
7	$S = \alpha \cdot V_{stem}{}^{\beta}$	Forest	2.62	0.21	0.67
8		Savanna	1.52	0.18	0.45

Root Area Index

Estimates of RAI_{fine} from core samples ranged from 4.5 m^2m^{-2} in the Cerrado aberto (STM-03) to 7.4 m^2m^{-2} in both of the dense savanna ('*Cerrado sensu stricto'*) plots studied (STM-01 & NXV-01; Table 2.4-3 & Figure 2.4-4). In contrast, to scale $RAI_{\text{absorbing}}$ to the stand level we used a random effects model correlating absorbing root area with A_{bas} independently for each plot (AIC=98.11). We found plot level differences to be significant (p=0.02). The resulting estimates of $RAI_{\text{absorbing}}$ across all the plots ranged from 0.01 in the *Cerrado aberto* (STM-03), to 0.13 m^2 m^{-2} in the *Brosimum* mono-dominant forest (VCR-01). We found no significant correlation between RAI_{fine} and $RAI_{\text{absorbing}}$ (p=0.87; Figure 2.4-5A).

Table 2.4-5: Stomatal dimensions of species represented in four plots in the Nova Xavantina municipality.

VEGETATION/ Species	Importance value (IV)		Stomatal density (mm^{-2})	Guard cell length (µm)	Percent epidermal area occupied by stomata (%)
CERRADO *sensu strict*					
Qualea parviflora	1st	27.9	499.2 (±23.5)	17.4 (±0.7)	7.6 (±0.5)
Davila elliptica	2nd	19.9	492.8 (±23.5)	17.6 (±0.4)	7.7 (±0.5)
Roupala montana	3rd	13.8	326.4 (±8.9)	24.9 (±0.8)	10.1 (±0.7)
Vochysia rufa	7th	8.2	620.8 (±10.3)	20.6 (±0.7)	13.1 (±0.6)
Kielmeyera rubriflora	8th	8.2	281.6 (±19.8)	20.7 (±0.9)	5.9 (±0.3)
Byrsonima pachyphylla	10th	8.0	552.0 (±17.8)	17.8 (±0.3)	8.7 (±0.1)
CERRADÃO					
Hirtella glandulosa	1st	41.7	233.6 (±17.2)	18.2 (±0.2)	3.8 (±0.2)
Sclerolobium paniculatum	2nd	24.1	435.2 (±16.7)	19.7 (±0.7)	8.5 (±0.7)
Xylopia aromatica	3rd	20.8	633.6 (±23.5)	17.3 (±0.3)	9.4 (±0.3)
Eriotheca gracilipes	4th	11.5	206.4 (±11.1)	36.2 (±0.5)	13.4 (±0.6)
Guapira graciliflora	6th	11.3	361.6 (±15.9)	20.5 (±0.5)	7.5 (±0.3)
Roupala montana	7th	11.2	307.2 (±29.4)	20.7 (±0.8)	6.4 (±0.4)
DRY DECIDUOUS FOREST					
Cheiloclinium cognatum	1st	36.0	478.4 (±17.2)	11.5 (±0.7)	3.2 (±0.4)
Amaioua guianensis	2nd	29.3	204.8 (±16.7)	17.9 (±0.7)	3.2 (±0.04)
Tetragastris altissima	3rd	23.6	643.2 (±29.0)	9.6 (±0.6)	2.9 (±0.2)
Himenaea courbaril	4th	17.0	528.0 (±21.9)	18.2 (±0.6)	8.7 (±0.6)
Mabea fistulifera	7th	13.4	521.6 (±13.5)	14.4 (±0.5)	5.4 (±0.2)
BROSIMUM MONO-DOMINANT EVERGREEN FOREST					
Brosimum rubescens	1st	131.9	243.2 (±16.9)	18.3 (±0.8)	4.1 (±0.4)
Amaioua guianensis	2nd	29.9	275.2 (±13.0)	19.2 (±0.4)	5.1 (±0.04)
Cheiloclinium cognatum	3rd	29.6	536.0 (±12.6)	9.9 (±0.2)	2.6 (±0.2)
Tetragastris altissima	4th	18.3	848.0 (±20.4)	9.3 (±0.2)	3.6 (±0.2)
Ephedranthus parviflorus	10th	4.2	684.8 (±13.5)	18.1 (±0.1)	11.2 (±0.3)

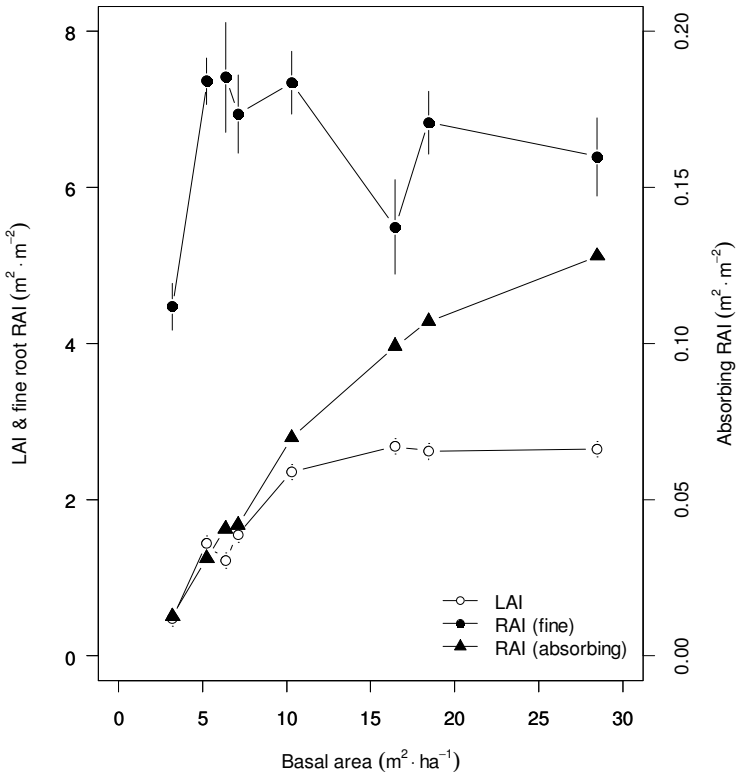

Figure 2.4-4: Ecosystem level resource exchange surface area indices across a gradient of basal area. Indices include leaf area index (*LAI*) and root area index (*RAI*) based on the earth impedance method ($RAI_{absorbing}$) and fine root surface area (RAI_{fine}), across eight one hectare plots representing tropical forest and savanna vegetation types (error bars represent standard errors were applicable).

We found the RAI_{fine}:*LAI* ratio to be inversely proportional to basal area across all the study sites ($p \leq 0.05$, $R^2=0.85$; Figure 2.4-5B), with savanna vegetation having more fine root area relative to leaf area. In contrast, the ratio of $RAI_{absorbing}$ to *LAI* was directly proportional to both basal area ($p \leq 0.05$, $R^2=0.85$; Figure 2.4-5C) and mean tree height ($p \leq 0.05$, $R^2=0.83$; Figure 2.4-5D). Consequently, the forest

plots with taller trees had a higher $RAI_{absorbing}$:LAI ratio than their savanna counterparts.

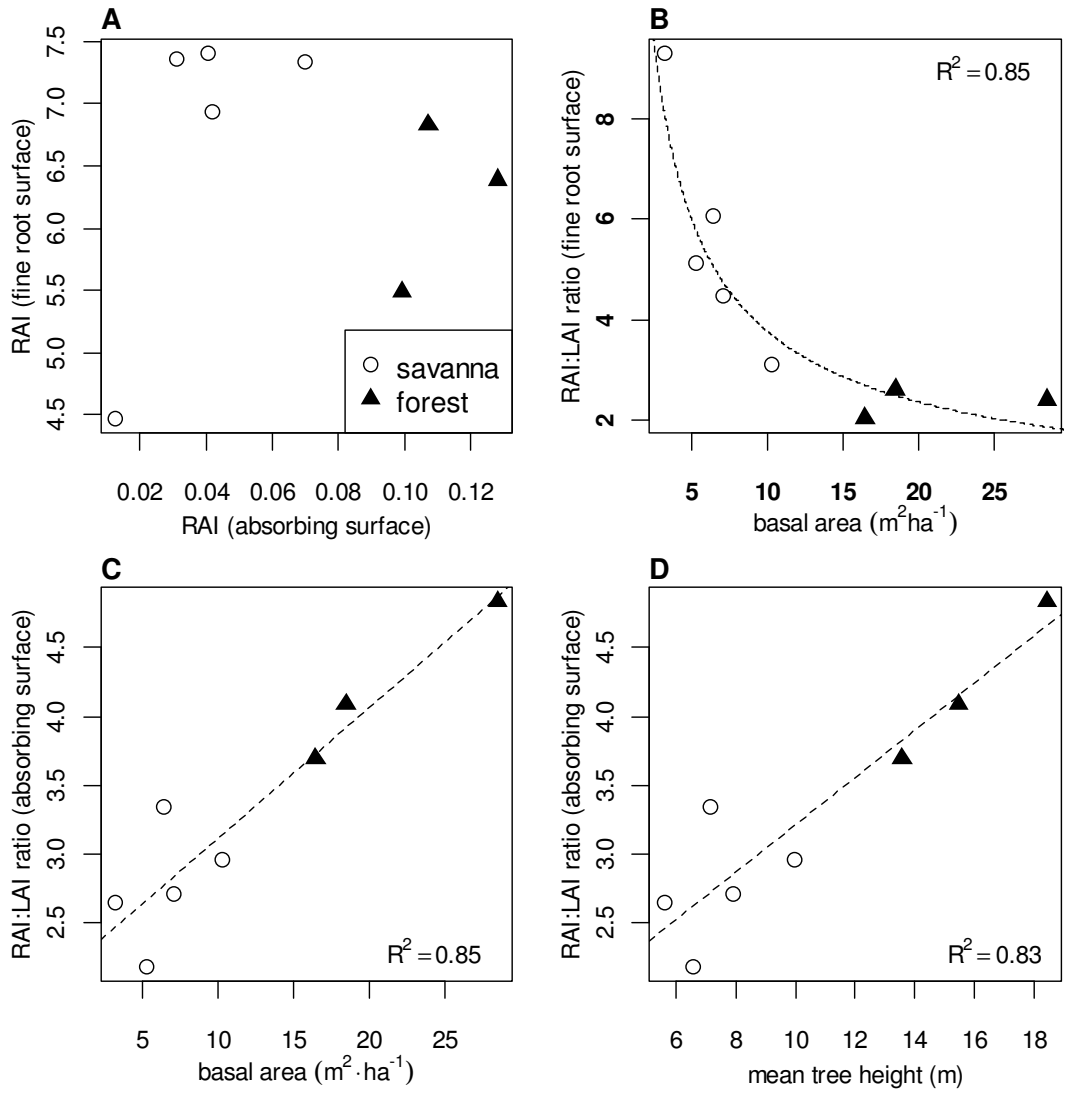

Figure 2.4-5: Comparison of root area index (*RAI*) based on the earth impedance method ($RAI_{absorbing}$) and fine root surface area (RAI_{fine}), across eight one hectare plots representing tropical forest and savanna vegetation types. (**A**) relationship between $RAI_{absorbing}$ and RAI_{fine}. (**B**) Relationship between RAI_{fine}:LAI ratio and stand basal area. (**C**) Relationship between $RAI_{absorbing}$:LAI ratio and stand basal area. (**D**) Relationship between $RAI_{absorbing}$:LAI ratio and mean tree height. $RAI_{absorbing}$:LAI ratios are multiplied by a factor of 100.

The stomatal pore area index ranged from 0.11 to 0.17, while the ratio of $RAI_{absorbing}$:$LAI_{transpiring}$ ranged from 0.26 to 1.23 across the four plots (Figure 2.4-6). The *Brosimum* forest (VCR-01) was the only vegetation type to have a ratio greater than one, indicating a higher surface area at the root-soil interface. In contrast, only a quarter of the aboveground exchange surface area is mirrored belowground in the Cerrado (NXV-01) vegetation (Figure 2.4-6).

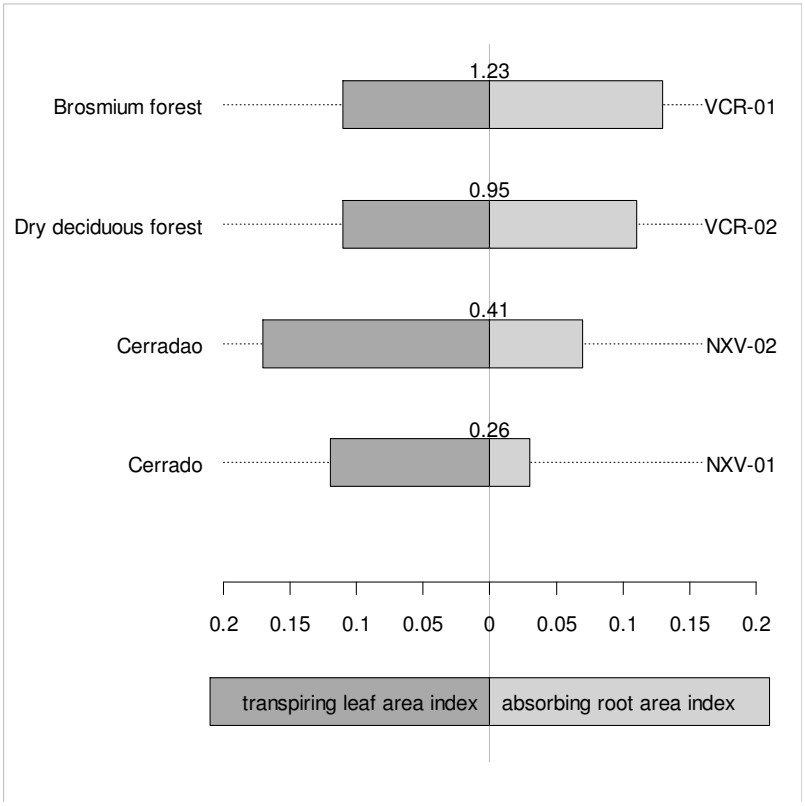

Figure 2.4-6: Comparison of absorbing root surface area index with transpiring leaf area index (stomatal pore area per unit ground area) of two forest and two savanna vegetation types. Ratios of $RAI_{absorbing}$:$LAI_{transpiring}$ are presented above each bar.

Discussion

Absorbing Root Surface Area

In general we would expect a given unit of absorbing root area to support a proportional amount of leaf area or water conducting tissue (Shinozaki et al., 1964; Sperry et al., 1998). Accordingly, the results from more than a hundred trees representing a high diversity of species show a consistent and reasonably strong relationship between absorbing root area and both basal area and crown projected area (Figure 2.4-3). However, within these relationships there is a divergence between forest and savanna species, with savanna trees surprisingly showing less absorbing root surface area for a given basal area. We speculate that the difference between these relationships could be related to the attainment of maximum tree height. A large root absorbing area will reduce the resistance to water flow across the soil-root boundary, thereby offsetting any increase in hydraulic resistance associated with tall trees (Magnani et al., 2000). This theory is additionally supported by the linear relationship between tree height and root absorbing area (Figure 2.4-3B). Alternatively, savanna trees have a greater proportion of their fine roots deeper in the soil profile (Jackson et al., 1997). Therefore, if the EI method only measures the surface roots this will result in an underestimate of the absorbing root surface areas of savanna trees.

Root Area Index

Up to now, root area index has been estimated from the geometric surface area of fine roots (Jackson et al., 1997). *RAI* estimates from similar vegetation to that in our study fall in the range of 6.3 in tropical deciduous forests to 42.5 in tropical grasslands (Jackson et al., 1997). Our estimates of RAI_{fine} across all the study sites, all of which were dominated by trees, are most similar to those reported for tropical deciduous forests. However, the suitability of fine roots to represent absorbing root area has been questioned in recent studies (Butler et al., 2010). We have therefore used an alternative approach to isolate the absorbing area of roots, which has resulted in estimates of $RAI_{\text{absorbing}}$. The earth impedance method was used on individual trees (Aubrecht et al., 2006; Čermák et al., 2006; Butler et al., 2010), and these measurements were scaled to the stand level to provide estimates of the functional soil-root interface ($RAI_{\text{absorbing}}$). These values fell in the range of 0.01 to 0.13, and are more than an order of magnitude smaller than RAI_{fine} (Figure 2.4-4). Surprisingly, we found that $RAI_{\text{absorbing}}$ was not correlated with RAI_{fine}, which implies that fine root surface area is not necessarily equivalent to the belowground absorptive surface area (Butler et al. 2010). We acknowledge that there are discrepancies between these two estimates of *RAI*; for example, $RAI_{\text{absorbing}}$ only includes the larger trees (≥10 cm *DBH*), while RAI_{fine} encompasses the vegetation as a whole. However, these discrepancies would not account for the size of the differences between the two estimates.

Root to Leaf Area Ratios

A fundamental adaptation for maintaining an efficient water balance in arid climates is the absorbing root area to leaf area ratio (Shackleton et al., 1988; Sperry et al., 1998; Litton et al., 2003). In this study we have compared our estimates of *RAI* to the analogous *LAI*. The RAI_{fine}:*LAI* ratio varied widely across the eight study sites and was strongly correlated with basal area; with low basal areas corresponding to the highest root to leaf area ratios. Generally we observed that savanna ecosystems allocate more resources to fine roots relative to leaves, suggesting that they are limited by belowground resources. In contrast to the RAI_{fine}:*LAI* ratio, we found that the $RAI_{absorbing}$:*LAI* ratio showed the opposite trend with basal area, with forest vegetation types having the highest values. This paradox may be explained by a dichotomy between the requirements for the acquisition of nutrients and water. It has been proposed that a dominant limitation to growth in Brazilian Cerrado environments such as the ones under study here is a severe shortage of nutrients in the soil (Arens, 1963). Accordingly, several authors have found a correlation between basal area and soil fertility in the cerrado (Goodland and Pollard, 1973; Lopes and Cox, 1977). Additionally, pronounced differences in soil fertility have also been found between semi-deciduous forest and cerrado ecosystems (Ruggiero et al. 2002). Cerrado soils also have high levels of soluble aluminium which compete with other essential nutrients for the same chemical sites on the soil particles, thus further promoting soil impoverishment (Arens, 1963; Furley and Ratter, 1988). We

therefore speculate that Cerrado vegetation requires a proportionally larger fine root network to explore an adequate soil volume to supply a given leaf area with nutrients. A similarly large network of fine roots near the soil surface may not be needed for water acquisition alone.

Differences in the $RAI_{absorbing}$:*LAI* ratios between different vegetation types are strongly correlated with canopy height. As stated above, there is a potential advantage of increasing the absorbing root to leaf area ratio with tree height (Magnani et al., 2000; McDowell et al., 2002), and it is interesting that we found that all the vegetation types fell on the same regression line. This suggests a homeostatic balance in the way in which these vegetation types adapt to hydrological pressures (Figure 2.4-5).

Stomatal Area

Canopy conductance is influenced by the combination of the total leaf area and the proportion of that area which is occupied by stomata. At the individual leaf level it has been shown that SPI correlates well with leaf laminar conductance (Sack et al., 2005). Overall we found that the *SPI* was significantly less for forest species than for savanna trees. This indicates that forest species will also have a lower stomatal conductance, which we would expect due to the hydraulic constraints imposed by increased tree height (Sack et al., 2003, 2005; England and Attiwill, 2006). However,

this difference in *SPI* is driven by a reduction in the size of the stomatal aperture in forest leaves rather than a change in stomatal density. Smaller stomata have been shown to enhance water use efficiency, both by responding faster to reduced soil water supply, and also by having a shorter diffusion distance that would allow for more efficient gas exchange (Aasamaa and Sober, 2001; Franks and Farquhar, 2007). Consequently, smaller stomata would minimise exposure to excessive leaf water potential deficits, thereby helping to protect plants from hydraulic damage.

We scaled the porous leaf-atmosphere interface represented by stomata to the stand level which is directly analogous to the porous soil-root interface measured by the EI method. We found that the differences in leaf area between the plots were counterbalanced by differences in stomatal pore area, resulting in largely similar values of $LAI_{\text{transpiring}}$ across the different vegetation types. It has been well documented that stomatal conductance decreases with tree height to control the minimum leaf water potential (Ryan and Yoder, 1997; Magnani et al., 2000). However, the benefits of increased root absorbing area to avoid potentially damaging effects of large water potential deficits of tall trees has not been previously investigated. Increasing the surface area for water exchange between the roots and the soil, relative to the leaf area, may allow taller trees to avoid dangerously negative water potential deficits, while limiting any reduction in the supply of water to the canopy (Sperry et al., 1998; Magnani et al., 2000).

Conclusions

The results from this study have demonstrated that measures of fine root area and absorbing root area (using the EI method) are not direct substitutes. Allocation patterns between leaves and fine roots are associated with a gradient of aboveground biomass, with savanna vegetation having the highest fine root to leaf area ratio. However, this measure of fine roots is not reflected in the functionally absorbing area for water uptake. We propose that excessive investment in fine root area relative to leaf area may reflect the requirement for nutrient uptake in poor soils. This finding questions the use of fine roots as a measure of water uptake ability, which highlights the need to develop an alternative approach for estimating water absorption in terrestrial vegetation models.

Part III: Belowground Carbon Cycling

3.1 Ecosystem Carbon Cycling

Ecosystem carbon cycling starts when plants fix CO_2 from the atmosphere and convert it to organic carbon compounds through photosynthesis. These organic carbon compounds are used for both the growth of new plant tissue as well as the maintenance of existing biomass. At the same time, plants discard dead plant material (i.e. litter) which is decomposed by microorganisms in the soil to provide energy for microbial growth. During this process of microbial respiration, CO_2 is released back to the atmosphere. The plant also breaks down some of the generated organic carbon compounds through respiration to supply the plant with energy, and through this process CO_2 is also released back into the atmosphere. Plant respiration takes place both aboveground through leaves and branches, as well as belowground through living roots and their mycorrhizal fungal partners. Thus, ecosystem respiration can be analysed as the equivalent of the total CO_2 emissions from these different processes.

In temperate forests, soil respiration typically contributes between 30%-80% of the total ecosystem respiration (Curtis et al., 2005), while estimates from tropical Amazonian forests represent approximately 46% (Chambers et al., 2004). Chen et al.

(2003) produced one of the first comprehensive studies of an ecosystem carbon balance in a tropical savanna in northern Australia. The authors estimated that soil respiration represented approximately 84% of the total ecosystem respiration, highlighting the importance of belowground carbon dynamics in tropical savannas.

Table 3.1-1: Mean rates of soil respiration in different types of vegetation (Raich and Schlesinger, 1992).

Vegetation Type	**Soil Respiration Rate ($gC/m^2/yr$) (mean ± se.)**
Tundra	60 (± 6)
Boreal forests and woodlands	322 (± 31)
Temperate grasslands	442 (± 78)
Temperate deciduous forests	681 (± 95)
Mediterranean woodlands and heath	647 (± 51)
Croplands, fields, etc.	713 (± 88)
Desert Scrub	544 (± 80)
Tropical savannas and grasslands	224 (± 38)
Tropical dry forests	629 (± 53)
Tropical moist forests	1260 (± 57)
Northern bogs and mires	94 (± 16)
Marshes	413 (± 76)

Mean rates of soil respiration have been shown to vary widely within and among major vegetation types (Table 3.1-1) (Raich and Schlesinger, 1992). Globally, these variations are driven by temperature and moisture. The lowest rates of soil

respiration occur in the cold and dry tundra, while the highest rates occur in tropical moist forests where both temperature and moisture are high throughout the year. Improved understanding of the controlling factors influencing the patterns of soil respiration in this region would be an important contribution to our knowledge of global carbon cycling.

The efflux of CO_2 from the soil surface alone (R_{soil}) is the product of both autotrophic respiration (R_a, contributed by living plant roots and their symbiotic mycorrhizal fungal partners) and heterotrophic respiration (R_h, contributed by microbial decomposition of detritus and soil organic matter) (Figure 3.3-1):

$$R_{soil} = R_h + R_a \quad (1)$$

There is mounting evidence that as much as half of the soil CO_2 efflux originates from an autotrophic source (Craine et al., 1999; Hogberg et al., 2001; Leake et al., 2006). Within tropical environments it is estimated that autotrophic respiration contributes 46-63% of the total soil CO_2 efflux (Trumbore et al., 1995; Malhi et al., 1999; Metcalfe et al., 2007). There is also evidence to suggest that these distinct sources of CO_2 respond differently to environmental variables (Pregitzer et al., 2000; Law et al., 2002), highlighting the need to consider them as independent processes.

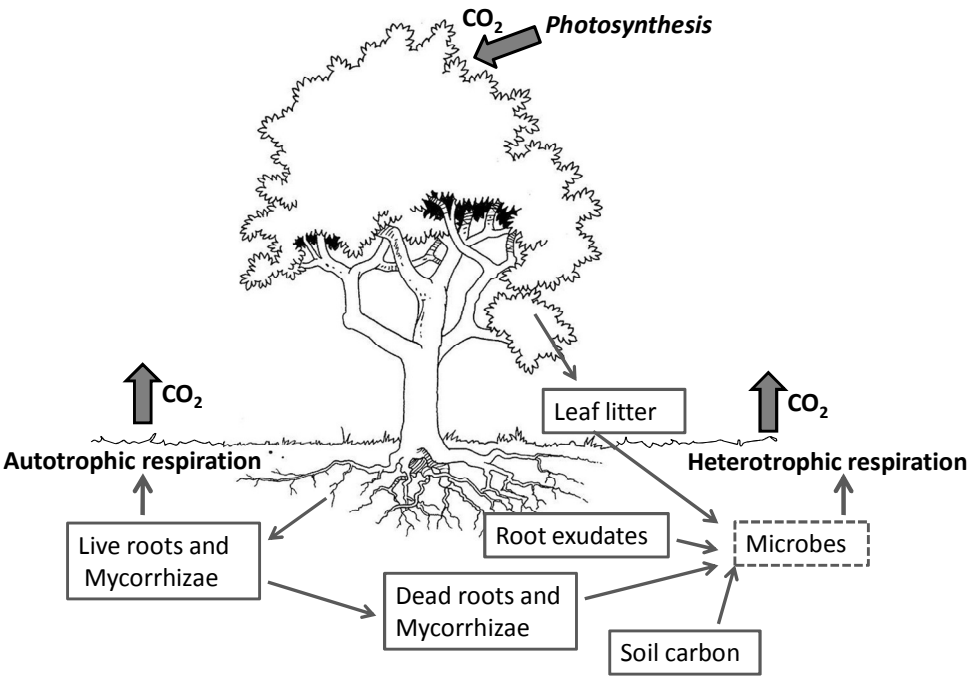

Figure 3.1-1: Ecosystem carbon processes.

3.2 Soil Respiration: Processes and Controls

In order to understand soil respiration rates and their patterns in changing environments it is important that we understand all the controlling factors that affect the associated CO_2 fluxes. It has been well documented that the most important factors which influence soil respiration are substrate supply and quality, temperature, and moisture.

Substrate Supply

Heterotrophic respiration mainly depends on the supply of plant litter to the soil environment. On average, and across all forest ecosystems, Davidson et al. (2002), estimated that about 25% of total soil CO_2 efflux is contributed by aboveground litter. In contrast, Chen et al. (2003) estimated that only 6% of total soil respiration was contributed by aboveground litter fall in a tropical savanna of northern Australia. Furthermore, the authors estimated that as much as 49% of total soil respiration is represented by fine root litter input, demonstrating a dominance of belowground processes in tropical savannas. There is also growing evidence that dead mycorrhizea and root exudates may represent significant sources of carbon for heterotrophic respiration (McDowell et al., 2001; Hobbie et al., 2004). It has been estimated that as much as 62% of the carbon entering the soil organic matter pool can come from mycorrhizal turnover, exceeding the input of both leaf litter and fine root turnover (Godbold et al., 2006).

Autotrophic respiration, conversely, is directly dependent on aboveground photosynthesis. A multitude of field experiments using physiological manipulations and canopy-labelling techniques have demonstrated that as much as half of soil CO_2 efflux has its origins in the recently fixed carbon by the canopy (Andrews et al., 1999; Craine et al., 1999; Hogberg et al., 2001). This connection between soil respiration and aboveground photosynthesis has also been demonstrated by other studies which looked at the impact of factors determining aboveground capacity to

assimilate carbon including; availability of nutrients (Nadelhoffer, 2000), light (Craine et al., 1999), and leaf area (Curiel-Yuste et al., 2004).

Temperature

Temperature primarily influences soil respiration at the biochemical and physiological levels. Low temperatures can limit the effectiveness of both the soluble and membrane-bound enzymes, while high temperatures can restrict the transport of the products from metabolism via diffusion processes. Consequently, the temperature sensitivity of metabolic processes associated with soil respiration are not constant (Lloyd and Taylor, 1994). The relationship between temperature and the biochemical processes of soil respiration have most commonly been described by the following equations:

$$\text{Van't Hoff: } R_{soil} = \alpha e^{\beta T} \text{ (where } Q_{10}=e^{\beta \times 10}) \quad (1)$$

$$\text{Arrhenius: } R_{soil} = \alpha e^{\left(-E_a / \Re T\right)} \quad (2)$$

$$\text{Lloyd \& Taylor: } R_{soil} = \alpha e^{\left(-E_0 / (T - T_0)\right)} \quad (3)$$

where R_{soil} is soil respiration, α, β, E_a (activation energy), E_0, *and* T_0 are fitted parameters, T is measured temperature (in degrees Kelvin for the Arrhenius function), $\Re$ is the universal gas constant, and Q_{10} is a quotient of change in respiration caused by a change in temperature of 10 degrees Celsius.

The temperature sensitivity of soil respiration varies widely between geographic location and ecosystem type. Q_{10} values are generally derived from seasonal variation in temperature. Resulting temperature sensitivity may therefore be the consequence of the confounding effects of temperature with covarying variables such as light, moisture, phenological patterns in photosynthetic activity (Davidson et al., 1998; Curiel-Yuste et al., 2004). Additionally, there is evidence to suggest that autotrophic and heterotrophic components of soil respiration are differentially influenced by temperature (Boone et al., 1998; Schindlbacher et al., 2008). In a field warming experiment, which excluded confounding effects of soil moisture and carbon flow from the canopy, Schindlbacher et al. (2008) estimated that the autotrophic Q_{10} response was twice as high as the heterotrophic component of soil respiration in a mature coniferous forest.

Soil Moisture

Soil moisture affects soil respiration both directly through its effect on physiological processes of roots and microorganisms, as well as indirectly via diffusion of substrates and oxygen. Conceptually, soil CO_2 efflux is thought to be low in dry conditions, to reach an optimal rate in intermediate moisture levels, and to decrease at high soil moisture content. The optimal water content for soil respiration is when

the macropore spaces are mostly air-filled, thereby facilitating oxygen diffusion, and the micropore spaces are mostly water-filled, thus allowing diffusion of soluble substrates. However, there is no consensus on the best way to mathematically describe the effects of soil moisture on soil respiration. Numerous equations have been proposed with soil water content being expressed in a variety of forms (Table 3.2-1).

The few studies describing soil respiration in tropical savanna environments indicate that soil moisture has a dominant influence (Gupta and Singh, 1981; Pinto et al., 2002; Chen et al., 2002a). Pinto et al. (2002) collected data over one wetting-drying cycle in the Brazillian Cerrado. They found that the stochastic effect of rainfall and the great fluctuations in soil moisture led to significant variation in soil respiration. However, fitting a single straightforward relationship to this variation is very difficult. The data showed that when soil was dry before rainfall, soil respiration was very low. Rainfall, when added to dry soil surfaces resulted in bursts of CO_2 released from the soil, which declined over time. The lack of consensus on how to relate soil moisture to respiration processes is a reflection of the numerous mechanisms involved in the process between soil environments, roots and microbial activities throughout different regions and seasons.

Table 3.2-1: Selected functions relating CO_2 production in soils to soil water content. (α & β represent fitted parameters.)

Orchard & Cook (1983) **lab incubations.**
$R = \alpha \ln(-\psi) + \beta$

ψ = water potential

Wildung et al. (1975) field fluxes in an arid grassland in central Washington State.

$$R = \alpha \pm \beta(\theta)(T)$$

θ = % water content, T = temperature

Howard & Howard (1993) lab incubations.

$$\ln R = \alpha + \beta_1(T + T^*) + \beta_2(T - T^*)^2 + Y_1(M - M^*) + Y_2(M - M^*)^2$$

M = % water holding capacity, M^* = mean M, T = temperature, T^* = mean T

Raich & Potter (1995) global analysis of published field fluxes.

$$R = F \times e^{Q \times T} \times \left(P \big/ K + P\right)$$

F = flux when temperature is zero and moisture is not limiting, Q = Q_{10} factor,

P = mean monthly precipitation, K = half saturation coefficient of precipitation

Hanson et al. (1993) field fluxes in a mixed hardwood forest, Tennessee.

$$R = \left(R_b \cdot \alpha^{(T/10)}\right)\left(1 - Cf \big/ 100\right) \qquad R_b = \left(\beta \cdot \theta \cdot R_{\max}\right) \big/ \left((\beta \cdot \theta) + R_{\max}\right)$$

θ = volumetric water content, Cf = course soil fraction, T = temperature,

R_{max} = maximum flux when W_s = 100%

Tang & Baldocchi (2005) field fluxes in an oak-grass savanna, California.

$$R = \alpha \cdot e^{\beta_1 T} \cdot e^{\beta_2 \theta + \beta_3 \theta^2}$$

θ = volumetric water content, T = temperature

Schlentner & Van Cleve (1985) field CO_2 fluxes in Alaskan forests.

$$R = \left(\frac{W_s}{(\alpha_1 + W_s)}\right)\left(\frac{\alpha_2}{(\alpha_2 + W_s)}\right) \times \alpha_3 \times \alpha_4^{\left((T-10)/10\right)}$$

W_s = volumetric water content, T = temperature

Understanding the factors that control the CO_2 efflux from the soil is central to our ability to predict the influence of a changing climate on the storage of carbon

sequestered from the atmosphere. Generally, the belowground carbon budget depends on the balance of carbon inputs and fluxes at the soil surface. However, this balance varies temporally in response to a multitude of environmental drivers. Additionally, there is growing evidence that heterotrophic and autotrophic components may respond differently to these drivers. Consequently, in order to construct accurate global carbon budgets there is a need for detailed local scale studies from a diverse range of ecosystems which isolate individual respiration components.

3.3 Soil respiration and belowground carbon cycling dynamics in two structurally contrasting woody savannas in Central Brazil

Submitted to *Plant and Soil*

Abstract

Trees allocate a large portion of gross primary production belowground for the growth and maintenance of roots and mycorrhizae. The ecosystem processes controlling belowground carbon dynamics are central to understanding the transfers of carbon between the atmosphere and terrestrial systems. Here we examine the soil CO_2 fluxes within the context of a belowground carbon budget for two structurally contrasting woody savannas in central Brazil. Mean monthly soil CO_2 efflux ranged from 1.5 to 12.6 μmol m^{-2} s^{-1} across both study sites. This resulted in an average annual losses of carbon from soil respiration of 17.3 Mg C ha^{-1}.Between 60-66% of the total soil CO_2 efflux was accounted for by autotrophic respiration. Seasonal fluctuations of soil respiration were strongly correlated with soil moisture for both the autotrophic (R^2=0.79, *p*-value<0.05) and heterotrophic (R^2=0.90, *p*-value<*0.05)* components, with maximum flux rates corresponding with 16.4 and 17.7% soil moisture content respectively. Furthermore, seasonal fluctuations in autotrophic

respiration were strongly correlated to phenological patterns of fine root production (R^2=0.80, p-value<0.05). Diurnal fluctuations of heterotrophic CO_2 efflux were correlated with soil temperature (R^2=0.74, p-value<0.05), demonstrating a Q_{10} value of 1.6 across both sites. In contrast, total soil CO_2 efflux was not correlated with temperature (p-value=0.31), providing evidence that autotrophic respiration does not respond to temperature in cerrado environments.

Introduction

Terrestrial ecosystems are sustained by the photosynthetic fixation of carbon, most of which is then released by respiratory processes occurring belowground. Globally, soil respiration releases 68-80 billion tons of carbon each year (Raich and Schlesinger, 1992; Raich et al., 2002). This represents the second largest carbon flux between ecosystems and the atmosphere, corresponding to more than 10 times the current rate of fossil fuel emissions (Reichstein et al., 2003). Therefore, even small changes in soil respiration have the potential to influence atmospheric CO_2 concentrations associated with climate change (Jenkinson et al., 1991). Understanding the factors that control belowground terrestrial carbon cycling is critical for estimating global carbon budgets.

The efflux of CO_2 from the soil surface originates from two distinct sources: autotrophic respiration (contributed by living plant roots and their symbiotic mycorrhizal fungal partners) and heterotrophic respiration (contributed by microbes involved in the decomposition of detritus and soil organic matter). The dynamics of these different components are controlled by a variety of biotic and abiotic variables including: temperature (Lloyd and Taylor, 1994; Davidson and Janssens, 2006), soil moisture (Bunnell et al., 1977; Davidson et al., 2000), litter quality (Raich and Tufekciogul, 2000), aboveground vegetation structure (Tang and Baldocchi, 2005), and photosynthetic activity (Curiel-Yuste et al., 2004). Despite this complexity, modelling soil respiration on large spatial scales requires simple empirically derived relations with easily measured parameters. Consequently, modelling soil respiration relies heavily on simple Q_{10} or Arhennius-derived functions of temperature sensitivity, which are often combined with a water availability function (Davidson et al., 2005). The temperature response of soil respiration has been shown to vary between its different components, with autotrophic respiration generally being more sensitive within temperate forests (Boone et al., 1998). In contrast, studies that have compared the differential response of the component parts of soil respiration in seasonally dry environments have found confounding effects of temperature and moisture (Rey et al., 2002; Almagro et al., 2009). These uncertainties have limited our understanding of how different components of soil respiration respond to soil moisture.

The cerrado (woody savanna) is the second most extensive biome in Latin America originally covering a land area of around 2×10^8 hectares . It is represented by a variety of physiognomic forms; including tall dense cerradão to the more widespread cerrado *sensu strictu*. The vast expanse of the land covered by cerrado vegetation means it plays a potentially significant role in both regional and global carbon budgets (Miranda et al., 1997). There is evidence to suggest that in these vegetation types soil CO_2 efflux is principally controlled by soil moisture (Pinto et al., 2002). However, it has also been widely reported that fine root productivity is limited by water supply within tropical regions with pronounced seasonality of rainfall (Chen et al., 2004; M'bou et al., 2008; Lima et al., 2010). However, very little is known about how such phenological processes influence the component parts of soil CO_2 efflux.

In this study, we compare the seasonal and diel patterns of both the autotrophic and heterotrophic components of soil CO_2 efflux in two adjacent, structurally contrasting forms of cerrado vegetation. This approach allows us to assess the influence of vegetation structure on the component parts of soil respiration under similar climatic regimes. Additionally, we coupled seasonal measures of autotrophic soil CO_2 efflux with phenological patterns of fine root proliferation. Thus, allowing us to isolate root growth respiration from total root respiration at the stand level. Consequently our aims were to (1) assess the seasonal variations in total,

autotrophic and heterotrophic soil CO_2 efflux at each site, (2) determine the contribution of each component to the annual soil carbon efflux, (3) to determine the environmental drivers of seasonal and diel patterns of the component parts of soil CO2 efflux, and (4) to explore the relationship between autotrophic respiration and fine root dynamics in these two semi-deciduous ecosystems. Finally, we will incorporate these measurements into a belowground carbon budget.

Materials and Methods

Study site

The study was carried out in the northeast region of the state of Mato Grosso, Brazil, within the Parque Municipal do Bacaba (14°41'S, 52°20'W) in the municipality of Nova Xavantina. The reserve lies at an altitude of 318 m. The mean annual temperature is 24.9°C and ranges between 14 and 33.4°C. The mean annual precipitation is 1500 mm, with a highly seasonal distribution resulting in close to no precipitation for three months of the year between June and August (Fig. 3.3-1a and 3.3-2a). The soils are characterised as deep, well drained dystrophic Ferrasols (Marimon Jr. and Haridasan, 2005). Within the reserve we established two 1 hectare plots representing two structurally distinct physiognomic forms of cerrado vegetation; cerrado *sensu stricto* (*s.s.*), and cerradão. The cerrado *s.s.* was

characterised by a basal area of 11.4 m^2 ha^{-1} and an open fragmented canopy (36% canopy cover; estimated from inventory of canopy dimensions of trees greater than 10 cm diameter at breast height). The three most dominant species in the cerrado *s.s.* were *Qualea parviflora*, *Davila eliptica*, and *Ropala Montana*. In contrast the cerradão had a basal area of 15.7 m^2 ha^{-1} and a closed canopy (69% canopy cover). The three most dominant species in the cerradão were *Hertella glandulosa*, *Sclerolobium paniculatum*, and *Xylopia aromatic*.

Soil respiration measurements

We used a root exclusion method to isolate the heterotrophic component of the total soil CO_2 efflux. All the roots were severed around the perimeter of treatment areas of 1 m^2, to a depth of 50 cm, and root re-growth into these areas was prevented. Twenty treatment areas were established within each plot on a 4 by 5 matrix with 20 meter spacing. Consequently, the input of recently fixed carbon from the canopy was excluded. We estimated the autotrophic flux component to be the difference between the mean monthly total soil respiration and the heterotrophic component for each plot.

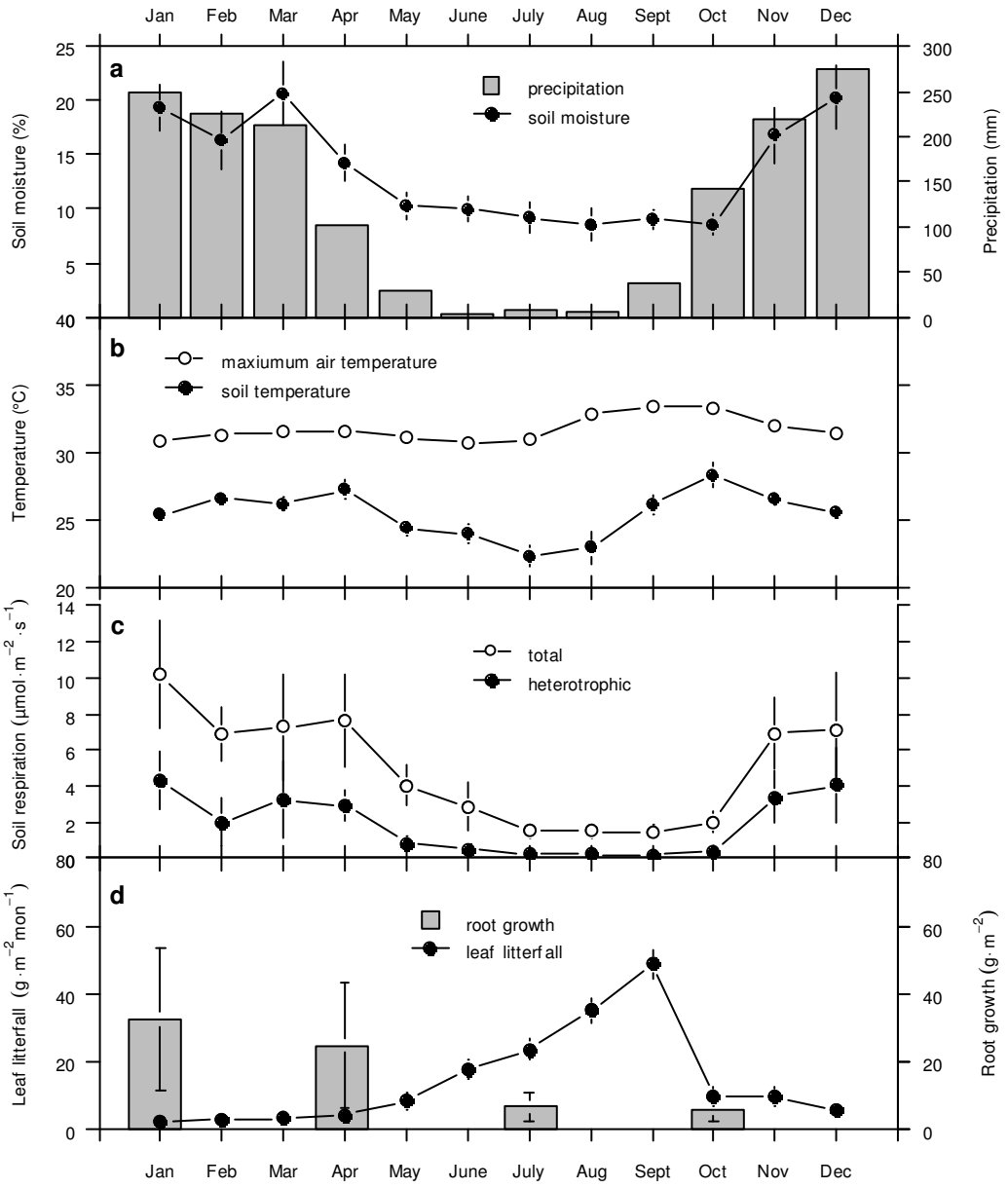

Fig. 3.3-1: Seasonal variations in biotic and abiotic factors that influence the carbon dynamics of a cerrado savanna near Nova Xavantina, Mato Grosso, Brazil. **(a)** Seasonal variation in monthly precipitation and volumetric soil moisture (at a depth of 0-30 cm, n=20). **(b)** Average maximum air temperature and average soil temperature (at a depth of 6 cm, n=20). **(c)** Average seasonal trend in heterotrophic and total soil respiration (n=20). **(d)** Average monthly leaf litterfall (n=20) and three monthly total fine root production (n=25). All error bars indicate ±1 standard deviation.

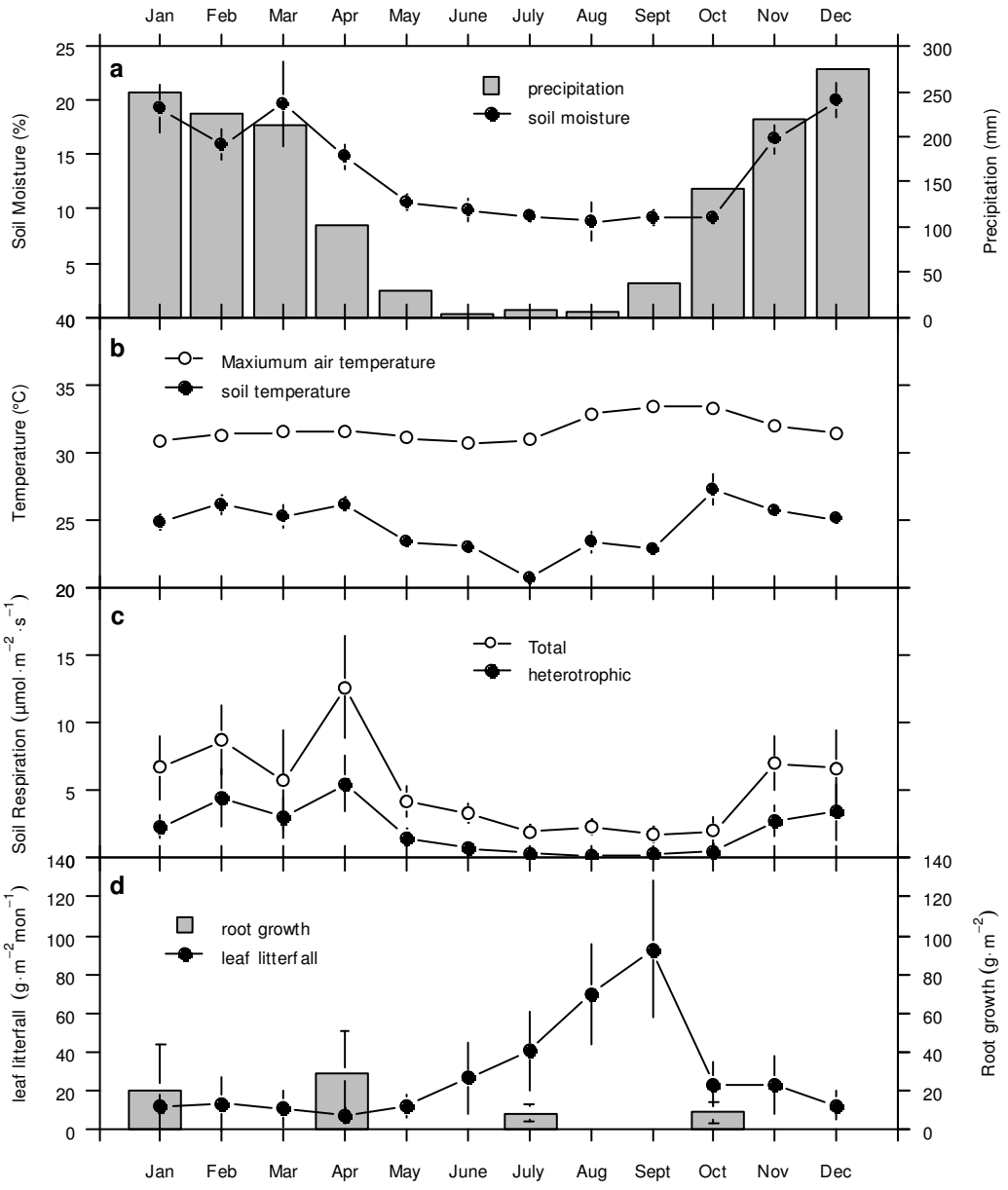

Fig. 3.3-2: Seasonal variations in biotic and abiotic factors that influence the carbon dynamics of a cerradão savanna near Nova Xavantina, Mato Grosso, Brazil. **(a)** Seasonal variation in monthly precipitation and volumetric soil moisture (at a depth of 0-30 cm, n=20). **(b)** Average maximum air temperature and average soil temperature (at a depth of 6 cm, n=20). **(c)** Average seasonal trend in heterotrophic and total soil respiration (n=20). **(d)** Average monthly leaf litterfall (n=20) and three monthly total fine root production (n=25). All error bars indicate ±1 standard deviation.

Flux measurements were made using a closed static system, by circulating air between a PP systems CIRAS-1 infrared gas analyzer and a flux chamber consisting of a PVC collar (15 cm diameter) and a vented PVC cover. The total volume of the sealed chamber was 3 litres. The collars were permanently inserted about 2 cm into the soil, two weeks before starting the measurements. In order to ensure the pressure within the chamber was at equilibrium with the atmosphere at all times, we used a stainless steel vent (10 cm long with an internal diameter of 2 mm). The CO_2 concentration was recorded at 10 second intervals. The rate of change in concentration was then estimated using the slope of a linear regression over a time period of about 2 minutes, beginning 30 seconds after placing the cover over the collar. The soil CO_2 efflux (R_{soil}, μmol m^{-2} s^{-1}) was calculated using the following equation:

$$R_{soil} = \frac{dCO_2}{dt} \times \frac{PV}{ART} \qquad \text{(eq. 1)}$$

where P is the atmospheric pressure (Pa), V is the volume of the chamber (m^3), A is the area of soil enclosed by the chamber (m^2), R is the universal gas constant, and T is the air temperature (K).

Each sampling location consisted of a root exclusion area (n=20), and an adjacent location which was not manipulated (n=20). Soil CO_2 efflux, soil temperature, and soil moisture measurements were made at each soil collar.

Measurements were made monthly, from April 2008 through March 2009, avoiding days when it was raining. Measurements were taken between 11 am and 2pm, during which time plants would have been photosynthetically active. We also measured diurnal variation of CO_2 efflux once, at the end of the wet season in April 2008, when soil respiration was not moisture limited. Measurements were taken once every half hour over a 24-hour period for both total and heterotrophic respiration within each plot. Soil temperature was measured at a soil depth of 6 cm. Soil moisture was measured to a depth of 30cm using a portable CS615 time domain reflectometer (TDR; Campbell enviScientific, Logan, UT) coupled with a digital multimeter (O'Brien and Oberbauer, 2001). We estimated annual emissions by extrapolating the measurement for each month to a 30-day period (15 days either side of the measurement date) and summing for a year.

Autotrophic respiration can be further divided into, growth respiration *a* (gC g^{-1}) and maintenance respiration *m* (gC g^{-1}) over the three month measurement period (Lehto and Grace, 1994). These can be estimated using the following linear regression equation:

$$\sum_{t_0}^{t_i} R_a = a\left(\frac{dw}{dt}\right) + m \qquad \text{(eq. 2)}$$

where R_a (gC m^{-2}) is the total autotrophic respiration per square meter over the same three month period during which fine root growth was measured (t_i=3 months), *w* is

root weight (g), and *t* is time (three month growth period). The cost of coarse root growth has been ignored in this estimation, however we believe fine root production to be the dominant source of CO_2 (Chen et al., 2003).

Table 3.3- 1: Methods for estimating components of the cerrado carbon balance.

Symbol	Component definition	Data source
ΔB_{leaf}	Leaf production	Leaf litter traps
ΔB_{fr}	Fine root production	Root in-growth cores (Vogt et al. 1998)
R_{soil}	Total soil respiration	Soil respiration was measured using closed chamber technique.
R_h	Heterotrophic respiration	Root exclusion method (Hanson et al. 2000)
R_a	Autotrophic respiration	$R_a=R_{soil} - R_h$
R_{rg}	Root growth respiration	Based on analysis in Lehto and Grace (1994)
R_{rm}	Root maintenance respiration	Based on analysis in Lehto and Grace (1994)
B_{ab}	Aboveground biomass	Based on allometric equations developed by Delitti, Meguro & Pausas (2006)
B_{bl}	Belowground biomass	The biomass of fine roots was estimated using soil cores, and that of coarse roots from root:shoot ratios reported by De Castro & Kauffman (1998)

Biomass and turnover

We measured the diameter at breast height (DBH, 1.30 m) of all the trees greater than 10 cm DBH. To estimate tree height, we measured a sub-sample of 50 trees and

developed allometric equations with DBH which were applied to the remaining trees. Additionally, we also measured the DBH and height of all the trees between 0.5-10cm DBH, in half the plot. Using these parameters, we calculated total leaf and stem biomass, using an allometric equation developed specifically for cerrado vegetation (Delitti et al., 2006). Within each plot leaf litterfall was recorded by measuring the monthly accumulation of litter within 20 mesh traps located on a 4 by 5 matrix with 20 meter spacing. Each trap covered 0.44 m^2 and was placed 1 m above the ground surface. The leaves from each trap were oven dried at 70^oC and weighed. Fine root biomass was measured from soil cores taken in the middle of the wet season (January) when biomass has been reported to be at its maximum (Delitti et al., 2001). Fine root production was measured using in-growth cores (Vogt et al. 1998). Soil cores (*n*=25) of 8 cm diameter and 30 cm deep were extracted from the soil within each plot. We carefully picked all the roots out the soil and separated the live and dead roots based on colour and resilience. The live roots ≤ 2 mm in diameter were then rinsed, oven dried at 70^oC, and weighed, giving an estimate of the maximum standing stock. The root free soil was then returned to the hole from which it came and the location was marked using a mesh crown. At three month intervals the cores were re-extracted and the newly grown roots were removed, to give an estimate of fine root production.

Assuming steady state conditions (i.e. annual changes in soil carbon storage are small relative to the carbon fluxes into and out of the soil) the belowground litter contribution was estimated as the difference between the heterotrophic soil respiration and aboveground litter contribution (Table 3.3-4). Changes in the carbon storage in the soil were probably quite small at our sites due to the fact that: (1) savanna vegetation is thought to acts as a carbon sink, particularly in the absence of fire (Miranda et al., 1997; Grace et al., 2006), (2) our sites had relatively low soil organic matter content (Scholes and Hall, 1996), (3) both sites hosted mature/climax vegetation, (4) the reserve was protected from fire which could stimulate abrupt changes in carbon flow dynamics (Bird et al., 2000). The methods used for estimating components of the carbon balance are summarised in Table 1.

Soil organic carbon stocks

We used a previously defined stratified sampling strategy for the determination of soil organic carbon (SOC) stocks, which accounts for the potential heterogeneity within tropical savanna ecosystems (Bird et al., 2004; Wynn et al., 2006). Accordingly ten sample locations were located within each plot with five of the samples taken near trees (at half the crown radius from the trunk) and five away from trees (at half the maximum distance between trees). Surface litter was removed previous to sampling and samples were collected using a stainless steel corer down to

a depth of 30 cm, and were oven-dried at 60^{o}C. Carbon content (%C) was determined with a ThermoQuest-Finnigan Delta Plus isotope ratio mass spectrometer (Finnigan-MAT; CA, USA) interfaced with an Elemental Analyzer (Carlo Erba, model 1110; Milan, Italy) at the Laboratory of Isotope Ecology (CENA-USP, Brazil). Soil bulk density was calculated by dividing the oven-dried weight of the soil sample by volume of soil corer. Accordingly, soil bulk density and organic carbon concentration determined at each sampling location were then used to calculate SOC stocks to a depth of 30 cm. The resulting SOC estimates near trees and away from trees were then weighed according to crown cover in order to obtain a representative average estimate.

Data analysis

To examine the influence of temperature and soil moisture on soil respiration we used ordinary least squares regression of a bivariate model (model 1) proposed by Tang and Baldocchi (2005). Additionally, we decomposed this function into individual moisture (model 2) and temperature (model 3) components.

$$R_i = \alpha e^{\beta_1 T} e^{\beta_2 \theta + \beta_3 \theta^2} \qquad \text{(model 1)}$$

$$R_i = \alpha e^{\beta_2 \theta + \beta_3 \theta^2} \qquad \text{(model 2)}$$

$$R_i = \alpha e^{\beta_1 T} \qquad \text{(model 3)}$$

where R is the rate of soil CO_2 efflux (μmol $m^{-2}s^{-1}$) from source i (total, heterotrophic, and autotrophic soil respiration), T is the mean soil temperature (^oC), θ is the mean volumetric water content (%), and α, β_1, β_2, and β_3 are the regression coefficients. We applied these three models individually to the monthly mean values of the total, heterotrophic, and autotrophic components of the soil CO_2 efflux.

The relationship between diurnal variation in soil respiration and temperature was based on repeated measures on individual soil collars. Therefore, the error terms will not be independent, it is thus reasonable to suspect some degree of heteroskedasticity. We used the Breusch-Pagan test for heteroskedasticity, and estimated our parameters using feasible generalized least-squares regression analysis

of model 3. A dummy variable was used to allow for differences in the slope and intercept between sites. The Q_{10} (the factor by which soil CO_2 efflux is multiplied for every 10°C increase in temperature) was calculated as $Q_{10}=e^{\beta\times10}$ for model 3. Finally, the influence of fine root growth on autotrophic soil respiration was assessed using ordinary least squares regression analysis of equation 2. All statistical tests were done in R (R Development Core Team, 2009).

Results

Ecosystem carbon stocks

Estimates for the carbon stocks of the above and belowground components (foliage, stem, fine roots and coarse roots) in the cerrado *s.s.* and cerradão environments are presented in Table 3. The total ecosystem carbon pool was 96.9 and 175.4 Mg C ha^{-1} for the cerrado *s.s.* and cerradão respectively. Of this total stock approximately 77% and 69% was stored belowground in each site respectively, of which the main component was coarse roots (approximately 53% and 72%). Soil organic carbon represented the second largest belowground carbon pool accounting for 38% and 23 % of the total (Table 3.3-2). Woody tissue accounted for 94% of the total aboveground carbon pool.

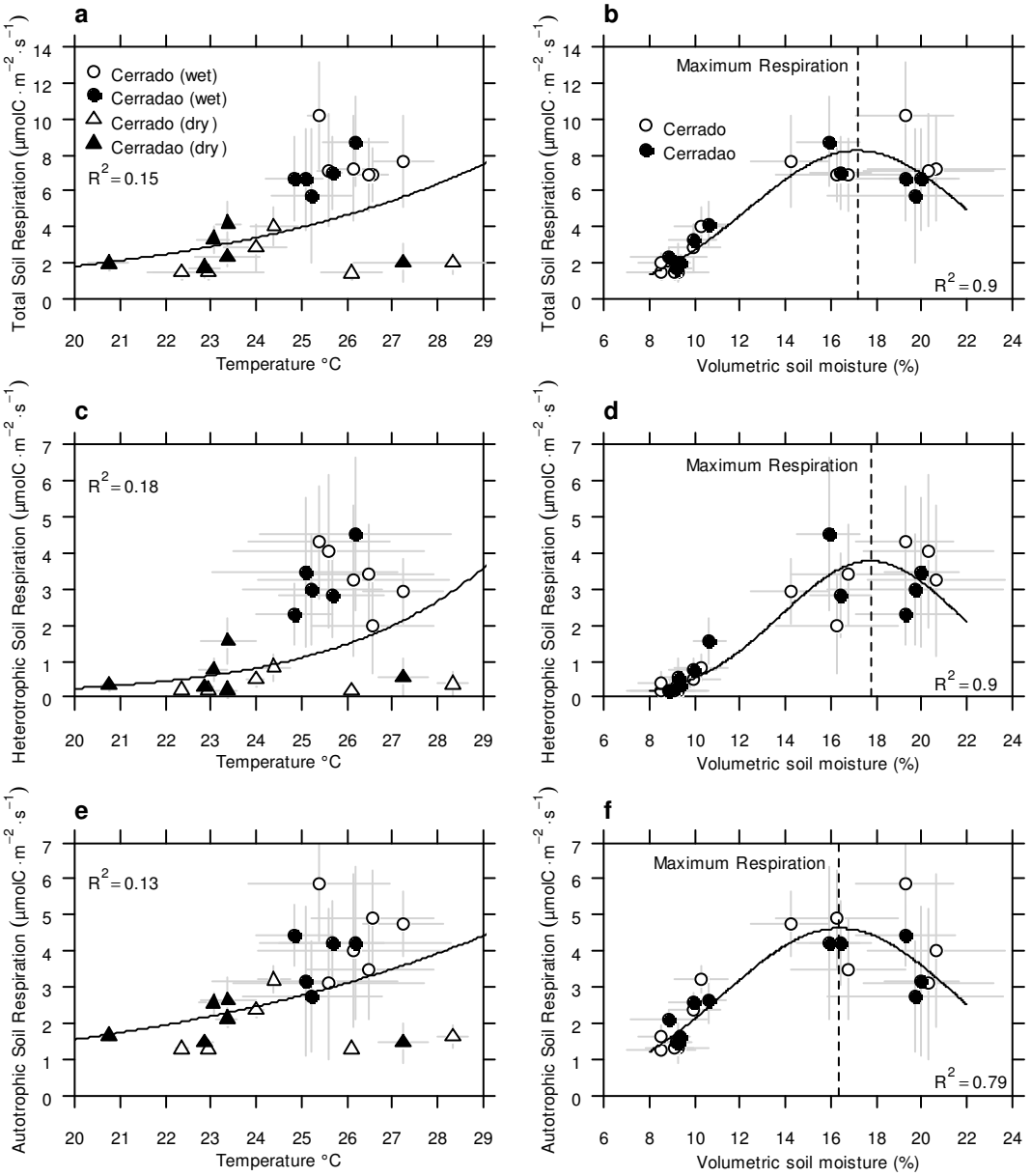

Figure 3.3-3: Total, heterotrophic and autotrophic components of soil respiration in two contrasting cerrado environments and their response to temperature, and soil moisture. Data points are monthly means (± one standard deviation, *n*=20).

Table 3.3-2: Ordinary least squared estimates for parameters in three different soil respiration models. Each model was applied to the total, heterotrophic, and autotrophic soil respiration components from two structurally contrasting cerrado environments.

Soil Respiration Component	Equation	Estimated parameters				R^2
		α	β_1	β_2	β_3	
Total	$R = \alpha e^{\beta_1 T} e^{\beta_2 \theta + \beta_3 \theta^2}$ (Model 1)	0.01 (±0.005)***	0.01 (±0.03)	0.73 (±0.11)***	-0.02 (±0.004)***	0.9
Heterotrophic		6.1×10^{-5} ($\pm4.8\times10^{-5}$)***	0.05 (±0.05)	1.11 (±0.2)***	-0.03 (±0.007)***	0.89
Autotrophic		0.02 (±0.009)***	2.3×10^{-3} (±0.03)	0.63 (±0.12)***	-0.02 (±0.004)***	0.78
Total	$R = \alpha e^{\beta_2 \theta + \beta_3 \theta^2}$ (Model 2)	0.01 (±0.003)***	—	0.74 (±0.1)***	-0.02 (±0.004)***	0.9
Heterotrophic		1.3×10^{-4} ($\pm9.3\times10^{-5}$)***	—	1.15 (±0.2)***	-0.03 (±0.007)***	0.9
Autotrophic		0.03 (±0.14)***	—	0.63 (±0.05)***	-0.02 (±0.004)***	0.79
Total	$R = \alpha e^{\beta_1 T}$ (Model 3)	0.08 (±0.07)	0.16 (±0.07)*	—	—	0.15
Heterotrophic		$6.\times10^{-4}$ (±0.0006)*	0.30 (±0.12)*	—	—	0.18
Autotrophic		0.20 (±0.14)	0.10 (±0.05)*	—	—	0.13

Notes: standard errors reported in parenthesis, *** indicates significance at less than 0.1%, ** indicates significance at less than 1%, * indicates significance at less than 5%.

Seasonal variation of soil respiration

Through the year mean monthly measurements of total soil CO_2 efflux ranged between 1.5 and 12.6 µmol $m^{-2}s^{-1}$ with a mean value of 5.2 µmol $m^{-2}s^{-1}$ across both the study sites. The variation in soil respiration closely followed seasonal variations in precipitation and consequently soil moisture (Fiure 3.3-1 and 3.3-2), where mean

wet season (November through April) soil CO_2 effluxes were 7.7 and 7.9 µmol $m^{-2}s^{-1}$, and mean dry season (May through October) fluxes were 2.2 and 2.6 µmol $m^{-2}s^{-1}$ for the cerrado *s.s.* and cerradão respectively. Therefore, about 75% of the total annual CO_2 efflux occurs during the wet season for both sites. Furthermore, during the wet season the heterotrophic component of the soil respiration accounted for 44 and 46% of the total, while in the dry season it only accounted for 17 and 24% for the cerrado *s.s.* and cerradão respectively (Figure 3.3-1c and Figure 3.3-2c).

Seasonal variation in soil temperature was found to be weakly correlated with all the components of soil respiration, within model 3 (Figure 3.3-3a, 3.3-3c, and 3.3-3d, and Table 2). Moreover, when accounting for soil moisture, within model 1, temperature was no longer a significant influence on any of the components of soil respiration (R^2 values and significance levels are reported in Table 3.3-2). In contrast, soil moisture (model 2) explained 90% of the seasonal variation in both the total and heterotrophic components of soil CO_2 efflux (Figure 3.3-3b and 3.3-3d), while the autotrophic respiration had an R^2 of 0.79 (Figure 3.3-3f and Table 3.3-2). The parabolic shape of the regression functions in Figure 3.3-3b, 3.3-3d, and 3.3-3f, demonstrate a diminishing effect of soil moisture on the individual components of soil respiration. Accordingly, the maximum respiration values occur at 17.2, 17.7 and 16.4 % soil moisture content for the total, heterotrophic, and autotrophic components respectively (Figure 3.3-3b, 3.3-3d, and 3.3-3f). Additionally, we relate autotrophic

respiration to fine root growth. Seasonal fluctuation in fine root productivity explained 80% of the seasonal variation in autotrophic respiration (Figure 3.3-4).

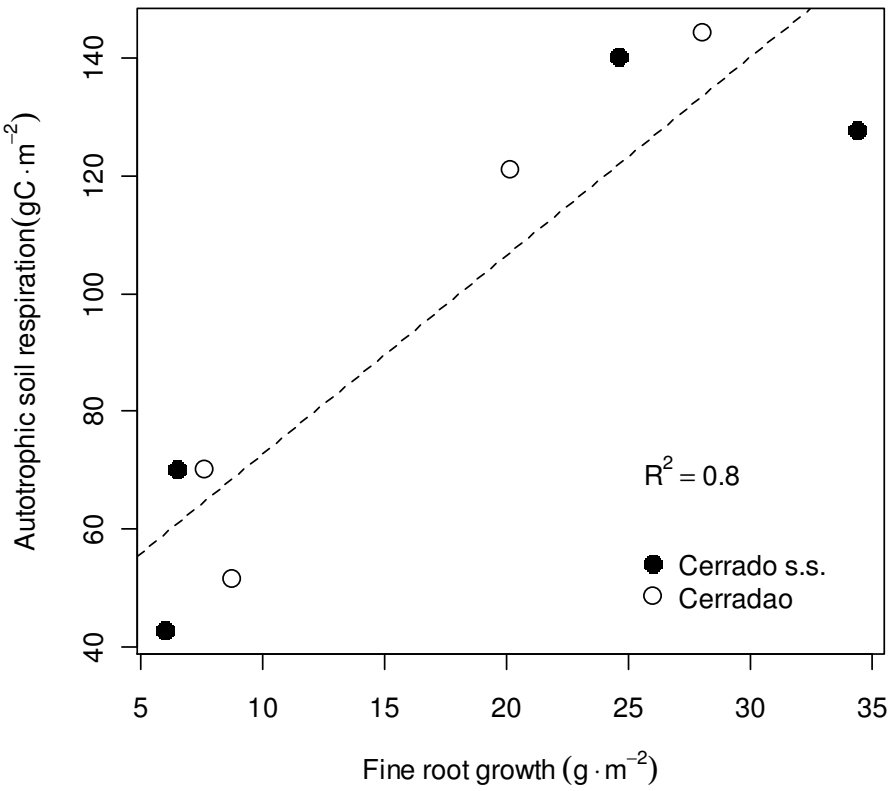

Figure 3.3-4: Response of autotrophic respiration to fine root growth in two contrasting cerrado environments. Each data point represents the mean (n=25) fine root growth over a three-month period and the total autotrophic respiration accumulated over the same time period. The regression line is linear: R_a=38.9+3.4(*dw*/*dt*) ($p<0.05$).

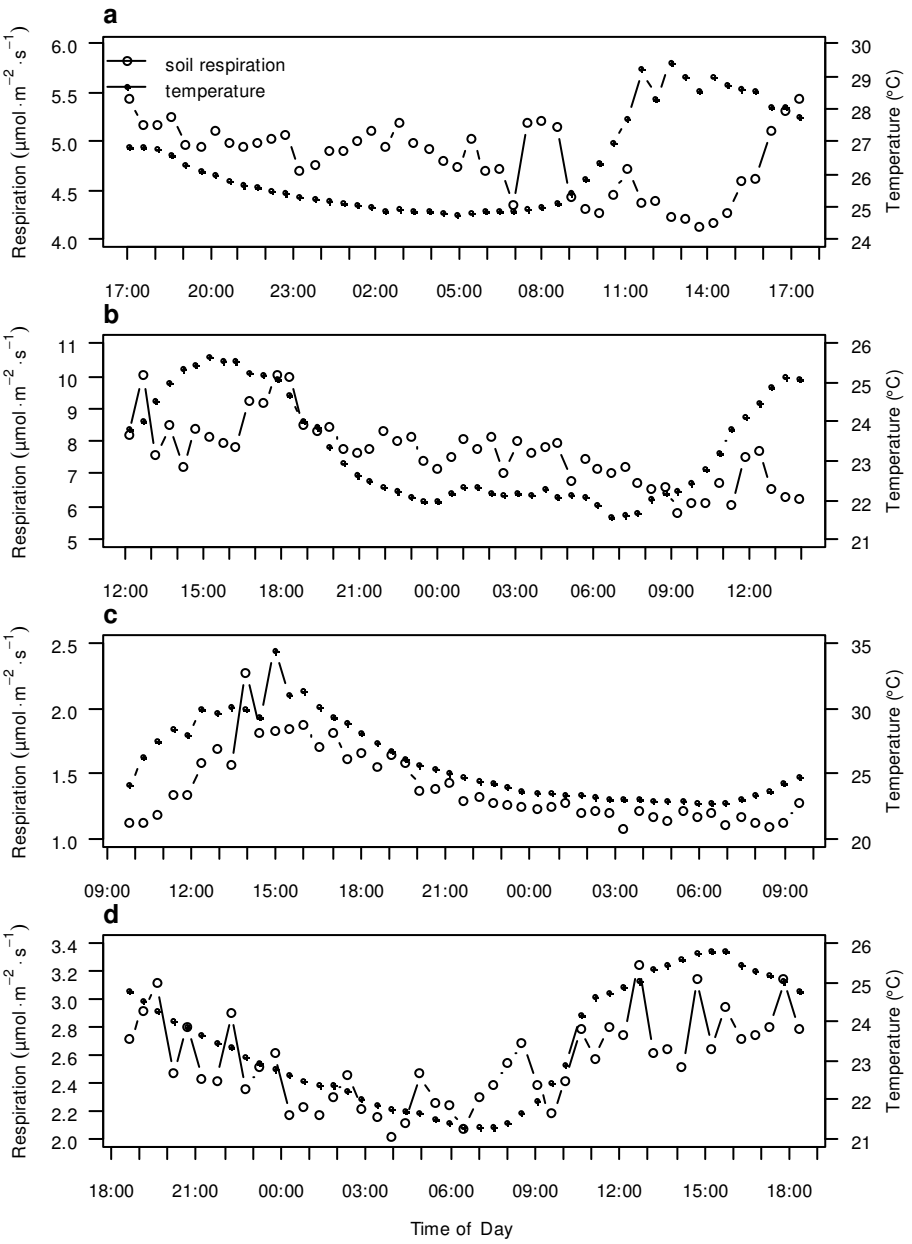

Figure 3.3-5: Diurnal variations in soil temperature and CO_2 efflux from two contrasting cerrado environments. (**a**) cerrado *s.s.*, total CO_2 efflux. (**b**) cerradão total CO_2 efflux. (**c**) cerrado *s.s.*, heterotrophic CO_2 efflux. (**d**) cerradão, heterotrophic CO_2 efflux.

Diurnal variation of soil respiration

Over a single diurnal cycle soil temperature in the cerrado *s.s.* varied by 11.8 ^{o}C while in the more shaded cerradão the variation was only 4.5 ^{o}C (Figure 3.3-5). Over the same diurnal cycle total CO_2 flux rates varied by 1.3 and 4.2 µmol $m^{-2}s^{-1}$ in the cerrado *s.s.* and cerradão respectively (Figure 3.3-5a and 3.3-5b). Furthermore, the flux variation for the heterotophic soil respiration for both sites was 1.2 µmol $m^{-2}s^{-1}$ (Figure 3.3-5c and 3.3-5d). The total soil CO_2 efflux was not correlated with temperature in either of the two sites (p=0.31), despite respiration rates varying by 4.23 µmol $m^{-2}s^{-1}$ across both sites (Figure 3.3-6a). In contrast, the heterotrophic CO_2 efflux was significantly correlated with temperature (p<0.05, R^2=0.74). After normalizing for site, the temperature response from the heterotrophic respiration corresponded to a Q_{10} of 1.6 (Figure 3.3-6b).

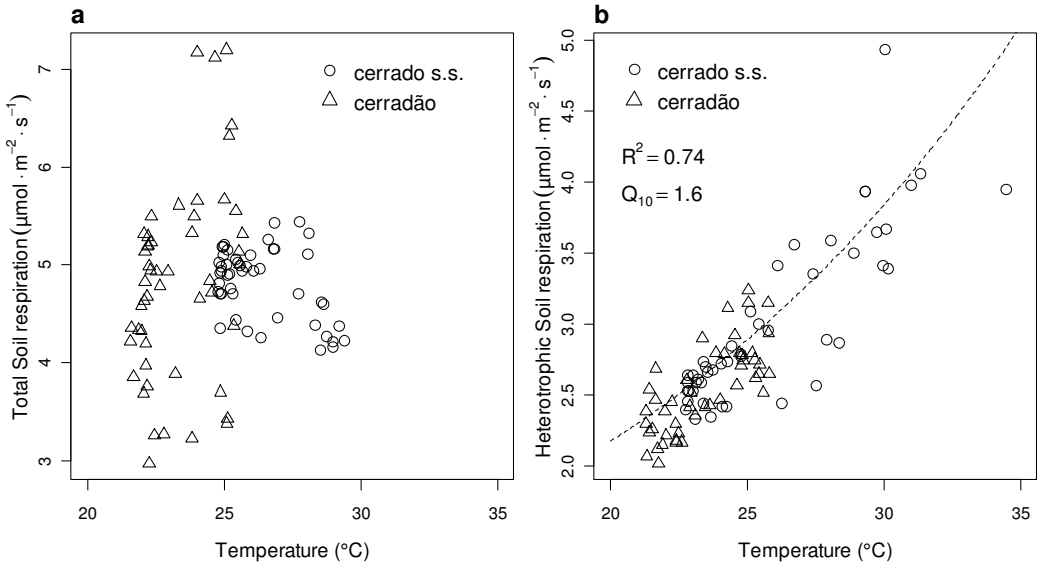

Figure 3.3-6: Relationship between diurnal variations in soil temperature and CO_2 efflux from two contrasting cerrado environments (flux values are normalised by site). (**a**) Total CO_2 efflux (p=0.31). (**b**) heterotrophic CO_2 efflux (p<0.05, R_h=0.7e$^{0.05T}$).

Contribution from the different components of soil CO_2 efflux

When estimating the annual carbon flux from soil respiration we excluded the unusually high flux measured in the cerradão plot in April (Figure 3.3-2c). Instead we estimated the flux for April from the average respiration rates from the two bracketing months. Accordingly, total soil respiration accounted for an annual carbon flux, of 17.41 and 17.22 Mg C ha^{-1} for the cerrado *s.s.* and cerradão respectively (Table 3.3-4). Autotrophic respiration was the main component of total soil respiration, accounting for 60 and 66% of the total in the cerradão and cerrado *s.s.* respectively. We observed a strong seasonal pattern of fine root production, with almost all growth occurring in the wet season (Figure 3.3-1d and Figure 3.3-2d). Furthermore, we estimate root growth accounted for 27% and 19% of the total

respiration for the cerrado *s.s.* and cerradão respectively. In the cerrado *s.s.* heterotrophic soil respiration resulted in an annual carbon flux of 6.49 Mg C ha^{-1}, while organic matter inputs amounted to 0.81 and 0.42 Mg C ha^{-1} from leaf litter fall and fine root production respectively. Similarly, in the cerradão heterotrophic soil respiration resulted in an annual carbon flux of 6.83 Mg C ha^{-1}, while organic matter inputs amounted to 1.64 and 0.29 Mg C ha^{-1} from leaf litter fall and fine root production respectively. Accordingly, there is 5.26 and 4.90 Mg C ha^{-1} being lost from the soil surface through heterotrophic respiration which is unaccounted for by measured organic matter input for the cerrado *s.s.* and cerradão respectively.

Table 3.3-3: Estimated stocks of carbon (Mg C ha^{-1}) in two cerrado environments.

Parameter	**Cerrado *s.s.***	**Cerradão**
Aboveground		
Tree foliage	1.6	2.9
Tree stem	21.1	51.9
Total tree	22.7	54.8
Belowground		
Fine roots	5.6 (±0.18)	5.5 (±0.22)
Course roots	39.9	87.4
Soil organic matter	28.7	27.7
Total belowground	74.2	120.6
Ecosystem		
Total ecosystem (above + belowground)	96.9	175.4

Discussion

Seasonal patterns of soil respiration

Mean monthly estimates of the rate of total soil CO_2 efflux (1.5-12.6 μmol m^{-2} s^{-1}) at both our study sites are at the high end of the range of reported fluxes in cerrado environments (Meir et al., 1996; Pinto et al., 2002).However, these results agree well with those of Valentine et al. (2008) who reported a range of 4.15 to 10.7 μmol m^2 s^{-1} in a deciduous dry forest within the zone of transition between the Amazonian rain forest and the cerrado in Mato Grosso, Brazil. Compared to other measurements in Amazonian forests our study shows greater seasonal variation, with wet season fluxes comparable to the maximum of previously measured flux rates (Davidson et al., 2000; Sotta et al., 2004).

Models of soil CO_2 efflux based on simple biochemical theory (Model 3) in which temperature governs enzyme activity, were a very poor predictor of the seasonal variation of all the soil respiration components in this study (Figure 3.3-3a, 3.3-3c, 3.3-3e, and Table 3.3-2). Furthermore, any correlation with soil temperature and soil respiration are confounded by seasonal variations in soil moisture. That is, soil temperature does not have a significant effect on soil CO_2 efflux if we account for seasonal variation in soil moisture (Table 2, Model 1). Therefore, within these seasonally dry ecosystems, soil moisture plays a central role in influencing the soil

CO_2 efflux for both the heterotrophic and autotrophic respiration components (Figure 3.3-3d and 3.3-3f). Conceptually, soil CO_2 efflux is thought to be low in dry conditions, increasing to a maximum rate for intermediate moisture levels, and decreasing at high soil moisture contents. The optimal water content for soil respiration is when the macropore spaces are mostly air-filled, thereby facilitating oxygen diffusion, and the micropore spaces are mostly water-filled, thus allowing diffusion of soluble substrates (Bunnell et al., 1977; Ilstedt et al., 2000). Accordingly, heterotrophic respiration appears to be limited by the diffusion capacity of soluble substrates at low soil moisture levels increasing to a maximum rate at 17.7% volumetric soil moisture.

There have been few studies that have addressed how soil moisture influences autotrophic soil respiration (Rey et al., 2002; Saiz et al., 2006; Almagro et al., 2009). At our study sites we observed a maximum soil respiration rate at 16.4% soil moisture for the autotrophic component. At low soil moisture levels, autotrophic respiration is likely limited by substrate supply from seasonal fluctuation in photosynthetic activity (Andrews et al., 1999; Craine et al., 1999; Högberg et al., 2001; Curiel-Yuste et al., 2004). As a result, during the wet season when productivity is highest fine root proliferation significantly increases soil CO_2 efflux (Fig. 4). In contrast, at high water content oxygen deficiency in the rooting zone may cause a depression in fine root proliferation and associated respiration (Drew, 1997).

Table 3.3-4: Estimated carbon fluxes (Mg C ha^{-1}) in two cerrado environments.

Processes	Cerrado *s.s.*			Cerradão		
	Wet season	**Dry season**	**Annual**	**Wet season**	**Dry season**	**Annual**
Aboveground						
Litter-fall	0.13 (±0.03)	0.68 (±0.09)	0.81 (±0.13)	0.37 (±0.06)	1.27 (±0.12)	1.64 (±0.18)
Belowground						
Belowground litter †	-	-	5.68 (±1.0)	-	-	5.19 (±0.96)
Fine root production	0.35 (±0.04)	0.07 (±0.01)	0.42 (±0.05)	0.22 (±0.04)	0.07 (±0.01)	0.29 (±0.05)
Total soil respiration	13.26 (±1.15)	4.15 (±0.32)	17.41 (±1.47)	12.37 (±1.15)	4.84 (±0.33)	17.22 (±1.48)
Heterotrophic respiration	5.78 (±0.77)	0.71 (±0.1)	6.49 (±0.87)	5.69 (±0.61)	1.14 (±0.17)	6.83 (±0.78)
Autotrophic respiration	8.12 (±1.97)	3.44 (±0.41)	11.56 (±2.38)	6.68 (±1.95)	3.70 (±0.5)	10.39 (±2.44)
Root growth respiration	2.58 (±0.34)	0.54 (±0.08)	3.12 (±0.42)	1.63 (±0.3)	0.54 (±0.08)	2.18 (±0.41)
Root maintenance respiration	5.54 (±2.54)	2.90 (±0.49)	8.44 (±2.8)	6.41 (±0.89)	3.16 (±0.58)	9.56 (±1.5)

Notes: propagated errors reported in parenthesis.
† Belowground litter is calculated as the difference between C loss from the soil via heterotrophic respiration and aboveground litter-fall, based on the assumption that soil C pool is in a steady and stable condition.

Diurnal patterns of soil respiration

In accordance with conventional biochemical theory, diurnal fluctuations of heterotrophic soil respiration responded to variations in soil temperature (Lloyd and Taylor, 1994). This relationship with temperature translates to a Q_{10} of 1.6 (Figure 3.3-6b), which is in agreement with other values reported for cerrado environments (Meir et al., 1996). Interestingly, diurnal fluctuations of the total soil CO_2 efflux in

the wet season showed no response to soil temperature (Figure 3.3-5a, 3.3-5b, and 3.3-6a). The decoupling of total soil CO_2 efflux from diurnal fluctuation in soil temperature indicates that autotrophic respiration was not influenced by temperature at our study sites. However, despite not responding to temperature, there was significant variation in total soil CO_2 efflux, particularly in the cerradão site, suggesting strong influence from other variables (Figure 3.3-5a and 3.3-5b). We speculate that autotrophic respiration may be limited by the photosynthetic supply of carbon, as stomata responded to high vapour pressure deficits associated with high mid-day temperatures (Tang and Baldocchi, 2005). Accordingly, we generally observe the lowest flux rates at both sites during the hottest part of the day giving tentative support to this theory. It appears that in dry tropical environments, the influence of diurnally fluctuating photosynthetic substrate supply on root respiration outweighs that of temperature.

Contribution from the different components of soil CO_2 efflux

Davidson et al. (2002) estimated that on average 25% of total soil CO_2 efflux is contributed by aboveground litter across all forest ecosystems. Our estimates are significantly lower, with aboveground litter only contributing between 5 to 8% of total annual CO_2 efflux. This probably reflects higher belowground carbon allocation

in the form of increased belowground productivity and associated autotrophic respiration (Chen et al., 2003). Based on the carbon-balance estimates for the cerrado *s.s.* and cerradão, belowground litter input was 5.7 and 5.2 Mg C $ha^{-1}yr^{-1}$ respectively, but only 6 to 7% of these carbon inputs could be accounted for by fine root production (Table 3.3-4). However, the values of net primary production of fine roots presented in this study (0.4 and 0.3 MgC ha^{-1}) are at the low end of the range (0.2-11.2 Mg C ha^{-1} yr^{-1}) of those reported for tropical forests (Priess et al., 1999; Trumbore et al., 2006; Metcalfe et al., 2008) and significantly lower than those reported for both drought-deciduous woodlands 5-19 Mg C ha^{-1} yr^{-1} (Menaut and Cesar, 1979), and tropical savannas 7-14.3 Mg C ha^{-1} yr^{-1} (Chen et al., 2003, 2004), indicating an underestimated values for our sites.

These relatively low values of fine root production could have resulted for several reasons including both methodological considerations and ecological processes. Fine root production estimates from ingrowth cores can result in underestimates due to unmeasured root mortality over the deployment period. It has been estimated in temperate forests that in-growth cores may underestimate fine root production by about 54% relative to the minirhizotron technique (Hendricks et al., 2006). Furthermore, ecological processes influencing belowground litter dynamics include carbon input from coarse root litter, mycorrhizae, and root exudates (McDowell et al., 2001; Hobbie et al., 2004). The low nutrient status of the soils at

our study site (Marimon Jr. and Haridasan, 2005) is a likely driver of a high level of mycorrhizal infection, which would allow host plants to access nutrients (Thomazini, 1974; Bustamante et al., 2004). It is therefore possible that a large proportion of the belowground litter contribution does not come directly from roots, but rather from their associated mycorrhizae. Högberg and Read (2006), suggested that we should view the finest roots as mycorrhizal hyphae, and that carbon in the fungal partner may turnover at a much faster rate than the fine roots themselves. It has been estimated that as much as 62% of the carbon entering the soil organic matter pool can come from mycorrhizal turnover, exceeding the input of both leaf litter and fine root turnover (Godbold et al., 2006). It is unlikely that any of these explanations alone can reconcile the magnitude of the discrepancy between the carbon balance and in-growth core approach for measuring belowground litter input. We propose a combination of these possible explanations, highlighting the need for further research in this area.

We estimate that 60 and 66% of the total soil CO_2 efflux originated from autotrophic respiration for the cerrado *s.s.* and cerradão respectively. This is at the high end of other estimates in tropical environments, which range from 46-63% (Trumbore et al., 1995; Malhi et al., 1999; Metcalfe et al., 2007), reflecting the high level of belowground carbon allocation in savanna ecosystems (De Castro and Kauffman, 1998). Autotrophic respiration consists of two components, growth

respiration and maintenance respiration. We estimate that approximately 23% of the autotrophic respiration can be attributed to growth at our study sites. Using this type of analysis we can identify the carbon balance associated with fine root growth, which is necessary to aquire new soil resources. We hypothesize that ecosystems with a fast turnover of fine roots will display higher respiration rates per unit belowground biomass, as they metabolise glucose associated with the synthesis of fine roots. In contrast, autotrophic respiration in ecosystems with slow fine root turnover may be expected to be dominated by maintenance respiration. However, an underestimate of fine root proliferation in this study would result in a over inflated estimate of root growth respiration.

Conclusions

Our study showed that more than 60% of the total CO_2 efflux originated from autotrophic respiration in cerrado environments, making it the dominant source of carbon released to the atmosphere. Therefore, it is important that we understand the mechanisms which control the seasonal and inter-annual fluctuations of this carbon source. Autotrophic respiration was strongly correlated with seasonal fluctuations of soil moisture, which may limit substrate supply from the canopy through a reduction in transpiration. Accordingly, seasonality in the synthesis of fine roots appears to the

main driver of fluctuations in autotrophic respiration. Heterotrophic decomposition was mainly governed by seasonal fluctuation in soil moisture, although diurnal temperature fluctuations were also shown to influence heterotrophic respiration. However, leaf and fine root litter combined to accounted for as little as 19-28 % of the heterotrophic respiration. Thus highlighting the need to better understand the belowground carbon input to heterotrophic soil respiration, including fine root proliferation, mycorrhizal turnover and root exudates, paying special attention to measurement techniques.

Part IV: Discussion

4.1 Critical Appraisal of the Earth Impedance Method

The earth impedance method is a recently established non-destructive method for measuring root surface area based on the electrical properties of root systems (Aubrecht et al., 2006; Čermák et al., 2006). In this method, the soil–root–stem system of an individual plant is connected to an electric circuit, and a low frequency current is applied through electrodes set in the stem and soil. According to the theory, the current passes between the plant root systems and the soil predominantly at the root tips through the same channels used in water up-take (Aubrecht et al., 2006). Accordingly, the measured electrical resistance is assumed to be related to absorbing root surface area when controlling for the longitudinal electrical resistance of the root system. Therefore based on the difference in conductivity of the tree tissue and the soil it is possible to estimate the magnitude of the contact surface area between the absorbing roots and the soil. The presumed relationships and contacts at the root soil interface are based on James Clerk Maxwell's equations of current continuity, which describes the movement of a conserved electrical charge. In the case of the single root and its interface with the soil the continuity equation can be expressed as:

$$I = \frac{U_1}{R_1} = \frac{U_2}{R_2} = \frac{U_1 S_1}{\rho L_1} = \frac{U_2 S_2}{\rho L_2} \qquad \text{(eq. 1)}$$

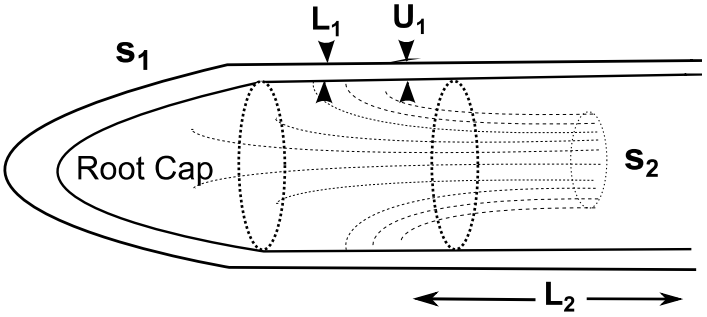

Figure 4.1-1: Current field passing between the soil solution and the conducting root cross-section (S_2). The thickness (L_1) of the absorbing zone (S_1) consists of the root cortex enveloped by an endo and exodermis (U_1 is the potential drop across distance L_1). L_2 is the distance between S_1 and S_2 (U_2 is the potential drop across distance L_2).

where I is the current (amperes) passing between the root and soil, ρ is the resistivity ($\Omega \cdot m$) of the respective water conducting tissue. The area (m^2) we are interested in is the magnitude of conducting root surface area (S_1). However, The drop in potential (U_1) across the radial path between the xylem and soil (L_1) is difficult to measure accurately particularly in the case of an entire root system. Consequently, the theoretical description of the method assumes that the conducting cross-sectional area of the xylem vessels is simply a continuation of the conducting root surface area, analogous to an open ended pipe, where S_1 is equivalent to S_2 (Aubrecht et al., 2006). Accordingly, the root is treated as a two-compartment system with an internal

compartment (xylem trachid elements) and an external (soil solution). The barrier between these two compartments is thus treated as a perfect conductor. However, in reality the barrier between the internal xylem elements and the soil potential electrode consists of the anatomically complex absorbing root tissue (Figure 4.1.2) and the soil solution between the absorbing root surfaces and the soil potential electrode. If the radial path between the xylem and soil solution were to significantly contribute to the measured resistance the magnitude of the conducting surface area would be larger.

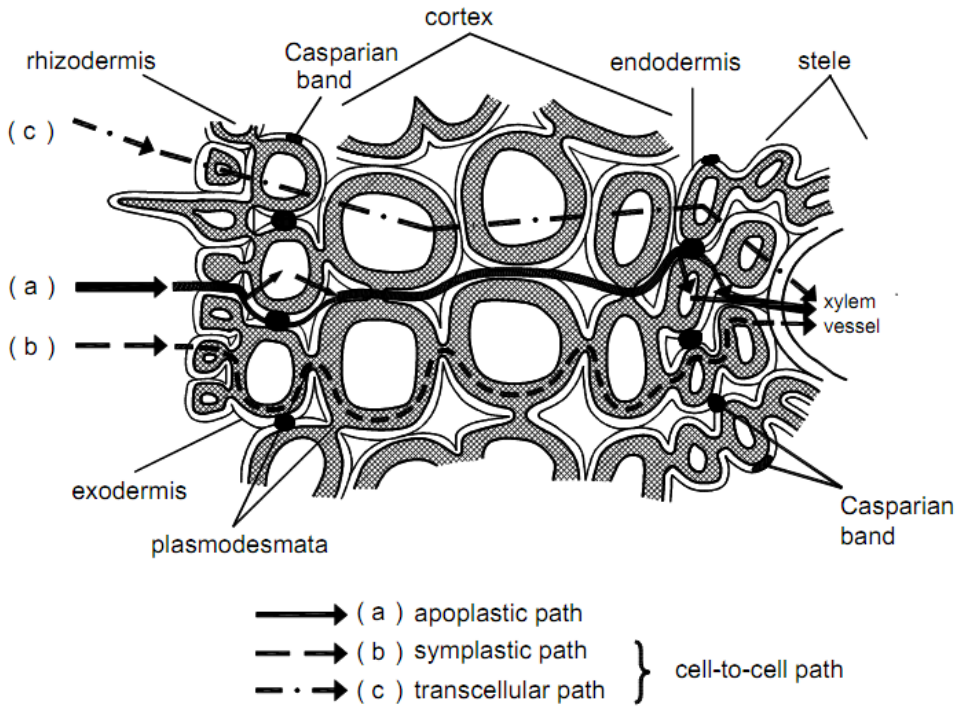

Figure 4.1-2: Pathway for the for the movement of water and solutes in absorbing roots. The apoplastic path **(a)** refers to the flow around protoplasts. The symplastic component defines flow from cell to cell via plasmodesmata **(b)**. Water passes across cell membranes within the trascellular path **(c)**. The Casparian bands in the exo- and endodermis partially interrupts the apoplastic path.

The radial hydraulic resistance of roots strongly depends on their anatomy, presenting a larger resistance to flow that the axial flow along the xylem vessels (Steudle, 2000a). The structure of absorbing roots optimally prevents leakage of nutrients from the xylem while at the same time offering an efficient path for the uptake of water (Steudle, 1994). A Casparian band forms in the radial wall of the endodermis, and acts as an osmotic barrier thus preventing leakage. There exists three parallel pathways for water uptake: (1) the apoplastic (which accounts for the vast majority of water uptake), (2), the symplastic, and (3) transcellular path (Steudle and Peterson, 1998). The Casparian band interupts the appoplastic path which is thought to be the rate limiting step to water transport across young roots (Steudle, 1994, 2000b; Steudle and Peterson, 1998). Furthermore, root anatomy which dictates water transport can be quite variable between species, habitats, and growth conditions. Therefore, it is likely that the same complex root anatomy that regulates water flow through roots will also present a significant resistance to electrical current flow. It seems reasonable that some datum on the electrical resistance of the absorbing root surfaces needs to be incorporated into any measurement of root area.

Current entering or exiting the root system of the tree must must pass through the soil before reaching the soil potential electrode. Therefore the resistivity of the soil will also play a significant role in our electrical circuit. The flow of electricity in

the soil is largely electrolytic, and is determined by the transport of ions dissolved in soil moisture. Consequently, soil moisture and highly mobile ions, such as K^+ and Cl^- could influence our measure of root surface area (Dvořák et al., 1981). Soil properties, such as soil moisture, salinity, and soil texture, have been observed to affect capacitance and impedance measurements of root systems (Dalton, 1995). Therefore, it is only reasonable to take measurements of absorbing root area using the earth impedance method when soil moisture content high enough (i.e. the field capacity), and consequently soil resistance will be minimized (Dalton, 1995; van Beem et al., 1998).

Another fundamental assumption of the earth impedance method is that the mature roots are electrically insulated from the soil. Therefore all current enters or exits the plant through its absorbing fine root surfaces. When a low frequency alternating current is a applied to plant tissue it flows through extracellular spaces (apoplastic channels), while its passage through the symplast is limited by the high impedance of the cellular membrane (Cole, 1968; Mancuso, 1999). The development of the Casparian band as roots mature, interrupts the apoplastic channels between the xylem and soil solution, thus increasing their electrical resistivity. However, the sympast becomes less resistant to the flow of current as the frequency increases (Cole, 1968; Cao et al., 2011). Therefore special attention should be paid to the frequency of current when measuring root systems. The use of high frequency

current may lead to the leakage of current into the soil through mature suberized roots which are not active in the uptake of water from the soil. However, fairly little is known about the contribution of older thickened roots to overall water uptake. Particularly for woody species, these roots are covered with several layers of suberized cells presumably acting as an electrical insulator. Usually it is thought that because of suberization, these arrays do not contribute significantly to overall water uptake. However, there is significant evidence suggesting older suberized roots may also contribute to water uptake (Kramer, 1946; MacFall et al., 1990; Macfall et al., 1991; Kramer and Boyer, 1995). It remains to be established if electrical current is also able to pass through these mature roots and how this may affect our estimate of absorbing root area (Urban et al., 2011).

4.2 Resource Capturing Ability: Links between form and function

Fundamental plant processes, such as carbon assimilation and associated evapo-transpiration, are significantly constrained by the supply of water from the soil to the leaf. Evaluation of hydraulic constraints on plant function could have considerable significance to models of forest productivity, and consequently biogeochemistry. However at present, most models of plant processes do not take account of hydraulic

limitations. A new generation of plant hydraulic models have identified the soil-root interface as the location of greatest hydraulic resistance, making it a fundamental factor affecting plant physiological processes (Sperry et al., 1998; Magnani et al., 2000; Williams et al., 2001). However, quantifying the soil-root interface at both the individual and stand level remains a significant challenge. Up to now, these models have been validated using fine root biomass measurements at the stand level (Magnani et al., 2000; Williams et al., 2001), or root length per leaf area of individual potted plants (Sperry et al., 1998). However, the recently developed EI method provides a means of measuring the soil-root interface of individual trees in the field, from which absorbing root surface area can be derived (Aubrecht et al., 2006; Čermák et al., 2006). The data obtained using this method can easily be scaled to the stand level (Butler et al., 2010).

How can we best quantify the absorbing surface area of root systems at the ecosystem level? Jackson et al. (1996, 1997) compiled published data on the global distribution of fine roots, introducing the idea of fine root area index (RAI_{fine}) as a parameter which is analogous and comparable with LAI. These authors estimated that tropical evergreen forests and tropical deciduous forests have a RAI_{fine} of 7.4 and 6.3 m^2m^{-2} respectively. Corresponding values for tropical grasslands/savannas are an order of magnitude higher (42.5); however this disparity may not be reflected in their water uptake per area of land. Our results for RAI_{fine} from tropical forests and woody

savannas are in strong agreement with values reported for deciduous forests, however we found no clear distinction between these different biomes (Table 2.4-2 & Figure 2.4-4). This suggests that simply compiling mean ecosystem values of RAI may not be very meaningful. Alternatively, the ratio of RAI_{fine} to LAI appears to be a more meaningful metric which varies along a continuum of vegetation structure (Figure 2.4-5). Here we introduce an alternative measure of root area index, $RAI_{absorbing}$, based on the EI method. The values of $RAI_{absorbing}$ recorded in this study vary by an order of magnitude, representing between 0.2 and 2.0 % of corresponding RAI_{fine} values within tropical ecosystems. Similarly, within a Sitka spruce forest the absorbing component accounted for between 3.7 and 19.6% of the total fine root surface area.

Why is there such a large disparity in the magnitude of values of RAI_{fine} and $RAI_{absorbing}$? The surface area of fine roots is conventionally estimated as the geometric surface area of small cylinders (fine roots are represented by small cylinders). In contrast, to quantify the soil-root contact surface area the EI method applies James Clerk Maxwell's (1861) equations of current continuity (Aubrecht et al., 2006). These equations are based on the fact that, in a similar way to mass or thermal energy, electrical charge cannot be destroyed and is therefore conserved in a closed system. For a steady state one dimensional flow in a pipe or channel with a cross sectional area S, the continuity equation shows a constancy of flow rate jS =

constant. Current density, *j*, is a measure of density of flow of a conserved electrical charge (amperes/m^2). Through this theory the EI method estimates the porous surface area used in water uptake. At present no alternative method allows us to independently verify the accuracy of this measure of absorbing root surface area. However, our estimates of $RAI_{absorbing}$ are similar in magnitude to the porous leaf surface area ($LAI_{transpiring}$ stomatal pore area per unit ground area). In accordance with pipe model theory (Shinozaki et al. 1964), this indicates that our measures of absorbing root surface are reasonable (Table 2.3-1 & Figure 2.4-6).

If we are to view mycorrhizal hyphae as the finest roots they must also be included in any estimate of the soil-root interface (Högberg and Read, 2006). Principally, rhizomorphs are considered to be a major site of nutrient and water transfer from mycorrhizal symbionts to the plant (Duddridge et al., 1980; Smith and Smith, 1990; Cui and Nobel, 1992; Smith et al., 1994, 2003). The efficiency of both nutrient and water transfer from the fungus to the plant (or carbon in the opposite direction) could be expressed as a flux per unit surface area. The surface area of the plant-fungal interface can now be quantified using laser scanning microscopy (Dickson and Kolesik, 1999; Schweiger et al., 2002). However, to the best of our knowledge there have been no attempts at ecosystem-level estimates. This issue is further complicated by evidence suggesting that fungal species differ in there capacity to transport water to recipient host plants (Plamboeck et al., 2007).

However, it remains unclear whether absorbing root area measured by the EI method represents only fine roots, or incorporates their mycorrhizal partners.

Here we have compared traditional measures of fine root surface area with estimates of absorbing root area at the stand level. Surprisingly, we found no strong correlation between fine root biomass and EI measurements of root absorbing surface area, which suggests that these different approaches to quantifying the resource exchange surface area between the vegetation and soil are not direct substitutes (Table 2.3-1 & Figure 2.4-5). Micro-scale investigation has identified a short zone (≈ 100–200 mm) behind the root tip as the absorbing surface area of fine roots (Steudle, 1994). Therefore the EI method is more likely to be correlated to the number of active root tips rather than fine root biomass as a whole. Our results lead us to questioning the suitability of fine root biomass as a proxy for water uptake ability.

The role of deep roots in water uptake is still not well understood, however in seasonally dry environments they are presumed to extend the period of photosynthesis and transpiration during the dry season. In eastern Amazonia an evergreen canopy, covering an area of more than 1,000,000 km^2, is sustained principally by water extracted from 2-8 meters below the soil surface (Nepstad et al., 1994). However, discrepancies exist between the amount of root biomass and the rate of water uptake from the soil; for example, low root densities in deep soil have been shown to significantly contribute to rates of evapo-transpiration during periods of

drought (Bruno et al., 2006; Quesada et al., 2008). Accordingly, further insight could be gained by adapting the EI method to differentiate absorbing root surface area measurements in distinct soil layers. This could be achieved by sequentially removing soil layers and their associated roots and repeatedly measuring the same individuals. These measurements could then be associated with fine root area measurements, thus allowing us to quantify the efficiency of deep roots for water uptake.

Over the short term plants respond to soil and plant water deficits by reducing stomatal conductance (Jarvis, 1976). However, over longer time periods adjustments in hydraulic architecture and intrinsic physiology can occur (Mencuccini and Grace, 1995; Magnani et al., 2000). For example, a combination of leaf shedding and fine root growth triggered by water stress can result in a higher root to leaf area ratio, thus maintaining a favourable water balance (Tyree et al., 1993; Ewers et al., 2000; Hacke et al., 2000). For example, Hacke et al. (2000) found that trees growing on sandy, drought-prone soil, showed a six-fold increase in the root to leaf area ratio relative to similar trees growing on loamy soil. However, there is growing evidence that both water and nutrient availability interact to influence root to leaf area ratios (Keyes and Grier, 1981; Haynes and Gower, 1995; Ewers et al., 2000). A study focusing on the hydraulic architecture of *Pinus taeda* trees found that a fertility treatment decreased the root to leaf area ratio without significantly limiting water extraction during

drought (Ewers et al., 2000). Similarly, our results demonstrate that tropical savanna vegetation growing on dystrophic soil had higher fine root to leaf area ratios than more fertile forest sites. However, the absorbing root area did not reflect this relatively high investment in fine roots. This apparently excessive investment in fine root area relative to leaf area likely reflects requirements for nutrient uptake rather than water (Sperry et al., 1998).

A related hypothesis is that plants growing in a seasonally dry climate should have a relatively high absorbing root to leaf area ratio, in order to minimize dangerous water potential deficits during periods of drought. However, we estimated dramatically higher $RAI_{absorbing}$:$LAI_{transpiring}$ ratios in a Sitka spruce forest in Scotland compared to the tropical dry-deciduous and woody savannas in central Brazil. The volume of water moving across a given surface area, A^i, (where i could be root absorbing surface area, sapwood area, or the transpiring leaf area) is also influenced by the volume flux density of water across component *i*, J_{Vw} (m^3 m^{-2} s^{-1}). In steady state conditions the flow of water across each component, $J_{Vw} \cdot A^i$ (m^3 s^{-1}), should be constant as nearly all the water taken up by the roots is lost through transpiration (Equation 1):

$$J_{Vw}^{i} \cdot A^{i} = \frac{\Delta \psi^{i}}{R^{i}} \cong CONSTANT \qquad (1)$$

Therefore any differences in the hydraulic resistances of water conducting organs (R^i) between these two contrasting environments will complicate any comparisons. Molecular studies of Aquaporins indicate they may be important for bulk water flow though absorbing roots (Luu and Maurel, 2005). Aquaporins are membrane water-channel proteins that facilitate water movement along a passive gradient in water potential. For example, the hydraulic conductivity of root cortex cells, as measured with a cell pressure probe, was reduced by upto 30% by altering the expression of an aquaporin gene (Javot et al., 2003), while elsewhere, over expression of aquaporins in rice plants was shown to increase the radial hydraulic conductivity by 140% which resulted in an increase in the mass ratio of shoot to root of 150% (Katsuhara et al., 2003). There is also evidence to suggest that aquaporins interact with mycorrhizal fungi to regulate root hydraulic properties (Aroca et al., 2007).

More generally, root:shoot biomass ratios have been estimated to be about three times higher in the Brazilian Cerrado relative to their forest counterparts (Castellanos et al., 1991; Abdala et al., 1998; De Castro and Kauffman, 1998). These distinct allocation patterns have often been interpreted to reflect a greater belowground resource capturing ability, however the absorbing root area data presented in this thesis have brought this interpretation into question (Figure 2.4-5). One alternative hypothesis is that the relatively high coarse root biomass found in savannas serves a capacitance (water storage) or energy storage (carbohydrates)

function. Domec et al. (2006) found that daily embolism in xylem conduits of lateral roots of neo-tropical savanna trees were refilled during night-time transpiration. The authors proposed that such a mechanism could allow the stomata to maintain the structural integrity of the hydraulic pipeline within the stem. Alternatively, high root: shoot ratios are also thought to be an adaptation to reduce exposure of biomass to fire (De Castro and Kauffman, 1998).

In 1948, van den Honert drew parallels between the movements of water in plants and the flow of electricity in accordance with Ohm's laws of electrical conductivity. With the development of the EI method we may now be able to physically quantify the relationship between hydraulic and electrical resistances. In this thesis we showed that stem resistivity varied with tree size and consequently tracheid diameter (Butler et al., 2010). Speculatively, we may be able to quantify xylem hydraulic resistance in terms of its electrical resistance. Similarly, axial root hydraulic resistance is proportional to the absorbing root surface area and axial root resistivity (specific resistance). Results from pressure probe experiments have provided estimates of hydraulic root resistivity, where flow is driven by both pressure and osmotic forces (Steudle, 1994). However, these estimates are expressed per unit surface area of fine root. Accordingly, there is an opportunity to combine root pressure probe data with electrical impedance measurements, resulting in hydraulic resistivity expressed per unit electrical impedance. This would allow us to

better interpret earth impedance data with respect to water relations. A foreseeable complication with this approach may arise because hydraulic resistances are not constant. At high water potential deficits the resistance to water flow increases. Nonetheless, this concept would merit further investigation.

In conclusion, within this thesis we have used a tested method for quantifying the absorbing root surface area. We have gone on to use the resulting data in a novel analysis, combing above and belowground exchange surface area for resource capture at the ecosystem level. Here we investigated potential links between biomass allocation patterns between leaves and fine roots and resource capturing ability. We found a consistent relationship for the allocation pattern between leaves and fine roots across a broad gradient of vegetation structure. Moving from dense forest to open savanna the fine root area to leaf area ratio increased dramatically. The absorbing root area (measured with the EI method) to leaf area ratio also showed a consistent and strong relationship across the same vegetation gradient. However, in contrast to the biomass allocation pattern (RAI_{fine}:LAI ratio) the absorbing root area to leaf area ratio decreased from dense forest to open savanna. Our results question the widely-held assumption that ecosystem fine root surface area provides a measure of water uptake ability. It appears that the use of fine root area measurements to estimate plant water uptake in terrestrial vegetation models may not always be appropriate, and instead the models need to be integrated with a better understanding

of the active area of exchange between the roots and soil (Aubrecht et al., 2006; Čermák et al., 2006; Butler et al., 2010). The analysis presented in this thesis examines a more mechanistic approach to understanding fine root functioning in relation to water uptake and how interaction with nutrient limitation may also be a controlling factor. We can now build on this initial analysis to create a more integrated approach which would incorporate $RAI_{absorbing}$ measurements and soil hydraulic properties along a depth profile allowing us to better quantify soil water supply to the canopy.

4.3 Belowground Carbon Cycling: Progress and challenges

Seasonally dry environments are prevalent within tropical regions; however they are dramatically under-represented in studies of soil respiration (Meir et al., 1996; Pinto et al., 2002; Chen et al., 2002b; Valentini et al., 2008). We have demonstrated in this study that soil respiration within these environments is strongly linked to plant phenology and to the belowground production of plant litter (Figure 3.3-6 & Figure 3.3-7). Therefore, to advance our understanding of the contribution of soil processes to the atmospheric concentration of carbon dioxide we must gain a greater appreciation of the coupling between the canopy and belowground processes.

The fraction of photosynthetically fixed carbon allocated belowground often exceeds the sum of aboveground litterfall and respiration, making it the dominant carbon sink component in an ecosystem (Janssens et al., 2001), but quantifying this fraction continues to be a major challenge at both short and long timescales. Davidson et al. (2002) used a carbon balance approach to quantify the belowground flux of carbon (assuming stocks of soil organic matter, roots and litter):

$$TBCA = R_{soil} - Litterfall \quad (1)$$

where *TBCA* is the total belowground carbon allocation, R_{soil} is total annual soil respiration, and *Litterfall* is the total annual leaf litterfall.

Davidson et al. (2002) estimated that TBCA in mature forest sites was on average twice the annual aboveground litterfall. The limited amount of comparable data from savanna vegetation indicates that soil respiration represents a larger flux relative to aboveground litterfall than that observed for mature forests (Figure 4.3-1). On average TBCA for three savanna sites (including the two sites from the study in this thesis) was ten times the annual aboveground litterfall. We acknowledge that significant respiration by grasses within woody savannas could be a confounding factor to estimates of belowground carbon allocation, but this is unlikely to account for the size of the difference estimated between forest and savanna.

Soil respiration is the dominant path for carbon leaving terrestrial ecosystems. In many models, soil respiration has been mostly treated as a heterotrophic process and assumed to respond to temperature and moisture (Raich and Schlesinger, 1992; Kicklighter et al., 1994). However, soil respiration processes includes both autotrophic respiration by roots, mycorrhizae, and the rhizosphere, as well as the decomposition of litter inputs comprising roots, mycorrhizae, and foliage (heterotrophic respiration) (Bhupinderpal et al., 2003; Godbold et al., 2006). Only soil organic matter consumed by heterotrophic micro-organisms has the potential to be stored as soil carbon. On the other hand, autotrophic respiration directly releases CO_2 from the soil. To be able to understand the underlying processes that contribute to this complex composite flux, as well as the factors which affect it, the individual components need to be disentangled. That is, the separation of these distinct respiration processes is vital for advancing our understanding and modelling of soil respiration.

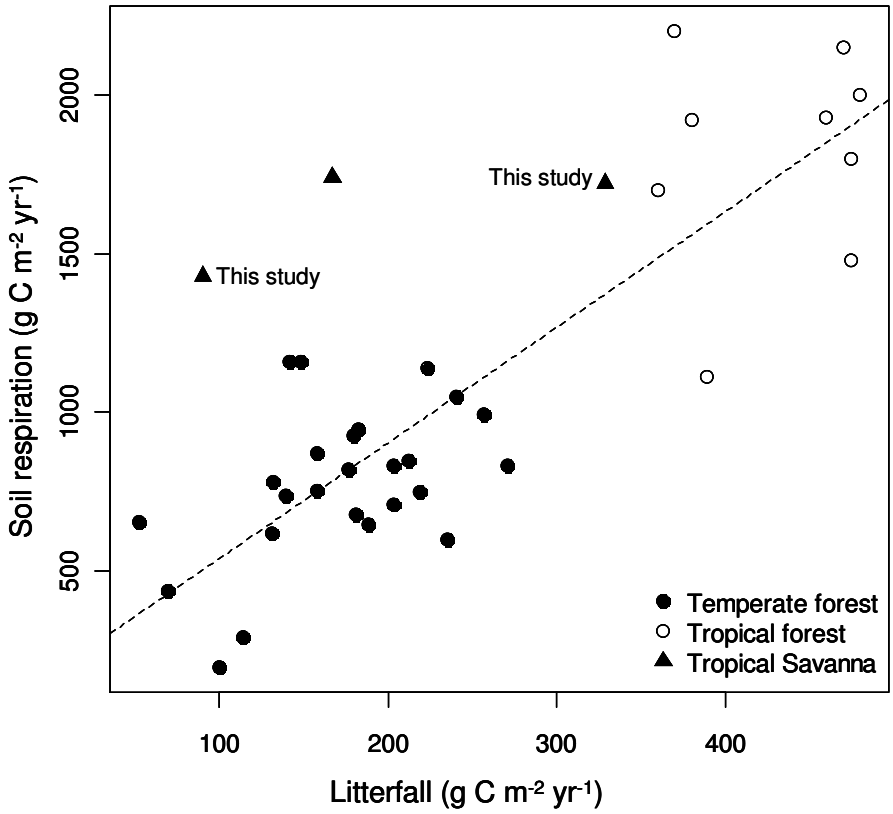

Figure 4.3-1: Correlation of soil respiration with the amount of aboveground litterfall across many forest and savanna ecosystems. Data were taken from Davidson et al. (2002) with additional savanna data points from Chen et al. (2003), and this study. The regression line excludes the savanna sites (p<0.01, R^2=0.73).

The autotrophic component of soil respiration is strongly dependent on recent aboveground photosynthesis. It has been clearly demonstrated that as much as half of

the soil CO_2 efflux has its origins in carbon recently fixed by the canopy (Andrews et al., 1999; Craine et al., 1999; Hogberg et al., 2001). Consequently, aboveground photosynthetic activity, in conjunction with the prevailing pattern of carbon allocation patterns is strongly linked to CO_2 efflux at the soil surface (Craine et al., 1999; Nadelhoffer, 2000; Curiel-Yuste et al., 2004). In this thesis we demonstrated links between phenological fluctuations in leaf area, root growth and soil respiration in a semi-deciduous savanna environment (Figure 3.3-6 & Figure 3.3-7). It follows that the extent to which phenological processes are genetically controlled will have important implications for the way in which soil respiration responds to a changing climate (Bullock and Solis-Magallanes, 1990; Williams et al., 1997, 2001; Oleksyn et al., 2000), although our understanding of both the biotic and abiotic control of root phenology is particularly limited in tropical environments (Pregitzer et al., 2000; Tierney et al., 2003).

Plant vegetative cycles, such as the timing and duration of both foliage and fine root shedding and re-growth, determine exchange periods of carbon dioxide and water between the earth surface and the atmosphere (Keeling et al., 1996). Within tropical ecosystems there is evidence to suggest there is some degree of plasticity in canopy phenology, with the controlling factors being seasonal rainfall (Bie et al., 1998; Bach, 2002) or photoperiod (Borchert and Rivera, 2001; Archibald and Scholes, 2007). However, these climatic factors often interact concurrently to control

phenology (Jolly et al., 2005). Nevertheless, this apparent plasticity may also be constrained by genetic limitations, consequently limiting the degree of response to environmental change (Billington and Pelham, 1991). Similarly, root growth and phenology are likely to be strongly linked to canopy processes and cycles (Comas et al., 2005).

In conclusion, the flux of carbon to the atmosphere is strongly dominated by soil respiration in savanna ecosystems. In this study we found that autotrophic respiration was the dominant source of CO_2 efflux at the soil surface. However, there were major fluctuations in this source between the wet and dry season, which we have directly linked to the seasonality of fine root growth. The observed reduction in root growth is likely to be limited by a lower photosynthetic capacity during the dry season. Importantly, we were unable to demonstrate that autotrophic respiration responded to temperature (Figure 3.3-1), probably because substrate supply from the canopy was limiting. Therefore, our data suggest that a measure of phenological processes is needed to realistically simulate belowground respiration within seasonally dry environments. Rates of heterotrophic respiration were related to temperature fluctuations (especially diurnal cycles), but seasonal changes in soil moisture were a dominant controlling factor over the course of the year. Since we found that root and leaf litter inputs to the soil only accounted for 28% of the heterotrophic respiration, it is likely that mycorrhizae make a dominant contribution

to the soil organic matter in these environments. This highlights the urgent need for further studies on mycorrhizal turnover within tropical savannas. It is becoming increasingly clear that roots and microbes respond differently to environmental conditions; therefore they should be treated as separate processes within a modelling context.

Part V: Appendix

5.1 Soil Respiration Chamber

Enclosed chambers have been used to measure soil respiration for many decades. However, when a chamber is placed over the soil surface the concentration of trace gases within the chamber headspace begins to rise, thus altering the natural diffusion gradient. Consequently, enclosure dimensions and deployment times should be carefully selected so that the negative feed back on the diffusion rate is minimised. In this study we used a chamber with a high volume:basal area ratio to avoid rapid feedback to the concentration gradient driving molecular diffusion (Figure 5.1-1) (Conen and Smith, 2000; Matthias et al., 1978).

Fans are sometimes used to mix the air within the chamber; however this can create artefacts by altering the concentration gradient (Le Dantec et al., 1999). Excessive air movement can disrupt the boundary layer at the soil surface thus increasing the CO_2 concentration gradient at the soil surface and over estimating the flux. Consequently, we adopted a method for mixing the air whereby air enters the chamber through a perforated circular manifold at the bottom of the chamber. Concurrently, air is extracted from the top of the chamber trough a similar manifold, thus naturally mixing the air (Figure 5.1-1).

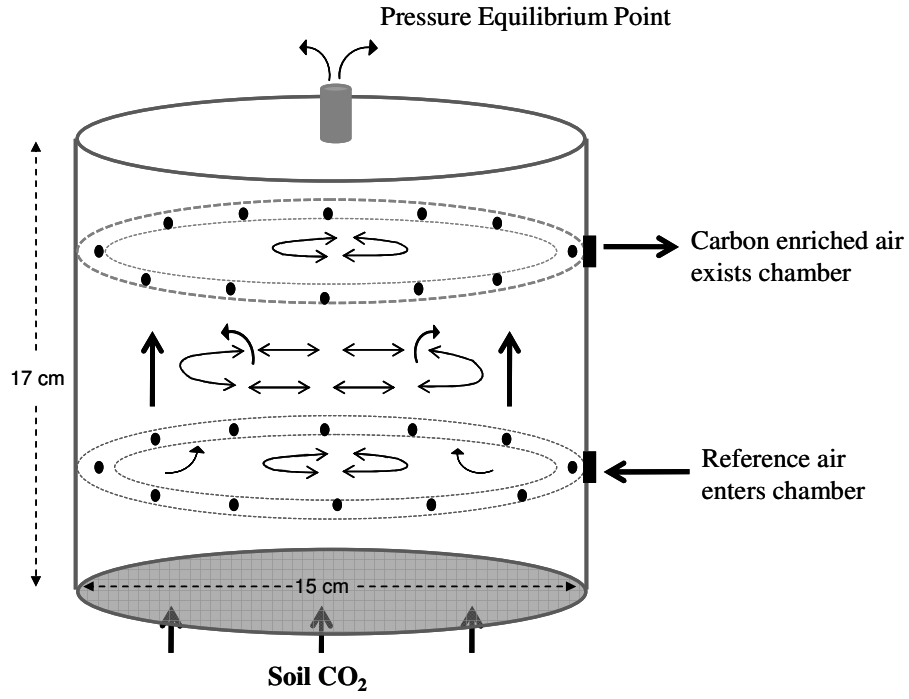

Figure 1: Soil respiration chamber design, showing dimensions and air flow.

It is generally recommended that flux chambers have vents to equilibrate the pressure between the chamber and atmosphere (Davidson et al., 2002). A small amount of gas exchange will occur through the vent, thus diluting the air in the chamber. However, it has been estimated that the resulting error is less than 3% (Longdoz et al., 2000). A much larger error can result either from an over pressurized chamber impeding diffusion, or an under pressurized chamber sucking air out of the soil. In order to ensure the pressure within the chamber was at equilibrium with the atmosphere at all times, we used a stainless steel vent 10 cm long with an internal diameter of 2 mm (Hutchinson and Mosier, 1981).

Bibliography

Aasamaa, K., Sober, A., 2001. Hydraulic conductance and stomatal sensitivity to changes of leaf water status in six deciduous tree species. Biologia Plantarum 44, 65–73.

Abdala, G., Caldas, L., Haridasan, M., Eiten, G., 1998. Above and belowground organic matter and root:shoot ratio in a cerrado in central Brazil. Brazilian Journal of Ecology 2, 11-23.

Almagro, M., López, J., Querejeta, J., Martínez-Mena, M., 2009. Temperature dependence of soil CO2 efflux is strongly modulated by seasonal patterns of moisture availability in a Mediterranean ecosystem. Soil Biology and Biochemistry 41, 594-605.

Andrews, J.A., Harrison, K.G., Matamala, R., Schlesinger, W.H., 1999. Separation of Root Respiration from Total Soil Respiration Using Carbon-13 Labeling during Free-Air Carbon Dioxide Enrichment (FACE). Soil Science Society of America Journal 63, 1429-1435.

Archibald, S., Scholes, R., 2007. Leaf green-up in a semi-arid African savanna - separating tree and grass responses to environmental cues. Journal of Vegetation Science 18, 583-594.

Arens, K., 1963. As plantas lenhosas dos campos cerrados como vegetação adaptada às deficiências minerais do solo, in: III Simpósio Sobre o Cerrado. Edgard Blucher /EDUSP, São Paulo, pp. 13–115.

Aroca, R., Porcel, R., Ruiz-Lozano, J.M., 2007. How does arbuscular mycorrhizal symbiosis regulate root hydraulic properties and plasma membrane aquaporins in Phaseolus vulgaris under drought, cold or salinity stresses? New Phytologist 173, 808-816.

Aubrecht, L., Stanek, Z., Koller, J., 2006. Electrical measurement of the absorption surfaces of tree roots by the earth impedance method: 1. Theory. Tree Physiology 26, 1105-1112.

Bach, C.S., 2002. Phenological patterns in monsoon rainforests in the Northern Territory, Australia. Austral Ecology 27, 477-489.

van Beem, J.S., Zobel, M.E., Rich, W., 1998. Estimating Root Mass in Maize Using a Portable Capacitance Meter. Agronomy Journal 90, 566.

Beerling, D.J., Osborne, C.P., 2006. The origin of the savanna biome. Global Change Biology 12, 2023-2031.

Belcher, J.W., Keddy, P.A., Twolan-Strutt, L., 1995. Root and shoot competition intensity along a soil depth gradient. Ecology 83, 673-682.

Bhupinderpal, S., Nordgren, A., Löfvenius, M., Högberg, M., Mellander, P., Högberg, P., 2003. Tree root and soil heterotrophic respiration as revealed by girdling of boreal Scots pine forest: extending observations beyond the first year. Plant, Cell & Environment 26, 1287-1296.

Bie, S.D., Ketner, P., Paasse, M., Geerling, C., 1998. Woody plant phenology in the West Africa savanna. Journal of Biogeography 25, 883-900.

Billington, H.L., Pelham, J., 1991. Genetic Variation in the Date of Budburst in Scottish Birch Populations: Implications for Climate Change. Functional Ecology 5, 403-409.

Bird, M.I., Veenendaal, E., Moyo, C., Lloyd, J., Frost, P., 2000. Effect of fire and soil texture on soil carbon in a sub-humid savanna (Matopos, Zimbabwe). Geoderma 94, 71-90.

Bird, M.I., Veenendaal, E.M., Lloyd, J.J., 2004. Soil carbon inventories and delta13C along a moisture gradient in Botswana. Global Change Biol 10, 342-349.

Bloom, A.J., Chapin III, F.S., Mooney, H.A., 1985. Resource limitation in plants-An economic analogy. Annual Reviews in Ecology and Systematics 16, 363-392.

Bond, W.J., Woodward, F.I., Midgley, G.F., 2005. The global distribution of ecosytems ina world without fire. New Phytologist 165, 525-538.

Boone, R.D., Nadelhoffer, K.J., Canary, J.D., Kaye, J.P., 1998. Roots exert a strong influence on the temperature sensitivityof soil respiration. Nature 396, 570-572.

Borchert, R., Rivera, G., 2001. Photoperiodic control of seasonal development and dormancy in tropical stem-succulent trees. Tree Physiol 21, 213-221.

Brazier, J.D., 1970. The effect of spacing on the wood density and wood yields of Sitka spruce. Forestry 43, 22-28.

Breda, N.J.J., 2003. Ground-based measurements of leaf area index: a review of methods, instruments and current controversies. Journal of Experimental Botany 54, 2403-2417.

Breshears, D.D., 2006. The grassland–forest continuum: trends in ecosystem properties for woody plant mosaics? Frontiers in Ecology and the Environment 4, 96-104.

Bristow, K.L., Campbell, G.S., Calissendorff, C., 1984. The effects of texture on the resistance to water movement within the rhizosphere. Soil Science Society of America Journal 48, 266.

Bruno, R.D., Rocha, H.R.D., Freitas, H.C.D., Goulden, M.L., Miller, S.D., 2006. Soil moisture dynamics in an eastern Amazonian tropical forest. Hydrological Processes 20, 2477-2489.

Bullock, S.H., Solis-Magallanes, J.A., 1990. Phenology of Canopy Trees of a Tropical Deciduous Forest in Mexico. Biotropica 22, 22-35.

Bunnell, F., Tait, D., Flanagan, P., Van Clever, K., 1977. Microbial respiration and substrate weight loss--I: A general model of the influences of abiotic variables. Soil Biology and Biochemistry 9, 33-40.

Bustamante, M.M.C., Martinelli, L.A., Silva, D.A., Camargo, P.B., Klink, C.A., Domingues, T.F., Santos, R.V., 2004. 15N natural abundance in woody plants and soils of central Brazillian savannas (Cerrado). Ecological Applications 14, 200-213.

Butler, A., Barbier, N., Cermak, J., Koller, J., Thornily, C., McEvoy, C., Nicoll, B., Perks, M., Grace, J., Meir, P., 2010. Estimates and relationships between aboveground and belowground resource exchange surface areas in a Sitka spruce managed forest. Tree Physiol doi:10.1093/treephys/tpq022.

Cao, Y., Repo, T., Silvennoinen, R., Lehto, T., Pelkonen, P., 2010. An appraisal of the electrical resistance method for assessing root surface area. J. Exp. Bot. erq078.

Cao, Y., Repo, T., Silvennoinen, R., Lehto, T., Pelkonen, P., 2011. Analysis of the willow root system by electrical impedance spectroscopy. Journal of Experimental Botany 62, 351 -358.

Carvalheiro, K.D., Nepstad, D.C., 1996. Deep soil heterogeneity and fine root distribution in forests and pastures of eastern Amazonia. Plant and Soil 182, 279-285.

Castellanos, J., Maass, M., Kummerow, J., 1991. Root biomass of a dry deciduous tropical forest in Mexico. Plant and Soil 131, 225-228.

Čermák, J., Kucera, J., Nadezhdina, N., 2004. Sap flow measurements with some thermodynamic methods, flow integration within trees and scaling up from sample trees to entire forest stands. Trees-Structure and Function 18, 529-546.

Čermák, J., Nadezhdina, N., Meiresonne, L., Ceulemans, R., 2008. Scots pine root distribution derived from radial sap flow patterns in stems of large leaning trees. Plant and Soil 305, 61-75.

Čermák, J., Ulrich, R., Stanek, Z., Koller, J., Aubrecht, L., 2006. Electrical measurement of tree root absorbing surfaces by the earth impedance method: 2. Verification based on allometric relationships and root severing experiments. Tree Physiology 26, 1113-1121.

Chambers, J.Q., Tribuzy, E.S., Toledo, L.C., Crispim, B.F., Higuchi, N., Santos, J.D., Araújo, A.C., Kruijt, B., Nobre, A.D., Trumbore, S.E., 2004. Respiration from a tropical forest ecosystem: partitioning of sources and low carbon use efficiency. Ecological Applications 14, 72-88.

Chen, X., Eamus, D., Hutley, L.B., 2002a. Corrigendum to: Seasonal patterns of soil carbon dioxide efflux from a wet¿dry tropical savanna of northern Australia. Aust. J. Bot. 50, 373.

Chen, X., Eamus, D., Hutley, L.B., 2002b. Seasonal patterns of soil carbon dioxide efflux from a wet-dry tropical savanna of northern Australia. Aust. J. Bot. 50, 373.

Chen, X., Eamus, D., Hutley, L.B., 2004. Seasonal Patterns of Fine-Root Productivity and Turnover in a Tropical Savanna of Northern Australia. Journal of Tropical Ecology 20, 221-224.

Chen, X., Hutley, L., Eamus, D., 2003. Carbon balance of a tropical savanna of northern Australia. Oecologia 137, 405-416.

Chloupek, O., 1977. Evaluation of the size of a plant's root system using its electrical capacitance. Plant and Soil 48, 525-532.

Cole, K.S., 1968. Membranes, ions, and impulses: a chapter of classical biophysics. University of California Press.

Comas, L.H., Anderson, L.J., Dunst, R.M., Lakso, A.N., Eissenstat, D.M., 2005. Canopy and environmental control of root dynamics in a long-term study of Concord grape. New Phytologist 167, 829-840.

Conen, F., Smith, K.A., 2000. An explanation of linear increases in gas concentration under closed chambers used to measure gas exchange between soil and the atmosphere. European Journal of Soil Science 51, 111-117.

Cox, P.M., Betts, R.A., Jones, C.D., Spall, S.A., Totterdell, I.J., 2000. Acceleration of global warming due to carbon-cycle feedbacks in a coupled climate model. Nature 408, 184-187.

Craine, J., Wedin, D., Chapin, F., 1999. Predominance of ecophysiological controls on soil CO2 flux in a Minnesota grassland. Plant and Soil 207, 77-86.

Cui, M., Nobel, P.S., 1992. Nutrient Status, Water Uptake and Gas Exchange for Three Desert Succulents Infected with Mycorrhizal Fungi. New Phytologist 122, 643-649.

Curiel-Yuste, C., Janssens, I.A., Carrara, A., Ceulemans, R., 2004. Annual Q10 of soil respiration reflects plant phenological patterns as well as temperature sensitivity. Global Change Biology 10, 161-169.

Curtis, P.S., Vogel, C.S., Gough, C.M., Schmid, H.P., Su, H., Bovard, B.D., 2005. Respiratory carbon losses and the carbon-use efficiency of a northern hardwood forest, 1999-2003. New Phytologist 167, 437-456.

Dalton, F.N., 1995. In-situ root extent measurements by electrical capacitance methods. Plant and Soil 173, 157-165.

Davidson, E.A., Janssens, I.A., Luo, Y.Q., 2005. On the variability of respiration in terrestrial ecosystems: moving beyond Q(10). Global Change Biology 12, 154-164.

Davidson, E.A., Savage, K., Bolstad, P., Clark, D.A., Curtis, P.S., Ellsworth, D.S., Hanson, P.J., Law, B.E., Luo, Y., Pregitzer, K.S., 2002. Belowground carbon allocation in forests estimated from litterfall and IRGA-based soil respiration measurements. Agricultural and Forest Meteorology 113, 39-51.

Davidson, E.A., Verchot, L.V., CattÃ¢nio, J.H., Ackerman, I.L., Carvalho, J.E.M., 2000. Effects of soil water content on soil respiration in forests and cattle pastures of eastern Amazonia. Biogeochemistry 48, 53-69.

Davidson, E.A., Janssens, I.A., 2006. Temperature sensitivity of soil carbon decomposition and feedbacks to climate change. Nature 440, 165-173.

Davidson, E.A., Belk, E., Boone, R.D., 1998. Soil water content and temperature as independent or confounded factors controlling soil respiration in a temperate mixed hardwood forest. Global Change Biology 4, 217-227.

De Castro, E.A., Kauffman, J.B., 1998. Ecosystem structure in the Brazilian Cerrado: a vegetation gradient of aboveground biomass, root mass and consumption by fire. Journal of Tropical Ecology 14, 263-283.

Delitti, W.B.C., Meguro, M., Pausas, J.G., 2006. Biomass and mineralmass estimates in a "cerrado" ecosystem. Rev. bras. Bot. 29, 531-540.

Delitti, W.B.C., Pausas, J.G., Burger, D.M., 2001. Belowground biomass seasonal variation in two Neotropical savannahs (Brazilian Cerrados) with different fire histories. Annals of Forest Science 58, 10.

Dickson, S., Kolesik, P., 1999. Visualisation of mycorrhizal fungal structures and quantification of their surface area and volume using laser scanning confocal microscopy. Mycorrhiza 9, 205-213.

Domec, J., Scholz, F.G., Bucci, S.J., Meinzer, F.C., Goldstein, G., Villalobos-Vega, R., 2006. Diurnal and seasonal variation in root xylem embolism in neotropical savanna woody species: impact on stomatal control of plant water status. Plant, Cell & Environment 29, 26-35.

Drew, M.C., 1997. OXYGEN DEFICIENCY AND ROOT METABOLISM: Injury and Acclimation Under Hypoxia and Anoxia. Annu. Rev. Plant. Physiol. Plant. Mol. Biol. 48, 223-250.

Duddridge, J.A., Malibari, A., Read, D.J., 1980. Structure and function of mycorrhizal rhizomorphs with special reference to their role in water transport. Nature 287, 834-836.

Dvořák, M., Černohorská, J., Janáček, K., 1981. Characteristics of current passage through plant tissue. Biologia Plantarum 23, 306-310.

Eastman, J.L., Coughenour, M.B., Pielke, R.A., 2001. The regional effects of CO2 and landscape change using a coupled plant and meteorological model. Global Change Biology 7, 797-815.

Eissenstat, D.M., Wells, C.E., Yanai, R.D., Whitbeck, J.L., 2000. Building roots in a changing environment: implications for root longevity. New Phytologist 147, 33-42.

England, J.R., Attiwill, P.M., 2006. Changes in leaf morphology and anatomy with tree age and height in the broadleaved evergreen species, Eucalyptus regnans F. Muell. Trees-Structure and Function 20, 79-90.

Ewers, B.E., Oren, R., Sperry, J.S., 2000. Influence of nutrient versus water supply on hydraulic architecture and water balance in Pinus taeda. Plant, Cell & Environment 23, 1055-1066.

Foley, J.A., Levis, S., Prentice, I.C., Pollard, D., Thompson, S.L., 1998. Coupling dynamic models of climate and vegetation. Global Change Biology 4, 561-579.

Franks, P.J., Farquhar, G.D., 2007. The mechanical diversity of stomata and its significance in gas exchange control. Plant Physiology 143, 78–87.

Furley, P., 2010. Tropical savannas: Biomass, plant ecology, and the role of fire and soil on vegetation. Progress in Physical Geography 34, 563-585.

Furley, P.A., Ratter, J.A., 1988. Soil resources and plant communities of the central Brazilian cerrado and their development. Journal of Biogeography 15, 97-108.

Gedroc, J.J., McConnaughay, K.D.M., Coleman, J.S., 1996. Plasticity in Root/Shoot Partitioning: Optimal, Ontogenetic, or Both? Functional Ecology 10, 44-50.

Gersani, M., Brown, J., O'Brien, E.E., Maina, G.M., Abramsky, Z., 2001. Tragedy of the commons as a result of root competition. Journal of Ecology 89, 660-669.

Gersani, M., Sachs, T., 1992. Development correlations between roots in heterogeneous environments. Plant, Cell and Environment 15, 463-469.

Gill, R.A., Jackson, R.B., 2000. Global patterns of root turnover for terrestrial ecosystems. New Phytologist 147, 13-31.

Godbold, D., Hoosbeek, M., Lukac, M., Cotrufo, M., Janssens, I., Ceulemans, R., Polle, A., Velthorst, E., Scarascia-Mugnozza, G., De Angelis, P., Miglietta, F., Peressotti, A., 2006. Mycorrhizal Hyphal Turnover as a Dominant Process for Carbon Input into Soil Organic Matter. Plant and Soil 281, 15-24.

Goodland, R., Pollard, R., 1973. The Brazilian Cerrado Vegetation: A Fertility Gradient. Journal of Ecology 61, 219-224.

Gotsch, S., Geiger, E., Franco, A., Goldstein, G., Meinzer, F., Hoffmann, W., 2010. Allocation to leaf area and sapwood area affects water relations of co-occurring savanna and forest trees. Oecologia 163, 291-301.

Grace, J., San Jose, J., Meir, P., Miranda, H.S., Montes, R.A., 2006. Productivity and carbon fluxes of tropical savannas. Journal of Biogeography 33, 387-400.

Graf, H.F., 2004. Atmospheric science - The complex interaction of aerosols and clouds. Science 303, 1309-1311.

Greens, S.R., Grace, J., Hutchings, N.J., 1995. Observations of turbulent air flow in three stands of widely spaced Sitka spruce. Agricultural and Forest Meteorology 74, 205-225.

Gupta, S.R., Singh, J.S., 1981. Soil respiration in a tropical grassland. Soil Biology and Biochemistry 13, 261-268.

Hacke, U.G., Sperry, J.S., Ewers, B.E., Ellsworth, D.S., Schäfer, K.V.R., Oren, R., 2000. Influence of soil porosity on water use in Pinus taeda. Oecologia 124, 495-505.

Hanson, P.J., Wullschleger, S.D., Bohlman, S.A., Todd, D.E., 1993. Seasonal and topographic patterns of forest floor CO2 efflux from an upland oak forest. Tree Physiol 13, 1-15.

Haynes, B.E., Gower, S.T., 1995. Belowground carbon allocation in unfertilized and fertilized red pine plantations in northern Wisconsin. Tree Physiol 15, 317-325.

Hendrick, R.L., Pregitzer, K.S., 1992. The demography of fine roots in a northern hardwood forest. Ecology 73, 1094-1104.

Hendricks, J.J., Hendrick, R.L., Wilson, C.A., Mitchell, R.J., Pecot, S.D., Guo, D., 2006. Assessing the patterns and controls of fine root dynamics: an empirical test and methodological review. J Ecology 94, 40-57.

Himmelbauer, M., Loiskandl, ¡., Kastanek, ¡., 2004. Estimating length, average diameter and surface area of roots using two different Image analyses systems. Plant and Soil 260, 111-120.

Hobbie, E., Johnson, M., Rygiewicz, P., Tingey, D., Olszyk, D., 2004. Isotopic estimates of new carbon inputs into litter and soils in a four-year climate change experiment with Douglas-fir. Plant and Soil 259, 331-343.

Hoffmann, W.A., da Silva, E.R., Machado, G.C., Bucci, S.J., Scholz, F.G., Goldstein, G., Meinzer, F.C., 2005. Seasonal leaf dynamics across a tree density gradient in a Brazilian savanna. Oecologia 145, 306-315.

Hoffmann, W.A., Franco, A.C., 2003. Comparative growth analysis of tropical forest and savanna woody plants using phylogenetically independent contrasts. Journal of Ecology 475-484.

Hoffmann, W.A., Adasme, R., Haridasan, M., T. de Carvalho, M., Geiger, E.L., Pereira, M.A.B., Gotsch, S.G., Franco, A.C., 2009. Tree topkill, not mortality, governs the dynamics of savanna–forest boundaries under frequent fire in central Brazil. Ecology 90, 1326-1337.

Hogberg, P., Nordgren, A., Buchmann, N., Taylor, A.F.S., Ekblad, A., Hogberg, M.N., Nyberg, G., Ottosson-Lofvenius, M., Read, D.J., 2001. Large-scale forest girdling shows that current photosynthesis drives soil respiration. Nature 411, 789-792.

Högberg, P., Nordgren, A., Buchmann, N., Taylor, A.F.S., Ekblad, A., Hogberg, M.N., Nyberg, G., Ottosson-Lofvenius, M., Read, D.J., 2001. Large-scale forest girdling shows that current photosynthesis drives soil respiration. Nature 411, 789-792.

Högberg, P., Read, D.J., 2006. Towards a more plant physiological perspective on soil ecology. Trends in Ecology & Evolution 21, 548-554.

House, J.I., Archer, S., Breshears, D.D., Scholes, R.J., 2003. Conundrums in mixed woody-herbaceous plant systems. Journal of Biogeography 30, 1763-1777.

Howard, D., Howard, P., 1993. Relationships between CO2 evolution, moisture content and temperature for a range of soil types. Soil Biology and Biochemistry 25, 1537-1546.

Hutchinson, G.L., Mosier, A.R., 1981. Improved Soil Cover Method for Field Measurement of Nitrous Oxide Fluxes. Soil Sci Soc Am J 45, 311-316.

IBGE, 1993. Mapa de Vegetaçao do Brasil. Fundaçao Instituto Brasileiro de Geographia e Estatistica.

Ilstedt, U., Nordgren, A., Malmer, A., 2000. Optimum soil water for soil respiration before and after amendment with glucose in humid tropical acrisols and a boreal mor layer. Soil Biology and Biochemistry 32, 1591-1599.

Jackson, R.B., Canadell, J., Ehleringer, J.R., Mooney, H.A., Sala, O.E., Schulze, E.D., 1996. A global analysis of root distributions for terrestrial biomes. Oecologia 108, 389-411.

Jackson, R.B., Mooney, H.A., Schulze, E.D., 1997. A global budget for fine root biomass, surface area, and nutrient contents. Proceedings of the National Academy of Sciences of the United States of America 94, 7362-7366.

Janssens, I.A., Lankreijer, H., Matteucci, G., Kowalski, A.S., Buchmann, N., Epron, D., Pilegaard, K., Kutsch, W., Longdoz, B., Grünwald, T., Montagnani, L., Dore, S., Rebmann, C., Moors, E.J., Grelle, A., Rannik, Ü., Morgenstern, K., Oltchev, S., Clement, R., Guðmundsson, J., Minerbi, S., Berbigier, P., Ibrom, A., Moncrieff, J., Aubinet, M., Bernhofer, C., Jensen, N.O., Vesala, T., Granier, A., Schulze, E.-., Lindroth, A., Dolman, A.J., Jarvis, P.G., Ceulemans, R., Valentini, R., 2001. Productivity overshadows temperature in determining soil and ecosystem respiration across European forests. Global Change Biology 7, 269-278.

Jarvis, P.G., 1976. The Interpretation of the Variations in Leaf Water Potential and Stomatal Conductance Found in Canopies in the Field. Philosophical Transactions of the Royal Society of London. Series B, Biological Sciences (1934-1990) 273, 593-610.

Javot, H., Lauvergeat, V., Santoni, V., Martin-Laurent, F., Guclu, J., Vinh, J., Heyes, J., Franck, K.I., Schaffner, A.R., Bouchez, D., Maurel, C., 2003. Role of a Single Aquaporin Isoform in Root Water Uptake. Plant Cell 15, 509-522.

Jeffree, C.E., Johnson, R.P.C., Jarvis, P.G., 1971. Epicuticular wax in the stomatal antechamber of sitka spruce and its effects on the diffusion of water vapour and carbon dioxide. Planta 98, 1-10.

Jenkinson, D.S., Adams, D.E., Wild, A., 1991. Model estimates of CO2 emissions from soil in response to global warming. Nature 351, 304-306.

Johnson, I.R., Thornley, J.H.M., 1987. A Model of Shoot: Root Partitioning with Optimal Growth. Ann Bot 60, 133-142.

Jolly, W.M., Nemani, R., Running, S.W., 2005. A generalized, bioclimatic index to predict foliar phenology in response to climate. Global Change Biology 11, 619-632.

Joslin, J.D., Wolfe, M.H., Hanson, P.J., 2000. Effects of altered water regimes on forest root systems. New Phytologist 147, 117-129.

Katsuhara, M., Koshio, K., Shibasaka, M., Hayashi, Y., Hayakawa, T., Kasamo, K., 2003. Over-expression of a Barley Aquaporin Increased the Shoot/Root Ratio and Raised Salt Sensitivity in Transgenic Rice Plants. Plant Cell Physiol. 44, 1378-1383.

Keeling, C.D., Chin, J.F.S., Whorf, T.P., 1996. Increased activity of northern vegetation inferred from atmospheric CO2 measurements. Nature 382, 146-149.

Keyes, M.R., Grier, C.C., 1981. Above- and below-ground net production in 40-year-old Douglas-fir stands on low and high productivity sites. Can. J. For. Res. 11, 599-605.

Kicklighter, D.W., Melillo, J.M., Peterjohn, W.T., Rastetter, E.B., McGuire, A.D., 1994. Aspects of spatial and temporal aggregation in estimating regional carbon dioxide fluxes from temperate forest soils. Journal of Geophysical Research 99, 1303-1315.

Koch, G.W., Sillett, S.C., Jennings, G.M., Davis, S.D., 2004. The limits to tree height. Nature 428, 851-854.

Koren, I., Kaufman, Y.J., Remer, L.A., Martins, J.V., 2004. Measurement of the effect of Amazon smoke on inhibition of cloud formation. Science 303, 1342-1345.

Körner, C., 1994. Biomass fractionation in plants: a reconsideration of definitions based on plant functions., in: A Whole Plant Perspective on Carbon–Nitrogen Interactions. Academic Publishing, The Hague, Netherlands, pp. 173-185.

Kramer, P.J., Boyer, J.S., 1995. Water relations of plants and soils. Academic Press, Inc., San Diego.

Kramer, P.J., 1946. Absorption of Water through Suberized Roots of Trees. Plant Physiology 21, 37-41.

Lauenroth, W.K., Gill, R., 2003. Turnover of root systems, Root Ecology. Springer, Berlin.

Law, B.E., Falge, E., Gu, L., Baldocchi, D.D., Bakwin, P., Berbigier, P., Davis, K., Dolman, A.J., Falk, M., Fuentes, J.D., Goldstein, A., Granier, A., Grelle, A., Hollinger, D., Janssens, I.A., Jarvis, P., Jensen, N.O., Katul, G., Mahli, Y., Matteucci, G., Meyers, T., Monson, R., Munger, W., Oechel, W., Olson, R., Pilegaard, K., Paw U, K.T., Thorgeirsson, H., Valentini, R., Verma, S., Vesala, T., Wilson, K., Wofsy, S., 2002. Environmental controls over carbon dioxide and water vapor exchange of terrestrial vegetation. Agricultural and Forest Meteorology 113, 97-120.

Le Dantec, V., Epron, D., Dufrêne, E., 1999. Soil CO2 efflux in a beech forest: comparison of two closed dynamic systems. Plant and Soil 214, 125-132.

Leake, J.R., Ostle, N.J., Rangel-Castro, J.I., Johnson, D., 2006. Carbon fluxes from plants through soil organisms determined by field 13CO2 pulse-labelling in an upland grassland. Applied Soil Ecology 33, 152-175.

Lehto, T., Grace, J., 1994. Carbon Balance of Tropical Tree Seedlings: A Comparison of Two Species. New Phytologist 127, 455-463.

Leuning, R., Cleugh, H.A., Zegelin, S.J., Hughes, D., 2005. Carbon and water fluxes over a temperate Eucalyptus forest and a tropical wet/dry savanna in Australia: measurements and comparison with MODIS remote sensing estimates. Agricultural and Forest Meteorology 129, 151-173.

Lima, T.T.S., Miranda, I.S., Vasconcelos, S.S., 2010. Effects of water and nutrient availability on fine root growth in eastern Amazonian forest regrowth, Brazil. New Phytologist 187, 622-630.

Litton, C., Ryan, M., Tinker, D., Knight, D., 2003. Belowground and aboveground biomass in young postfire lodgepole pine forests of contrasting tree density. Canadian Journal of Forest Research 33, 351-363.

Lloyd, J., Taylor, J.A., 1994. On the Temperature Dependence of Soil Respiration. Functional Ecology 8, 315-323.

Longdoz, B., Yernaux, M., Aubinet, M., 2000. Soil CO2 efflux measurements in a mixed forest: impact of chamber disturbances, spatial variability and seasonal evolution. Global Change Biology 6, 907-917.

Lopes, A.S., Cox, F.R., 1977. Cerrado Vegetation in Brazil: An Edaphic Gradient. Agron J 69, 828-831.

Luu, D., Maurel, C., 2005. Aquaporins in a challenging environment: molecular gears for adjusting plant water status. Plant, Cell & Environment 28, 85-96.

MacFall, J.S., Johnson, G.A., Kramer, P.J., 1990. Observation of a water-depletion region surrounding loblolly pine roots by magnetic resonance imaging. Proceedings of the National Academy of Sciences of the United States of America 87, 1203 -1207.

Macfall, J.S., Johnson, G.A., Kramer, P.J., 1991. Comparative water uptake by roots of different ages in seedlings of loblolly pine (Pinus taeda L.). New Phytol 119, 551-560.

Magnani, F., Leonardi, S., Tognetti, R., Grace, J., Borghetti, M., 1998. Modelling the surface conductance of a broad-leaf canopy: effects of partial decoupling from the atmosphere. Plant, Cell & Environment 21, 867-879.

Magnani, F., Mencuccini, M., Grace, J., 2000. Age-related decline in stand productivity: the role of structural acclimation under hydraulic constraints. Plant, Cell & Environment 23, 251-263.

Malhi, Y., Baldocchi, D.D., Jarvis, P.G., 1999. The carbon balance of tropical, temperate and boreal forests. Plant, Cell & Environment 22, 715-740.

Malhi, Y., Aragão, L.E.O.C., Galbraith, D., Huntingford, C., Fisher, R., Zelazowski, P., Sitch, S., McSweeney, C., Meir, P., 2009. Exploring the likelihood and

mechanism of a climate-change-induced dieback of the Amazon rainforest. Proceedings of the National Academy of Sciences 106, 20610-20615.

Maliakal, S.K., McDonnell, K., Dudley, S.A., Schmitt, J., 1999. Effects of red to far-red ratio and plant density on biomass allocation and gas exchange in Impatiens capensis. International Journal of Plant Sciences 160, 723-733.

Mancuso, S., 1999. Seasonal dynamics of electrical impedance parameters in shoots and leaves related to rooting ability of olive (Olea europea) cuttings. Tree Physiology 19, 95 -101.

Marimon Jr., B.H., Haridasan, M., 2005. Comparação da vegetação arbórea e características edáficas de um cerradão e um cerrado sensu stricto em áreas adjacentes sobre solo distrófico no leste de Mato Grosso, Brasil. Acta Bot. Bras. 19, 913-926.

Matthias, A.D., Yarger, D.N., Weinbeck, R.S., 1978. A numerical evaluation of chamber methods for determining gas fluxes. Geophys. Res. Lett. 5, PP. 765-768.

Mayle, F.E., Langstroth, R.P., Fisher, R.A., Meir, P., 2007. Long-term forest–savannah dynamics in the Bolivian Amazon: implications for conservation. Philosophical Transactions of the Royal Society B: Biological Sciences 362, 291 -307.

M'bou, A.T., Jourdan, C., Deleporte, P., Nouvellon, Y., Saint-André, L., Bouillet, J., Mialoundama, F., Mabiala, A., Epron, D., 2008. Root elongation in tropical Eucalyptus plantations: effect of soil water content. Annals of Forest Science 65, 7.

McBride, R., Candido, M., Ferguson, J., 2008. Estimating root mass in maize genotypes using the electrical capacitance method. Archives of Agronomy and Soil Science 54, 215-226.

McDowell, N. McDowell, Barnard, H. Barnard, Bond, B. Bond, Hinckley, T. Hinckley, Hubbard, R. Hubbard, Ishii, H. Ishii, Köstner, B. Köstner, Magnani, F. Magnani, Marshall, J. Marshall, Meinzer, F. Meinzer, Phillips, N. Phillips, Ryan, M. Ryan, Whitehead, D. Whitehead, 2002. The

relationship between tree height and leaf area: sapwood area ratio. Oecologia 132, 12-20.

McDowell, N.G., Balster, N.J., Marshall, J.D., 2001. Belowground carbon allocation of Rocky Mountain Douglas-fir. Can. J. For. Res. 31, 1425-1436.

Meir, P., Grace, J., Miranda, A.C., Lloyd, J., 1996. Soil respiration in a rainforest in Amazonia and in cerrado in central Brazil. In Amazonian Deforestation and Climate.(Eds JHC Gash, CA Nobre, J. Roberts and RL Victoria.) pp. 319-330, in: . John Wiley: Chichester.

Menaut, J.C., Cesar, J., 1979. Structure and Primary Productivty of Lamto Savannas, Ivory Coast. Ecology 60, 1197.

Mencuccini, M., Grace, J., 1995. Climate influences the leaf area/sapwood area ratio in Scots pine. Tree Physiology 15, 1-10.

Metcalfe, D.B., Meir, P., Aragão, L.E.O.C., Malhi, Y., Costa, A.C.L.D., Braga, A., Gonçalves, P.H.L., Athaydes, J.D., Almeida, S.S.D., Williams, M., 2007. Factors controlling spatio-temporal variation in carbon dioxide efflux from surface litter, roots, and soil organic matter at four rain forest sites in the eastern Amazon. J. Geophys. Res. 112, doi:10.1029/2007JG000443.

Metcalfe, D.B., Meir, P., Aragão, L.E.O.C., Costa, A.C.L., Braga, A.P., Gonçalves, P.H.L., Athaydes Silva Junior, J., Almeida, S.S., Dawson, L.A., Malhi, Y., Williams, M., 2008. The effects of water availability on root growth and morphology in an Amazon rainforest. Plant Soil 311, 189-199.

Miranda, A.C., Miranda, H.S., Lloyd, J., Grace, J., Francey, R.J., McIntyre, J.A., Meir, P., Riggan, P., Lockwood, R., Brass, J., 1997. Fluxes of carbon, water and energy over Brazilian cerrado: An analysis using eddy covariance and stable isotopes. Plant Cell and Environment 20, 315-328.

Mitchell, M.D., Denne, M.P., 1997. Variation in density of Picea sitchensis in relation to within-tree trends in tracheid diameter and wall thickness. Forestry 70, 47.

Murphy, P.G., Lugo, A.E., 1986. Ecology of Tropical Dry Forest. Annu. Rev. Ecol. Syst. 17, 67-88.

Nadelhoffer, K.J., 2000. Research Review: The Potential Effects of Nitrogen Deposition on Fine-Root Production in Forest Ecosystems. New Phytologist 147, 131-139.

Neilson, R.P., 1993. Vegetation redistribution: A possible biosphere source of CO2 during climatic change. Water, Air, & Soil Pollution 70, 659-673.

Nepstad, D., Lefebvre, P., Da Silva, U.L., Tomasella, J., Schlesinger, P., Solorzano, L., Moutinho, P., Ray, D., Benito, J.G., 2004. Amazon drought and its implications for forest flammability and tree growth: a basin-wide analysis. Global Change Biology 10, 704-717.

Nepstad, D.C., Decarvalho, C.R., Davidson, E.A., Jipp, P.H., Lefebvre, P.A., Negreiros, G.H., Dasilva, E.D., Stone, T.A., Trumbore, S.E., Vieira, S., 1994. The Role of Deep Roots in the Hydrological and Carbon Cycles of Amazonian Forests and Pastures. Nature 372, 666-669.

Newman, E.I., 1969. Resistance to water flow in soil and plant. I. Soil resistance in relation to amounts of root: theoretical estimates. Journal of Applied Ecology 6, 1-12.

Nicoll, B.C., Ray, D., 1996. Adaptive growth of tree root systems in response to wind action and site conditions. Tree physiology 16, 891.

Niklas, K.J., 2004. Plant allometry: is there a grand unifying theory? Biological Reviews 79, 871-889.

Nobre, C.A., Sellers, P.J., Shukla, J., 1991. Amazonian Deforestation and Regional Climate Change. Journal of Climate 4, 957-988.

Norby, R.J., Jackson, R.B., 2000. Root dynamics and global change: seeking an ecosystem perspective. New Phytologist 147, 3-12.

O'Brien, J.J., Oberbauer, S.F., 2001. An inexpensive, portable meter for measuring soil moisture. Soil Sci Soc Am J 65, 1081-1083.

Oleksyn, J., Zytkowiak, R., Karolewski, P., Reich, P.B., Tjoelker, M.G., 2000. Genetic and environmental control of seasonal carbohydrate dynamics in trees of diverse Pinus sylvestris populations. Tree Physiol 20, 837-847.

Persson, H., Fircks, Y., Majdi, H., Nilsson, L.O., 1995. Root distribution in a Norway spruce (Picea abies (L.) Karst.) stand subjected to drought and ammonium-sulphate application. Plant and Soil 168, 161-165.

Petty, J.A., Macmillan, D.C., Steward, C.M., 1990. Variation of density and growth ring width in stems of Sitka and Norway spruce. Forestry 63, 39.

Pinto, A.D., Bustamante, M.M.C., Kisselle, K., Burke, R., Zepp, R., Viana, L.T., Varella, R.F., Molina, M., 2002. Soil emissions of N2O, NO, and CO2 in Brazilian Savannas: Effects of vegetation type, seasonality, and prescribed fires. Journal of Geophysical Research-Atmospheres 107.

Plamboeck, A.H., Dawson, T.E., Egerton-Warburton, L.M., North, M., Bruns, T.D., Querejeta, J.I., 2007. Water transfer via ectomycorrhizal fungal hyphae to conifer seedlings. Mycorrhiza 17, 439-447.

Pregitzer, K.S., 2002. Fine roots of trees - a new perspective. New Phytologist 154, 267-270.

Pregitzer, K.S., DeForest, J.L., Burton, A.J., Allen, M.F., Ruess, R.W., Hendrick, R.L., 2002. Fine root architecture of nine north american trees. Ecological Monographs 72, 293-309.

Pregitzer, K.S., Hendrick, R.L., Fogel, R., 1993. The Demography of Fine Roots in Response to Patches of Water and Nitrogen. New Phytologist 125, 575-580.

Pregitzer, K.S., King, J.A., Burton, A.J., Brown, S.E., 2000. Responses of tree fine roots to temperature. New Phytologist 147, 105-115.

Pregitzer, K.S., Laskowski, M.J., Burton, A.J., Lessard, V.C., Zak, D.R., 1998. Variation in sugar maple root respiration with root diameter and soil depth. Tree Physiology 18, 665-670.

Preston, G., McBride, R., Bryan, J., Candido, M., 2004. Estimating root mass in young hybrid poplar trees using the electrical capacitance method. Agroforestry Systems 60, 305-309.

Priess, J., Then, C., Fölster, H., 1999. Litter and Fine-Root Production in Three Types of Tropical Premontane Rain Forest in SE Venezuela. Plant Ecology 143, 171-187.

Quesada, C.A., Hodnett, M.G., Breyer, L.M., Santos, A.J., Andrade, S., Miranda, H.S., Miranda, A.C., Lloyd, J., 2008. Seasonal variations in soil water in two woodland savannas of central Brazil with different fire histories. Tree Physiol 28, 405-415.

R Development Core Team, 2009. R: A Language and Environment for Statistical Computing. Vienna, Austria.

Raich, J.W., Potter, C.S., Bhagawati, D., 2002. Interannual variability in global soil respiration, 1980-94. Global Change Biology 8, 800-812.

Raich, J.W., Schlesinger, W.H., 1992. The global carbon dioxide flux in soil respiration and its relationship to vegetation and climate. Tellus B 44, 81-99.

Raich, J.W., Potter, C.S., 1995. Global patterns of carbon dioxide emissions from soils. Global Biogeochemical Cycles 9, 23-36.

Raich, J.W., Tufekciogul, A., 2000. Vegetation and soil respiration: Correlations and controls. Biogeochemistry 48, 71-90.

Reichstein, M., Rey, A., Freibauer, A., Tenhunen, J., Valentini, R., Banza, J., Casals, P., Cheng, Y., Grünzweig, J.M., Irvine, J., Joffre, R., Law, B.E., Loustau, D., Miglietta, F., Oechel, W., Ourcival, J., Pereira, J.S., Peressotti, A., Ponti, F., Qi, Y., Rambal, S., Rayment, M., Romanya, J., Rossi, F., Tedeschi, V., Tirone, G., Xu, M., Yakir, D., 2003. Modeling temporal and large-scale spatial variability of soil respiration from soil water availability, temperature and vegetation productivity indices. Global Biogeochemical Cycles 17, 15-1.

Repo, T., Laukkanen, J., Silvennoinen, R., 2005. Measurement of the tree root growth using electrical impedance spectroscopy. Silva Fennica 39, 159–166.

Rey, A., Pegoraro, E., Tedeschi, V., De Parri, I., Jarvis, P.G., Valentini, R., 2002. Annual variation in soil respiration and its components in a coppice oak forest in Central Italy. Global Change Biol 8, 851-866.

Reynolds, H.L., Pacala, S.W., 1993. An Analytical Treatment of Root-to-Shoot Ratio and Plant Competition for Soil Nutrient and Light. American Naturalist 141, 51.

Robinson, D., 1986. Compensatory Changes in the Partitioning of Dry Matter in Relation to Nitrogen Uptake and Optimal Variations in Growth. Ann Bot 58, 841-848.

Ryan, M.G., Yoder, B.J., 1997. Hydraulic limits to tree height and tree growth. Bioscience 47, 235–242.

Sack, L., Cowan, P.D., Jaikumar, N., Holbrook, N.M., 2003. The'hydrology'of leaves: co-ordination of structure and function in temperate woody species. Plant, Cell & Environment 26, 1343-1356.

Sack, L., Tyree, M.T., Holbrook, N.M., 2005. Leaf hydraulic architecture correlates with regeneration irradiance in tropical rainforest trees. New Phytologist 167, 403–413.

Saiz, G., Green, C., Butterbach-Bahl, K., Kiese, R., Avitabile, V., Farrell, E.P., 2006. Seasonal and spatial variability of soil respiration in four Sitka spruce stands. Plant Soil 287, 161-176.

Sankaran, M., Ratnam, J., Hanan, N., 2008. Woody cover in African savannas: the role of resources, fire and herbivory. Global Ecology and Biogeography 17, 236-245.

Savill, P.S., 1976. The Effects of Drainage and Ploughing of Surface Water Gleys on Rooting and Windthrow of Sitka Spruce in Northern Ireland. Forestry 49, 133.

Schafer, K.V.R., Oren, R., Tenhunen, J.D., 2000. The effect of tree height on crown level stomatal conductance. Plant, Cell & Environment 23, 365-375.

Schenk, H.J., Jackson, R.B., 2002. Rooting depths, lateral root spreads and below-ground/above-ground allometries of plants in water-limited ecosystems. Journal of Ecology 90, 480-494.

Schindlbacher, A., Zechmeister-Boltenstern, S., Kitzler, B., Jandl, R., 2008. Experimental forest soil warming: response of autotrophic and heterotrophic soil respiration to a short-term 10°C temperature rise. Plant and Soil 303, 323-330.

Schlentner, R., Cleve, K., 1985. Relationships between CO2 evolution from soil, substrate temperature, and substrate moisture in four mature forest types in interior Alaska. Canadian Journal of Forest Research 15, 97-106.

Scholes, R., Hall, D.O., 1996. The carbon budget of tropical savannas, woodlands and grasslands, in: Global Change: effects on coniferous forests and grasslands. Wiley, New York, pp. 69-100.

Schulze, E.D., Schilling, K., Nagarajah, S., 1983. Carbohydrate partitioning in relation to whole plant production and water use of Vigna unguiculata (L.) Walp. Oecologia 58, 169-177.

Schweiger, P.F., Rouhier, H., Söderström, B., 2002. Visualisation of ectomycorrhizal rhizomorph structure using laser scanning confocal microscopy. Mycological Research 106, 349-354.

Sellers, P.J., Dickinson, R.E., Randall, D.A., Betts, A.K., Hall, F.G., Berry, J.A., Collatz, G.J., Denning, A.S., Mooney, H.A., Nobre, C.A., Sato, N., Field, C.B., Henderson-Sellers, A., 1997. Modeling the Exchanges of Energy, Water, and Carbon Between Continents and the Atmosphere. Science 275, 502-509.

Shackleton, C.M., McKenzie, B., Granger, J.E., 1988. Seasonal changes in root biomass, root/shoot ratios and turnover in two coastal grassland communities in Transkei. South African Journal of Botany 54, 465-471.

Sheppard, L.J., Leith, I.D., Smith, C.M.S., Kennedy, V., 1995. Effects of soil chemistry on the response of potted Sitka spruce to acid mist in open-top chambers. Water, Air, & Soil Pollution 84, 347-366.

Shinozaki, K., Yoda, K., Hozumi, K., Kira, T., 1964. A quantitative analysis of plant form - the pipe model theory I. Basic analysis. Japanese Journal of Ecology 14, 97-105.

Shipley, B., Meziane, D., 2002. The balanced-growth hypothesis and the allometry of leaf and root biomass allocation. Functional Ecology 16, 326-331.

Singh, J.S., Raghubanshi, A.S., Singh, R.S., Srivastava, S.C., 1989. Microbial biomass acts as a source of plant nutrients in dry tropical forest and savanna. Nature 338, 499-500.

Smith, S., Gianinazzi-Pearson, V., Koide, R., Cairney, J., 1994. Nutrient transport in mycorrhizas: structure, physiology and consequences for efficiency of the symbiosis. Plant and Soil 159, 103-113.

Smith, S.E., Smith, F.A., 1990. Structure and function of the interfaces in biotrophic symbioses as they relate to nutrient transport. New Phytologist 114, 1-38.

Smith, S.E., Smith, F.A., Jakobsen, I., 2003. Mycorrhizal Fungi Can Dominate Phosphate Supply to Plants Irrespective of Growth Responses. Plant Physiol. 133, 16-20.

Sotta, E., Meir, P., Malhi, Y., Nobre, A., Hodnett, M., Grace, J., 2004. Soil CO2 efflux in a tropical forest in the central Amazon. Global Change Biology 10, 601-617.

Sperry, J.S., Adler, F.R., Campbell, G.S., Comstock, J.P., 1998. Limitation of plant water use by rhizosphere and xylem conductance: results from a model. Plant, Cell & Environment 21, 347-359.

Sperry, J.S., Hacke, U.G., Oren, R., Comstock, J.P., 2002. Water deficits and hydraulic limits to leaf water supply. Plant, Cell & Environment 25, 251-263.

Steudle, E., 1994. Water transport across roots. Plant and Soil 167, 79-90.

Steudle, E., Peterson, C.A., 1998. How does water get through roots? Journal of Experimental Botany 49, 775-788.

Steudle, E., 2000a. Water uptake by roots: effects of water deficit. Journal of Experimental Botany 51, 1531 -1542.

Steudle, E., 2000b. Water uptake by roots: effects of water deficit. Journal of Experimental Botany 51, 1531 -1542.

Tang, J., Baldocchi, D.D., 2005. Spatial–temporal variation in soil respiration in an oak–grass savanna ecosystem in California and its partitioning into autotrophic and heterotrophic components. Biogeochemistry 73, 183-207.

Thomazini, L., 1974. Mycorrhiza in plants of the 'Cerrado'. Plant and Soil 41, 707-711.

Tierney, G.L., Fahey, T.J., Groffman, P.M., Hardy, J.P., Fitzhugh, R.D., Driscoll, C.T., Yavitt, J.B., 2003. Environmental control of fine root dynamics in a northern hardwood forest. Global Change Biology 9, 670-679.

Titlyanova, A.A., Romanova, I.P., Kosykh, N.P., Mironycheva-Tokareva, N.P., 1999. Pattern and Process in Above-Ground and Below-Ground Components of Grassland Ecosystems. Journal of Vegetation Science 10, 307-320.

Tobin, B., Black, K., Osborne, B., Reidy, B., Bolger, T., Nieuwenhuis, M., 2006. Assessment of allometric algorithms for estimating leaf biomass, leaf area index and litter fall in different-aged Sitka spruce forests. Forestry 79, 453.

Trumbore, S., Da Costa, E.S., Nepstad, D.C., De Camargo, P.B., Martinelli, L., Ray, D., Restom, T., Silver, W., 2006. Dynamics of fine root carbon in Amazonian tropical ecosystems and the contribution of roots to soil respiration. Global Change Biology 12, 217-229.

Trumbore, S.E., Gaudinski, J.B., 2003. The secret lives of roots. Science 302, 1344-1345.

Trumbore, S.E., Davidson, E.A., Camargo, P.B.D., Nepstad, D.C., Martinelli, L.A., 1995. Belowground Cycling of Carbon in Forests and Pastures of Eastern Amazonia. Global Biogeochem. Cycles 9, 515-528.

Tyree, M.T., Cochard, H., Cruiziat, P., Sinclair, B., Ameglio, T., 1993. Drought-induced leaf shedding in walnut: evidence for vulnerability segmentation. Plant, Cell and Environment 16, 879-882.

Urban, J., Bequet, R., Mainiero, R., 2011. Assessing the applicability of the earth impedance method for in situ studies of tree root systems. Journal of Experimental Botany.

Valentini, C.M.A., Sanches, L., de Paula, S.R., Vourlitis, G.L., de Souza Nogueira, J., Pinto, O.B., de Almeida Lobo, F., 2008. Soil respiration and aboveground litter dynamics of a tropical transitional forest in northwest Mato Grosso, Brazil. J. Geophys. Res. 113.

Vanninen, P., Makela, A., 1999. Fine root biomass of Scots pine stands differing in age and soil fertility in southern Finland. Tree Physiology 19, 823-830.

Vogt, K.A., Vogt, D.J., Bloomfield, J., 1998. Analysis of some direct and indirect methods for estimating root biomass and production of forests at an ecosystem level. Plant and Soil 200, 71-89.

Whitehead, D., Edwards, W., Jarvis, P., 1984. Conducting sapwood area, foliage area, and permeability in mature trees of Picea sitchensis and Pinus contorta. Canadian Journal of Forest Research 14, 940-947.

Wildung, R.E., Garland, T.R., Buschbom, R.L., 1975. The interdependent effects of soil temperature and water content on soil respiration rate and plant root decomposition in arid grassland soils. Soil Biology and Biochemistry 7, 373-378.

Williams, M., Bond, B.J., Ryan, M.G., 2001. Evaluating different soil and plant hydraulic constraints on tree function using a model and sap flow data from ponderosa pine. Plant, Cell & Environment 24, 679-690.

Williams, R.J., Myers, B.A., Muller, W.J., Duff, G.A., Eamus, D., 1997. Leaf phenology of woody species in a north australian tropical savanna. Ecology 78, 2542-2558.

Woodward, F.I., Osborne, C.P., 2000. The representation of root processes in models addressing the responses of vegetation to global change. New Phytologist 147, 223-232.

Wynn, J.G., Bird, M.I., Vellen, L., Grand-Clement, E., Carter, J., Berry, S.L., 2006. Continental-scale measurement of the soil organic carbon pool with climatic, edaphic, and biotic controls. Global Biogeochem. Cycles 20, 12 PP.

Zhang, H., HendersonSellers, A., McGuffie, K., 1996. Impacts of tropical deforestation .1. Process analysis of local climatic change. Journal of Climate 9, 1497-1517.